THE INTERACTIONS OF HOT SPHERES AND VOLATILE

LIQUIDS

A thesis submitted for the degree of PhD

by

MUSTAFA MEHMET KONURAY

in

The University of Aston in Birmingham

June 1975

Summary

A series of experiments involving explosions between molten metals
(aluminium, bismuth, lead and tin) and water is described. These
explosions result from a physical mechanism. An explosion is a
rapid disintegration of the molten metal into its fragments accompanied
by a noise and a pressure wave. High speed photography was used
to study this fragmentation phenomenon. Photographs provides the
time interval required for fragmentation. Results demonstrated that
an entire explosive interaction requires only 2 milli seconds for
completion.

The drops of molten metal were obtained using a tube, made of
graphite or inconel, with a nozzle at the end. The drops of molten
tin obtained from these tubes show a standard deviation in weight of
less than 5% and each weighed 0.26 grams. The availability of
known, repeatable drop configuration offered several advantages and
yielded quantitative data.

It is shown that there exists a water temperature above which
no explosion can occur. If water is at or above these temperatures,
explosions can be prevented.

It has been found that for tin temperatures just below that
necessary for explosions to occur, the tin drops suddenly deviate
from their vertical paths after falling a short distance below the
water surface. By stroboscopic illumination photography tracks of
these drops were observed and quantitative information on the dynamics
of the interaction obtained.

To the memory of

ERHAN NARLIOĞLU

This thesis 'The Interactions of Hot Spheres and Volatile
Liquids' is an account of the study done under the supervision
of Professor F M Page, BA, PhD, ScD, at the University of
Aston in Birmingham, during the period August 1972 to
July 1975.

The work described is original, except where stated, and
has not been, or is being, submitted for any other degree or
award.

June 1975   M M Konuray

Contents   Page

List of Tables

List of Figures

Acknowledgements

The author wishes to express his sincere gratitude to Professor F M Page for his help and patience over the last three years.

Thanks are also due to Professor W O Alexander and Mr A S Blower for their encouragement and also to the technical staff of the Chemistry and Metallurgy Departments.

The author wishes to express his heartiest thanks to Surendra Patel and Fikret Ateş for their co-operation in many aspects of life over the last three years.

Finally, thanks are due to Howard B Mead for many helpful discussions and to the Department of the Environment for their financial assistance.

Introduction

Considerable interest has been generated in recent years

concerning the devastating and destructive explosions which occur

when molten metal and water come in contact. These explosive

incidents may occur during casting of various metals by a continuous

process and similar explosions have occurred during the pouring of

liquified natural gas or molten sodium carbonate into water.

Some statistical evidence about casting of aluminium is

available which suggests strongly that of 40 major explosions, one

quarter may be termed catastrophic and more than half of these

associated with charging the furnace as are one third of the less

violent explosions (table 1). This type of explosion occurs when

solid scrap aluminium is being charged into a furnace containing

molten aluminium. Such an explosion is believed to be caused by

the presence of water in the scrap. When the scrap, particularly

light-weight sheet or foil scrap, has been stored in the open air.

Frost or moisture can easily be present. Some work done by

Johnson and Page[1] indicates that cold metal exposed to a

saturated atmosphere will take up several percent of water

permanently, and considerably more temporarily.

In one particular incident a soft drink bottle discarded in a

bale of scrap was believed to have been responsible for a catastrophic

explosion. However, as reported by Rengstorff[2] et al, attempts

Table 1

History of Industrial Explosions

	Catastrophic	Violent
Furnace tapping	0	4
Furnace charging	6	11
Charging of additives	0	3
Reduction of pot tapping	0	1
Furnace pour out	0	7
DC casting-runout	3	6
Unknown	1	0
	10	32

Prepared by Illinois Institute of Technology,
Research Institute in collaboration with the
Alluminium Association of America

to reproduce this form of explosion by dropping containers of water into molten aluminium have been unsuccessful. The less frequent, but less explicable explosions, are those derived from run out during casting. If a mechanical problem develops there is a chance that molten metal will escape through the shell and explosions have been reported when molten aluminium contacts patches of rust, moisture on horizontal surfaces or falls into a water-filled container. The conditions necessary for this kind of physical explosion have been qualitatively defined by Long[3] who carried out a systematic investigation using 23kg of commercially pure molten aluminium discharged through an 8.25cm diameter hole into water at $12^{\circ}C - 25^{\circ}C$ in a welded steel tank for a total of 880 tests. An 8.25cm diameter hole was chosen since explosions did not result from holes up to 6.35cm diameter. Also for a given tap-hole size there was a threshold amount of metal required to produce an explosion and greater amounts did not increase its violence. Explosions were produced by dropping metal from 45cm, 90 cm, 120cm but not from 300cm. It was thought that the metal stream broke up during the long fall and this was demonstrated by placing a grid at 45cm and pouring the metal through. There was no explosion.

The depth of the water and the metal temperature for an explosion to occur were interdependent. As the water depth is

increased so the metal temperature for an explosion increases.
As an example,

Metal at 670°C into 15.2cm water – explosion

Metal at 670°C into 25.4cm water – no explosion

Metal at 750°C into 25.4cm water – explosion

Metal at 750°C into 50.8cm water – no explosion

There was no explosion with 50.8cm water or less but this produced
a hazardous situation due to molten metal being blown out of the
container. The lateral dimensions of the tank were found to be less
important compared with the depth. If the water was warm
(60°C – 100°C) then no explosions resulted from conditions which
gave rise to explosions. Using cold water (0°C – 50°C), soluble
oils and wetting agents were found to prevent explosions by encouraging
vapour blanket production which prevents the necessary rapid heat
transfer while 15 percent sodium chloride promoted them. However,
soluble oils and wetting agents have an adverse effect on aluminium
ingot quenching, therefore, cannot be used in practice to prevent
the aluminium water explosions. Oxide and hydroxide coatings
were found to promote explosions. Small traces of grease on the
bottom of the container prevented the entrapment of water beneath
the molten metal and hence removed the cause of the triggering
reaction of steam production under the molten metal.

It would, therefore, appear that if a sufficiently large amount

of molten metal traps water beneath it on the bottom of a water container and that conditions are such that there is rapid heat transfer of a large quantity of heat to the water then an explosion will occur.

An alternative approach to that of Long has been proposed by Brauer[4] et al in which it is suggested that liquid water becomes entrained in the molten metal as it passes through the water and is rapidly vapourised causing a pressure pulse from steam generation. This fragments the metal drop and the increased heat transfer causes a violent explosion. In this case the molten metal is far from any container surface.

Flory et al[5][14] observed the formation of hollow thin shelled 'bubbles' of aluminium in water and the subsequent bursting of these bubbles. No evidence of a chemical reaction was found but some bubbles which did not burst were found to contain water. Those that did fragment did so after solidifying. It was thought that the water trapped inside the drop vapourises due to the heat and the surface tension of the molten metal holds the bubble together as it grows. Larger diameter drops fragmented more readily and more violently than smaller ones as did those released from greater heights. Vapour blanket formation appeared to prevent fragmentation.

Fragmentation may also be caused by violent boiling. When a sample is quenched in a liquid, the cooling is characterised by a boiling curve traced in reverse (from high to low temperature).

Molten metal is initially quenched by film boiling which is hydro-

namically quite. As the metal cools, the regime changes to transition

and later to nucleate boiling which are relatively violent. The

collapse and re-formation of vapour creates a rapidly varying pressure

field near the hot surface. During the transition range the forces

generated may overcome the surface tension of the molten mass and tear

it apart. Brauer[4], however, did not find any evidence that violent

boiling occurred with aluminium in water. Alternatively, fragmentation

may result when the inertial forces acting upon a sample overcome the

surface tension forces holding the sample together. The ratio of

these two forces is called the Weber number. An example of a steel-

water explosion has been reported by Lipsett[6]. He suggested that

it is the sudden conversion of water to steam which produces a shock

wave which in turn does the physical damage caused by the metal-

water explosion. In 1970 Witte et al[7] argued that the explosive

phenomenon between molten materials and cool liquids is believed

to result from a very rapid transfer of heat forming vapour in an

explosive manner rather than a release of chemical energy. In his

article, he described an explosive incident which occurred during

the development of the Bessemer process: "Once a careless worker,

in the last half of the 19th Century, poured two tons of molten metal

into a chilling pit in which there were only a few gallons of water.

The resulting explosion hurled a United States Senator who had come

to observe the new miracle, across the room and blew ^him backwards

out of the door and on to a scrap pile". Witte also explains the

Quebec foundry incident which occurred in a foundry building of

approximately 51,000cu m volume. 45kg of molten steel fell into a

shallow trough containing about $0.300m^3$ of water. The resulting

explosion injured mill personnel and cracked a half-inch concrete

floor. The data from the Quebec incident enables an estimation of the

heat transfer rates occurring during explosive vapour formation. He

calculated that a heat transfer rate of approximately 3000kw cm^{-2}

would be required, but the heat transfer rates during boiling processes

rarely exceed 3kw cm^{-2} three orders of magnitude smaller than that

required for the rapid energy release. If the 45.4kg of steel were

to fragment into smaller particles providing additional surface area

for heat transfer, the necessary total energy transfer could be

obtained with reasonable heat transfer rates. In view of ^the Lipsett[6] .

the explosions between molten materials and water are mechanical

(physical) rather than chemical. Lipsett also conducted similar

calculations as Witte from the data of Quebec incident. The amount

of heat in 45.4kg of molten steel could only have converted 13.5kg

of water to steam having a temperature of $326°C$ produces $36m^3$

steam at a pressure of 1 atmosphere. It is clear that such a volume

of steam could not, simply by its pressure effect, significantly increase

pressure within a building of several thousands cubic meter capacity.

This is a conclusion that has trapped many in investigators for upon reaching it, they then deduce that something other than the generation of steam must have caused the destruction. The view of the writer regarding this devastating explosion is that the sudden conversion of water to steam does not pressurise the whole atmosphere, but produces a shock wave in the air.

More support for the physical explanation of the explosion between molten metals and water has been supplied by Witte[8] in his 1973 article together with Vyas and Gelabert. The writers are of the opinion that the key to the occurrence of a vapour explosion is the very rapid transfer of heat which requires substantial surface area and the frag- mentation provides this necessary area. They carried out many experiments consisting of dropping small quantities of molten aluminium, tin, bismuth, lead, zinc and mercury into water. Their conclusion was that it is likely that the indirect cause of the break-up is the initial collapse of the vapour film (as film boiling around a sample becomes unstable).

The direct cause of fragmentation could be pressure differences, surface tension changes or a thermal phenomenon occurs so rapidly that it will be exceedingly difficult to capture photographically the sequence of events that initiate the fragmentation.

Elgert[9] discharged molten aluminium into water in a sealed container and measured the pressure generation resulting from the

aluminium water interaction. In experiments where pressure pulses of 1.5×10^3 bars were recorded, it was found that only 0.2% of the aluminium reacted chemically to produce aluminium oxide. The peak pressures were achieved in 1-3 milli-seconds. In the view of Elgert the explosions between molten metals and water are physical and their cause is the rapid transfer of heat which yields the flash vapourisation of the water in an explosive manner. Higgins[10] found very short reaction times during studies of metal water reactions comparing well with the time observed by Elgert. Using basic kinetic theory Epstein[11] found that the only way in which these very short reaction times could be obtained (from a chemical reaction view point) was to assume that every water molecule that struck the metal surface reacted to form oxide and liberate hydrogen. Clearly, this is a limiting case that would rarely occur in nature.

In 1969 Hess and Brondyke[12] repeated Long's experiments and verified his results. However, they distinguished three grades of explosion as moderate explosions, violent explosions and catastrophic explosions.

Moderate explosions are believed to be 'steam explosions'. Entrapment of water under the hot metal generates steam and rapid expansion of the vapour creates sufficient pressure to blow the metal out of the container. Violent explosions which destroy the container are believed to be 'contained steam explosions'. Metal enters the

water in a manner such that heat transfer is extremely rapid and pressure increases rapidly. Restraint, perhaps from a crust forming at the metal-water interface, causes an explosion violent enough to destroy the container. Catastrophic explosions which blow the container apart and are accompanied by a flash are believed to be chemical reaction.

Bradley and Witte[13] carried out a high-speed photographic investigation which enabled them to establish the general nature of the explosive interaction between hot molten metal jets and subcooled $(24^{\circ}C)$ distilled water. They hypothesised a thermally controlled initiation mechanism and their experimental evidence supports the hypothesis. Dimensional analysis of the problem yields a parameter dominated by the thermal characteristics of the jet system.

The writers believe that the use of a small jet of molten metal for the explosions between molten metals and water offers several advantages such as, known repeatable sample configuration constant sample velocity, pressure and surface termperature and continuous flow until an explosion occurs. They found that there were three basic types of interaction.

    1 Solidification, no fragmentation

    2 Porous expansion (pop corn) without fragmentation

    3 Extensive fragmentation

This type of interactions are dependent on temperature

difference between the jet surface and the water. There is, in general, a smooth transition between the three types of behaviour.

After a series of experiments on explosion between molten lead and water, Paoli and Mesler[14] obtained two methods to support the liquid entrapment hypothesis. They also used high-speed photography. The high-speed motion pictures were taken at speeds of 4000 and 8000 frames per second. As far as the writers are able to judge, the nature of the interaction between molten lead and water depends on the temperature of the molten lead. When fragmentation occurred it was always accompanied by an explosion or loud noise. Explosions occurred between $700^\circ C$ and $650^\circ C$ and above $750^\circ C$. Their results show that just above the melting point and at temperatures around $700^\circ C$ fragmentation did not occur and there was no explosion. Application of a close-up motion picture photograph revealed some information about the ripples found on the lead samples. The ripples could not be seen on the solidified sample. The formation of ripples on a fluid surface is a familiar occurrence in fluid mechanics. The development of ripples in this case is termed a Helmholtz instability because it results from a relative tangential velocity of one fluid over the surface of another. The explosion has been shown to occur at the instant of eruption of molten metal, also the existence of ripples indicating a Helmholtz instability has been shown. The

ripples suggest a possible way that the water can be entrapped within the molten metal. Consequently, the writers take the view that the liquid entrapment hypothesis can be supported as a possible mechanism for molten metal-water explosions.

In order to explain the occurrence of what they considered to be steam explosions between molten metal and water, Genco and Lemmon[15] in 1970 developed a model for the heat transfer and subsequent energy release due to steam formation from a collection of spherical metal drops surrounded by a fixed quantity of water. These molten drops were assumed to be result of molten metal-water intereaction, and metals considered were slag, pig-iron and aluminium. The controlling parameter for the explosions was thought to be primarily the heat transfer coefficient from metal to water. An empirical expression was derived from experimental data for solid 0.635cm diameter metal spheres moving through water. Molten drop sizes of 100 and 1000 microns were assumed and an explosion period of 15 mili-seconds was used based on data obtained by Higgins and Schultz[16]. Such data were high temperature chemical explosions, but their applicability to steam explosions was not demonstrated. Genco and Lemmon used different ratios of water to metal, and it was found that theoretically a ratio of between 1:10 and 1:5 for the weight of water to metal was the most explosive. Lower water temperatures were found to be

more explosive than high temperatures and high metal

temperatures to be more explosive than low temperatures.

Maischak and Feige[17] suggested that a catastrophic

aluminium-water explosion could be brought about by the presence

of an oxygen containing compound, such as rust, calcium hydroxide

or sodium or potassium sulphates. The local high temperature

resulting from reduction of these compounds by aluminium was

considered to be high enough to enable a major aluminium water

reaction to proceed. Bradley and Witte[13] claimed that the violent

explosion which can occur when molten metals come into contact

with water was not due to a chemical reaction and regarded this

fact as being firmly established. An explosive action was shown

by pouring heated mercury into water, the shrinking shell theory

of Hsiao et al[14] could be discounted. This hypothesis involved a

pressure increase on the molten interior of a sample due to

contraction of a solidified shell. This pressure increase causes

an explosive rupture of the solidified shell. Since mercury jets

exhibited explosive action, clearly without solidification, and by

injecting a sample of molten alloy at $88.5^{o}C$ into water and

obtaining mild fragmentation, Bradley and Witte concluded that

the proposition that transition-nucleate boiling was the cause of

the fragmentation had been some what discredited. However,

no mention was made of whether the distilled water used had been

degasified prior to its use. The expulsion of dissolved gases could have explained the mild fragmentation which occurred in this case. There is also no objective scale what really mild fragmentation is.

One explosive action had been initiated between a jet of molten metal and water, the explosion was extremely rapid, its period varying from between 200 and 500 micro seconds. Thus the time used in the model of Genco and Lemmon[15] was at least one order of magnitude too large. In fact, as previously mentioned the estimate of 15 milli seconds used by Genco and Lemmon[15] was based on work by Higgins and Schultz[16] which dealt with chemical explosion at high temperatures between high melting point metal and water whereas Genco and Lemmon were considering physical explosions.

In the operation of a water-cooled nuclear reactor the danger exists that in the event of a power excursion the metal from which the cooling tubes are built will melt and come into close contact with the cooling water. Any resulting explosion could be more dangerous than even the presence of the radio-active fuel. The Spert ID incident reported by the USAEC in 1964 was the first occasion on which a destructive test had been well monitored. The aluminium cooling tubes had melted and exploded with the water they contained. Because of the extreme rapidity of the explosion and

the small amount of aluminium oxide retrieved, the explosion

was regarded as physical in origin.[19]

Before this, in 1957, Higgins and Schultz[16] had investigated

the dispersion of various molten metals into water. Two methods

of dispersion were used. The first used an Aerojet explosion

dynamometer which sprayed molten metal into water, and the

second involved the use of a blasting cap to disperse molten metal

which had been dropped into a water filled container. The water

used was of a high degree of purity, and for the dynamometer tests

the droplet sizes ranged from 30 microns to 3000 microns. It was

found that for aluminium temperatures in excess of $1170^{\circ}C$ a violent

chemical explosion took place. On analysis of the residual particles

it was found the percentage of reaction, ie proportion of oxide to

metal, was higher for the smaller particles than for the larger, as

might be expected.

Following the Spert ID incident work was carried out by USAEC

to reproduce a physical aluminium-water explosion in the laboratory.

Water vapour blanket collapse was simulated on molten aluminium

and silver at metal temperatures up to $1000^{\circ}C$ for aluminium and

$1130^{\circ}C$ for silver[20]. Up to these temperatures the chemical

contribution to the pressure pulse produced by the vapour blanket

collapse was insignificant. The experimental procedure was to

drop water through a gap containing water vapour at a pressure of

1mm of mercury on to molten metal by breaking a diaphram which separated the water from the water vapour. The peak pressure produced by water impact increased very rapidly with aluminium temperature above the melting point. It was also found that only the non-latent heat present in the molten metal was available for high pressure steam generation.

Explosions involving liquified natural gas and water has also been reported. Liquified natural gas (LNG) is a mixture of hydro-carbons with boiling points ranging from methane at -161°C to isobutane at -11°C. Research carried out by Enger et al[21] and Boyle[22] has shown that on spilling LNG on to water stable film boiling is first maintained but as the lighter hydrocarbons fractions boil off preferentially, the remaining enriched liquified gas passes from film boiling to transition boiling which involves a series of minor 'pops' or explosions. No flame has been reported as a result of these 'pops', and at their most violent a shock wave has been emitted. If the water temperature was sufficiently low ice was formed before stable film boiling ceases, and the explosions were found to be prevented. This is analogous to the molten tin solidifying before the end of the stable film boiling regime in water above 60°C, as reported by Board et al[23]. The LNG explosions were explained by Boyle[22] and Katz and Sliepcevich[24] as the result of sudden vapourisation of super-heated liquified gas. They postulate that

because of the lack of nucleation sites at a liquid-liquid interface,
liquified gas is readily super-heated until explosive homogeneous
nucleation takes place. While this may seem reasonable for LNG
explosions, it is difficult to see how in an industrial application of
metal-water explosions a lack of nucleation sites would occur in
the unpurified cooling water used.

In their 1970 annual report Laber and Lemmon[25] performed
large scale experiments for the explosions between molten
aluminium and water. The experiments involved dropping 4.5 and
18kg of pure aluminium. It was found only the rusted-mild steel
bottomed water tanks would produce explosions. The glass,
aluminium or coated glass bottom did not yield explosions.

Zyszkowski[26] performed experiments to study the thermal
interaction between molten copper particles and water from about
$15^{\circ}C - 80^{\circ}C$. The initial temperatures of molten copper ranged
from the melting point of copper to $1800^{\circ}C$. The experiments
involved dropping pure copper weighing about 0.5g into water. The
copper heated and melted in the levitation coil. Strong and weak
thermal explosions below the water surface are distinguished.
When no thermal explosion occurs during the fall in water, the
particle moves quietly. The vapour air film moves ahead of the
copper particle and a steam air 'chimney' originates behind it. In
the view of the writer, the thermal explosion is caused by some

internal process in the molten metal during the rapid solidification of the molten mass in a relatively cold liquid. The heat transfer at the surface of the molten metal mass should be sufficiently high to subcool this metal below the solidification point. In such a case, where rapidly produced latent of fusion in a confined space cannot be transferred smoothly, the 'swelling out' forces originate which involve the fragmentation of the metal.

The above survey of the nature of explosive interactions between molten materials and water indicates the importance of physical approach to the problem. The danger of these explosions to human beings is considerably high compared to the present knowledge available for them.

Therefore, this Thesis will be concerned with the extension of the present knowledge available for the molten metal-water explosions.

It should be remembered all the time that the terms the explosion, steam (vapour) explosion, thermal explosion, fuel-coolant explosion, explosive interaction are used to describe the same phenomenon throughout this Thesis.

Theories about the explosions between molten metal and water

Whenever two liquids at widely different temperatures are brought together, an explosion may occur. An explosion is a rapid disintegration of the hot liquid into its fragments accompanied by a noise and a pressure wave whose force can be catastrophic.

The first step in an enquiry into molten metal–water explosions is to classify the phenomenon as a physical or chemical one, and to determine which of these mechanisms was dominant or occurred first. It could be that the cause for these explosions is physical and chemistry has no significant effect on the explosions. The view of the writers regarding the explosion is that they are mainly physical rather than chemical[3-9]. However, there is some evidence that chemical explosions may occur between molten aluminium and water[16-17]. As a result, the role of chemistry must be clearly stated on the explosions.

As is known, finely divided molten metals can undergo a chemical reaction with water such as

$$\text{Metal} + n\,H_2O \longrightarrow \text{Metal}\,O_n + n\,H_2 \qquad\qquad (2\text{-}1)$$
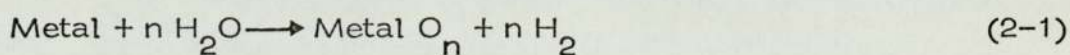
and the resulting products are the oxide of the given metal and hydrogen. An explosion is generally the result of this type of chemical reaction. When highly reactive metals like sodium and potassium contact water, there is a definite chemical reaction. The release of free hydrogen which ignites in an explosive manner

may very well be the cause of these explosions. However, it is very doubtful whether the ignition of hydrogen is at all effective on the explosive interactions between molten metals and water (eg aluminium—water, tin—water). Although chemistry has still some trumps to play on this matter. This is based on the hazardous chemical explosions between aluminium / air mixtures. This type of chemical explosion can occur when hot fragmented particles of molten aluminium react violently with air.

$$2Al + {}^3/_2 O_2 \longrightarrow Al_2O_3 \qquad\qquad (2-2)$$

The facts provide some evidence that formation of aluminium oxide has taken place during the explosion. It should be noted, however, that this type of explosion will require an initiation mechanism which causes the fragmentation of molten aluminium in the beginning phases.

If the treatment of the problem under these two explanations is summarised, it is possible to obtain a table which can describe the possible ways for the explosive interaction. As far as the current investigation is concerned, there are no observations recorded of direct chemical explosions, but there is some evidence from the previous workers[17] that the basis of the reaction is chemical. However, the overwhelming majority of the workers describe the phenomenon as physical. As far as the physical ways are concerned there are mainly five hypothesis about the interactions between

between molten metal and water, but all of these hypothesis have been developed to account for fragmentation of molten material.

1 Entrapment Theory – Liquid is trapped between the molten metal globule and the surface of the container. The liquid vapourises and rapidly expands, blowing the globule apart.

2 Violent Boiling Theory – When molten metal is quenched in a liquid the cooling is characterised by a boiling curve traced in reverse (figure 1). Film boiling is hydrodynamically quiet and little turbulence is attributed to film boiling. However, the transition and nucleate regimes are relatively violent. The collapse and reformation of vapour creates a rapidly varying pressure field near the hot surface. The violent boiling hypothesis states that, if the sample enters the transition–nucleate regime in the molten state, the hydrodynamic violence tears the particle apart.

3 Shrinking Shell Theory – This hypothesis involves a pressure increase on the molten interior of a sample due to contraction of a solidified shell. This pressure increase causes an explosive rupture of the solidified shell.

4 Entrainment Theory – The mechanism proposed for the entrainment of the water here is quite similar to that is called entrapment except in the method of trapping the water. In both cases, liquid water is believed trapped by the molten metal.

Figure 1
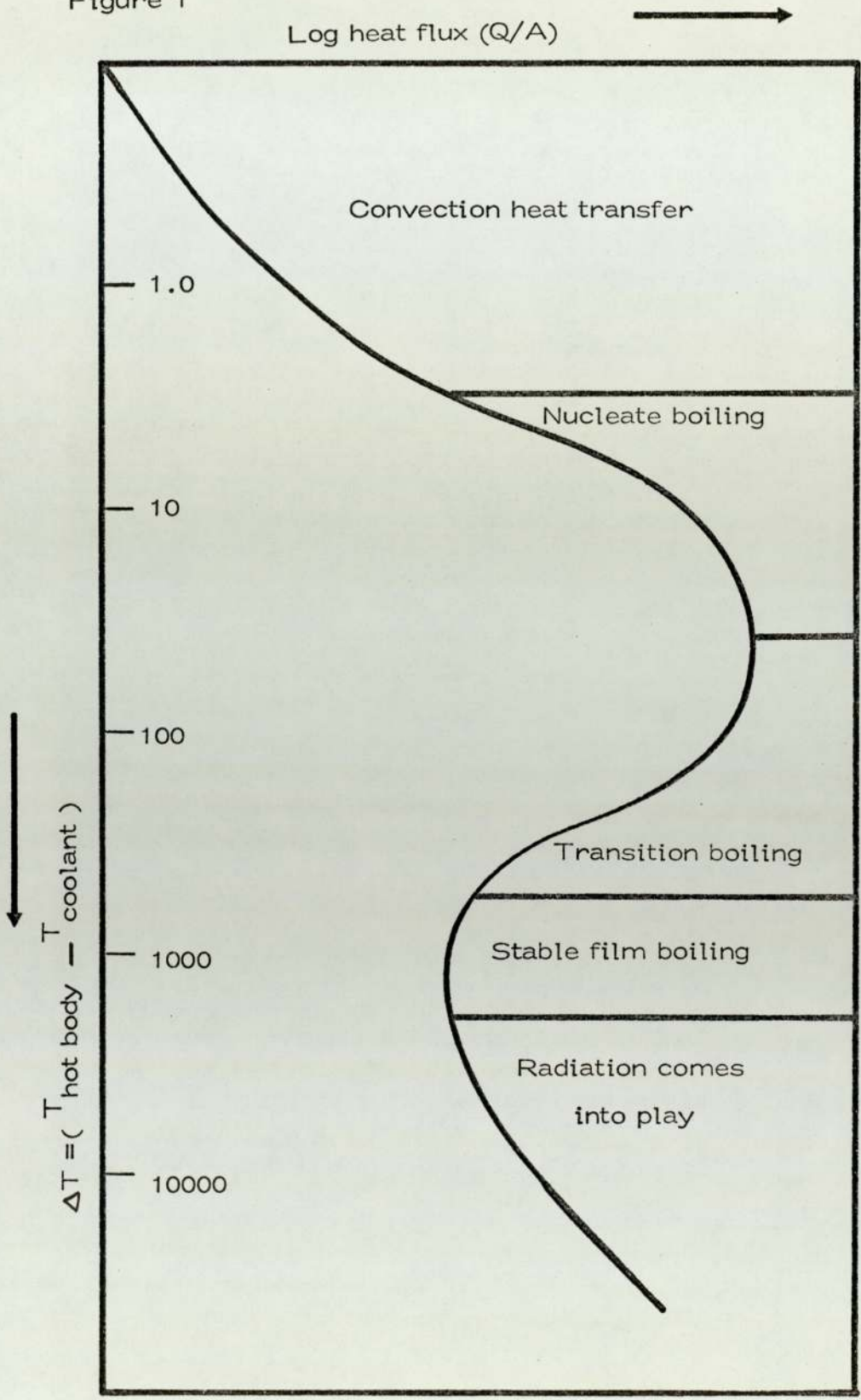
Boiling curve

Rapid vapourisation of the trapped water then leads to the

dispersal of the molten metal into water. Here water is

trapped in the falling drops of molten metal, while entrapment

theory is when the water is trapped beneath the incoming

metal as it strikes the bottom of the container.

5 Weber Number Effect – Fragmentation may occur when the

inertial forces acting on a particle overcome the surface

tension forces. The ratio of these two forces is the Weber

Number.

$$N_w = \frac{\rho R V^2}{\sigma}$$ (2-3)

where ρ is the density of the molten globule, V is the velocity of the

globule through the surrounding fluid. R is the effective radius of

the particle and σ is the surface tension. If the Weber Number

exceeds a critical value, the inertia overcomes the surface tension

and the globule fragments into smaller more stable sizes as

demonstrated by Hinze[27,28]

The experimental results which can provide some evidence to

these theories will be discussed later.

2.1 The relation between the explosion and the boiling

The possibility of an explosion resulting from the mixing of molten metal

and coolant has its relations with the boiling of the coolant around

these molten globules.

When a hot body is immersed in a cooler liquid, the transfer of heat takes place, until the body reaches thermal equilibrium with its surroundings. It is generally accepted that this type of heat transfer is associated with the phenomenon which is called boiling. Therefore, it is necessary to find out the relation between the explosions and the boiling phenomenon and this can be achieved by the explanation of the boiling processes which are relevant in thermal explosions.

The process of evaporation results in conversion of a liquid into a vapour. When this conversion occurs within a liquid, forming vapour bubbles, it is called boiling[29]. The forming of bubbles associated with transfer of heat from a hot body to a fluid. If the fluid is greatly subcooled, for example below boiling point temperature, the processes of evaporation of boiling may occur locally at the surface of the hot body accompanied by subsequent condensation in the colder bulk of the fluid, resulting in no net evaporation.

If one considers a situation where the body temperature T_w is increased (by body temperature, is meant for example, temperature of electric coil in a kettle) step by step above the temperature of bulk fluid, as T_w increased natural convection will occur without the formation of the bubbles of the fluid. Then as T_w is further

increased vapour bubbles form and agitate the liquid. This type

of boiling is nucleate boiling. These bubbles rise and break through

the free surface if the fluid is not subcooled. Eventually as Tw-Tf

is increased, the amount of body surface covered with vapour bubbles

is increased until the entire surface becomes vapour blanketed. This

results in a process called film boiling. The heat transfer rate

associated with dynamic nucleate boiling is very high because of

agitation by the bubbles. The heat transfer rate associated with

film boiling is much lower because of the insulating effect of the

vapour film. Figure 1 illustrates a boiling curve.

The transition from one type of boiling to another is a very

profound change, and is accompanied by sharp changes in hydro-

dynamic and thermal conditions of the cooling process taking place

at the cooling surface[30]. This problem is complicated by the

fact that there are not one but two crises in the boiling process.

One when the continuous vapour film is formed, and another when it

is destroyed and the bubble formation begins. The thermal flux

necessary to effect the first change is considerably greater than

that necessary to destroy the continuous film.

In nucleate boiling a temperature increase is accompanied by a

sharp increase of the heat flux and of the bubble population. The

spots where bubbles originate become more numerous until a

critical temperature is reached at which a maximum heat of flux is

attained. At that point the bubbles are so numerous that they interfere with each other. If the temperature is increased beyond the critical value by a few degrees the transition boiling begins. Westwater and Santangelo[31] have found that in this region no liquid-solid contact exists (in the case of molten metal drop, it is liquid-liquid contact). The surface is blanketed by an unstable irregular film of vapour which is in violent motion. As is known, a further increase of the temperature of the surface is followed by a decrease of heat flux until a minimum value is reached at which a stable film is formed. The stable film boiling is characterised by an orderly discharge of bubbles with a regular frequency and at regular intervals. It should be noted, however, that Bradfield did some experiments on quenching solid spheres under quasistatic conditions in water, he observed that there are intermittent liquid-solid contacts even in stable boiling. Consequently, it is possible that these intermittent contacts can also exist in transition boiling regimes.

The experimental evidence indicates that the large heat transfer rates associated with nucleate boiling are a consquence of the microconvection in the superheated liquid sublayer. This motion is caused by the dynamics of bubbles that nucleate and grow in this superheated film. As these bubbles are strong agitators and the heat flux appears to be independent of the geometry of the system,

it should be possible to scale boiling heat transfer in the nucleate

region by considerations arising from a study of the action of a

single bubble.

Zuber[32,33] formulates appropriate formula to characterise the

heat flux by the aid of agitating bubbles. His result is in the form

of:

$$Q/_A = \text{constant } \Delta T^n \qquad (2\text{-}1\text{-}1)$$

The constant includes Reynolds and Prandtl numbers. At a

constant pressure and for the same solid-liquid combination the

value of the exponent can be altered from 3 to 24.

Starting from non-linear Euler equation of motion for the two

phases and the heat transfer equations, Kutateladze[30] derived the

following criterion which describes maximum heat transfer rate in

the boiling processes.

$$\frac{Q/_A}{L(\rho_v \, g)^{1/2}(\sigma(\rho_L - \rho_v))^{1/4}} = K = \text{constant} \qquad (2\text{-}1\text{-}2)$$

This equation describes the heat transfer rate when the change over

from nucleate boiling to film boiling occurs, and it is usually called

first crisis in boiling process.

A molten metal drop, when falling into a pool of much cooler

liquid, will undergo the following sequence of events. Initially,

the heat transfer mechanism will be film boiling in which the cooling

rate of the drop is relatively low. After the particle has cooled

sufficiently, this stable film boiling will change to violent transition

boiling. Therefore, as far as molten metal water interaction is

concerned, the critical point is where film boiling gives way to

transition and consequently to nucleate boiling regimes. Kuteladze

describes this change over from stable film boiling to nucleate

boiling via transition boiling, 'A second crisis in the Boiling

Process' and he predicts that the critical heat flux can be represented

by this same formula (2-1-2). Because of the difference in the

initial structure of two phase boundary layer. However, the value

of the constant for the second crisis will be different from that for

the first.

If k_1 is the constant for the first crisis and k_2 is for the

second one, the ratio of these two constants will be

$$\frac{k_2}{k_1} = \text{constant} \tag{2-1-3}$$

Since the experiments have shown that Q_{cr_2} is less than Q_{cr_1}, the

constant in the above formula is less than unity. The above

equations have been derived on the basis that boiling around the hot

bodies was saturated. The liquids which are boiling around the hot

bodies are at their saturation temperature.

2.2 The effect of subcooling the liquid on the critical heat flux

When a bubble breaks away from the vapour film an equivalent

volume of liquid intrudes itself into the boundary region. When

this occurs, part of liquid obviously re-circulates and part travels

toward the centre of flow and is replaced by liquid from the latter

region.

To obtain a vapour film in a liquid, the main mass of which

cannot reach the saturation temperature, it is necessary that the

quantity of heat passing through the heating surface cannot be less

than that required attaining the critical rate of vapour formation in

a saturated liquid and heating the mass of liquid brought in

saturated liquid and heating the mass of liquid brought in from the

cold zone up to the saturation temperature.

The quantity of liquid flowing into the boundary region, if the

latter is not under heated, is equal to:

$$G = \frac{Q/A_{cr}}{\lambda \, f_v} \, f_L \, (1-n) \tag{2-1-4}$$

If the degree of subcooling to be slight, G is constant and it is

possible to write

$$\left(\frac{Q}{A}\right)_{cr} = \left(\frac{Q}{A}\right)_{,o,cr} \left[1 + (1-n)\right] \frac{c \, f_L \, \theta}{\lambda \, f_v} \tag{2-1-5}$$

where $\left(\frac{Q}{A}\right)_{cr}$ is the critical heat flux in a liquid which has not

been heated up to saturation temperature, $(Q/A)_{o,cr}$ is the same

quantity for a liquid, all of which is heated to saturation temperature

($\theta = 0$), all other conditions being the same.

$$\theta = t_{saturation} - t_{subcooling} \qquad (2\text{-}1\text{-}6)$$

θ is the degree of the subcooling of the main mass of the liquid

below saturation temperature t_s and c is the specific heat capacity

of the liquid. It follows from formula (2-1-5) that to a first

approximation, Q_{cr} is a linear function of θ. It should be noted,

however, that in general, the re-circulation coefficient n is

variable, and depends on a number of factors, including the relative

density of vapour.

The second crisis of boiling and corresponding rates of heat

transfer is often called Leiden frost points. In any liquid, film

boiling does not normally develop on surfaces cooler than the

Leidenfrost temperature. The Leidenfrost temperature in cryogenic

liquids may be well below normal ambient temperature, and the

film boiling. The reason why the minimum heat flux point in the

boiling curves is often called Leidenfrost point is that in 1756 a

German medical doctor, J G Leidenfrost[34] studied the boiling

of small liquid masses on a hot surface. Every house wife has

provoked the Leidenfrost phenomenon by spilling water on a hot

frying pan and watched the water drops dancing. These droplets

do not evaporate rapidly because an insulating vapour film forms

between the surface and the droplets.

Insaturated film boiling, all the liquid is at the boiling point
therefore temperature gradients exist only in the vapour as shown
in the sketch. The temperature difference between the surface and
the boiling point of the liquid is often termed the super heat. The
vapour around the hot body has a tendency to rise because of its
buoyancy against the liquid.

$T_i = T_s$

T_{HB}

$T_L = T_s$

Liquid

vapour

Temperature profile in saturated
film boiling

U_i

$U_i = 0$

Liquid

vapour

Velocity profile in saturated
film boiling
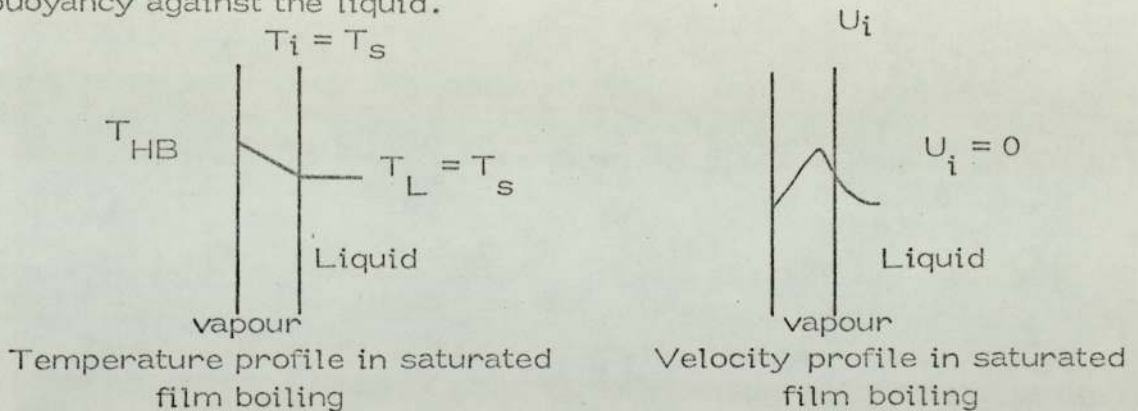
In subcooled film boiling the bulk liquid temperature is below
the boiling point, although the interface remains on that temperature.
The temperature difference between the bulk liquid and the boiling
point is known as the subcooling.

T_{HB}

T_s

T_L

Liquid

vapour

Temperature profile in subcooled
film boiling

U_i

$L = 0$

Liquid

vapour

Velocity profile in subcooled
film boiling
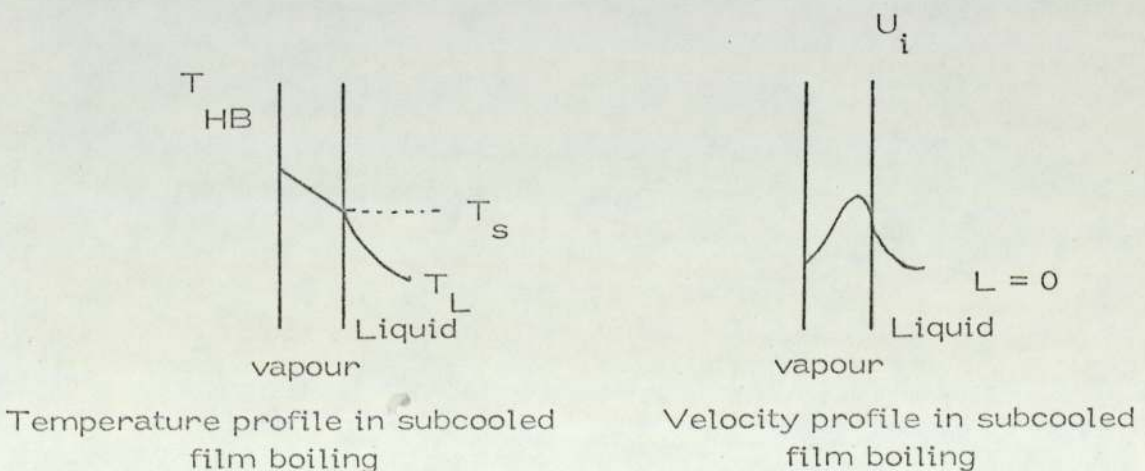
Paschkis et al[35,36,37,38] carried out experiments to obtain
boiling curves from a two-inch diameter sphere (850°C) in water,
aqueous solution of sodium hydroxide and oils. In water, increasing
the degree of subcooling increased the rates of heat transfer over the
whole range of super heat. The addition of sodium hydroxide to
water caused the replacement of film boiling by transition boiling at
higher body temperatures. This happens because sodium hydroxide
was deposited on the surface of the metal sphere as water was
evaporated at the interface. The surface on which boiling took
place was therefore one of soidum hydroxide. The relatively poor
thermal conductivity of sodium hydroxide meant the surface on
which boiling occurred was considerably cooler than the body
temperature.

It has been shown that the explosive interaction can be prevented
when the coolant is at its saturation point. The strong relation
between stable film boiling and the explosive interaction indicates
the importance of the understanding of boiling phenomenon.

It should be noted, however, the stability of the film boiling
may break down either because of external mechanical perturbation
or spontaneously as the surface cools. In fact it has been shown
that the onset of transition boiling is itself produced by small
mechanic perturbations and if such perturbations are absent, film
boiling continues until the surface cools to the saturation temperature.

It is possible that the role of triggering mechanisms in the

metal water explosions is merely to disturb the stability of film

boiling, but, the cause of the explosions cannot always be

explained by this instability. It could be that the collapse of the

film boiling is a triggering mechanism in these thermal

explosions

Vapour bubble collapse and jet penetration

One of the most important characteristics of molten metal—water

explosions is the release of excess energy in a very short time.

The observed timescale has been reported by many workers and it

is in order of a few mili—seconds. As a result, to transfer this

excess energy from the molten metal to coolant within such a short

period an extremely large contact area between molten metal and

water is required.

Witte et al[7] in 1970 have calculated the heat transfer rates

occurring during explosive vapour formation and they have shown

that a heat transfer rate of approximately $3000kW\,cm^{-2}$ would be

required. Heat transfer rates during boiling processes rarely

exceed $3kW\,cm^{-2}$ three orders of magnitude smaller than that

required for the rapid energy release. This result indicates that

the surface area for the energy release should increase by a factor

of 10^{3}. Experimental results have shown that once the onset of the

explosive interaction is established the later stages of the interaction

proceeds in a series of expansion and contraction. Every expansion

is followed by a contraction and every contraction is followed by an

expansion and this process continues until all molten metal is finely

dispersed in the coolant. It should be noted, however, that there is

some evidence about the cyclic behaviour of the vapour layer

surrounding the small molten metal drops before the explosive

interaction, but this could be the oscillations of the film boiling

regime, which is the first phenomenon^that occurs when molten metal

comes into contact with the coolant.

Any model which can describe the phenomenon should be

capable of explaining the large contact area required for the transfer of

energy in a very short time.

In 1972 Board, Farmer and Poole[23] postulated that the vapour

collapse is the main cause of dispersion in many thermal

explosions. In the view of the writers, the possible mechanism for

this is that during collapse a high speed liquid jet is formed, which

penetrates and disperses the molten material. It has been shown

that the jet penetration process can account for both the timescales

and energy transfer rates characteristic of thermal explosions.

Buchanan[39] in 1973 also proposed similar model in the view of

cyclic proceedings in these thermal explosions. Later Dullforce

and Buchanan[40] supplied additional evidence to the hypothesis put

by Buchanan.

The experimental results have shown that there exists a

threshold temperature for the coolant above which no explosion

occurs. Board et al, however, have shown that above the

threshold temperature, a mechanical disturbance initiates an

interaction.

According to Buchanan's hypothesis, there are five stages in

the interaction and the last four of which occur cyclically.

Stage 1

The onset of transition boiling causes the molten material to come in contact with the coolant and a vapour bubble is formed.

Stage 2

The expansion and the collapse of this vapour bubble occurs as a result of condensation in the subcooled coolant. The collapse of the bubble produces a high velocity jet of liquid coolant, directed towards the molten material.

Stage 3

The jet of liquid coolant penetrates the molten material and, since it has a high velocity, it disintegrates, and therefore increase in molten material coolant contact area is extremely rapid.

Stage 4

As the jet of coolant penetrates and breaks up heat is transferred from the surrounding molten material to the jet, and since the surface area is increasing rapidly the total heat transfer also increases rapidly.

Stage 5

When the jet has been heated to a certain temperature it suddenly vapourises and a high pressure vapour bubble forms. The rapid expansion of this bubble disperses the surrounding

molten material into the coolant.

The process now proceeds from stage 2 again.

Stage 1

This stage is only responsible to supply the initial perturbation. The model assumes that a vapour bubble has been formed in this stage. Although this stage is independent of the rest of the proposed mechanism nevertheless it can be an explanation for the initial triggering. This stage is also similar to that hypothesis called violent boiling. The only difference between these two models is that violent boiling theory states that the onset of transition boiling is enough to cause the explosive interactions but this model assumes the following stages are the main cause of the interaction, the only duty of the transition boiling is to supply the initial perturbation, consequently lead the way to other stages where interaction occurs.

Stage 2

When the vapour bubble is formed in the first stage is assumed to be spherical and has an initial pressure and radius R_i which expands in the surrounding incompressible coolant at density ρ and ambient pressure p_∞ . The assumptions that this model makes are that the bubble expands until the maximum radius is reached and that during this expansion phase no heat transfer occurs and conse- quently the mass of vapour in the bubble is constant. When the maximum radius is reached all the vapour suddenly condenses due to

the surrounding subcooled liquid. A cavity now exists in the coolant and this cavity collapses under the external pressure p .

A most important contribution to the understanding of cavity behaviour was made by Lord Rayleigh[41] in 1917. In his article he quoted Besant's[42] formulation of the problem for an empty cavity in a constant density liquid with constant pressure at infinity. "An infinite mass of homogeneous incompressible fluid acted upon by no forces is at rest, and a spherical portion of the fluid suddenly annihilated, it is required to find the instantaneous alteration of pressure at any point of the mass, and the time in which the cavity will be filled up, the pressure at an infinite distance being supposed to remain constant". Rayleight first set up an expression for the velocity u, at any radial distance r, where r is greater than R, the radius of the cavity wall U is the cavity wall velocity at time t. For spherical symmetry, velocity is given by

$$\frac{u}{U} = \frac{R^2}{r^2} \qquad (3-1)$$

the expression for the kinetic energy of the entire body of liquid at time t is developed by integrating the kinetic energy of a concentric fluid shell of thickness dr and density .

The result is:

$$(KE)_{liquid} = \frac{\rho}{2} \int_{R}^{\infty} u^2 4\pi r^2 dr = 2\pi \rho U^2 R^3 \qquad (3-2)$$

The work done on the entire body of fluid as the cavity is collapsing

from the initial radius, R_o to R, (R_o is the initial radius of the cavity

and is the same as maximum radius of the bubble which expands R_m)

is a product of the pressure p_∞ at infinity and the change in volume

of the cavity, since no work is done at the cavity wall where the

pressure is assumed to be zero, ie

$$\frac{4\pi P_\infty}{3} (R_o{}^3 - R^3) \tag{3-3}$$

If the fluid is inviscid as well as incompressible, the work done

appears as kinetic energy. Therefore equation (3-2) can be equated

to equation (3-3) which gives

$$U^2 = \frac{2p_\infty}{3\rho} \left(\frac{R_o{}^3}{R^3} - 1\right) \tag{3-4}$$

An expression for the time t required for a cavity to collapse from

R_o to R can be obtained from equation (3-4) by substituting for the

velocity U, of the boundary, its equivalent dR/dt and performing the

necessary integration.

$$t \doteq \frac{3\rho}{2p_\infty}^{1/2} \int_R^{R_o} \frac{R^{3/2}\,dR}{(R_o{}^3 - R^3)^{1/2}} \tag{3-5}$$

The new symbol β has been described as R/R_o. The time t of complete

collapse is obtained if equation (3-5) is evalued $\beta = 0$.

$$t = 0.91468\, R_o \sqrt{\frac{\rho}{P_\infty}} \tag{3-6}$$

Equation (3-4) shows that, as R decreases to 0, the velocity U

increases to infinity. However, the model of Buchanan assumes

vapour bubble contains some gas and has a constant pressure.

Rayleigh also did some calculations of a cavity which is filled with

a gas. (In Buchanan's model, the gas is vapour of the coolant

which is thermally compressed. Buchanan assumes while the

bubble expands, no heat transfer occurs). In such a case, the

external work done on the system as given by equation (3-3) is

equated to the sum of the kinetic energy of the liquid given by

(3-2) and the work of compression of the gas, which is $4\pi Q R_o^3 \ln$

(R_o/R), where Q is the initial pressure of the gas. Thus equation

(3-4) is replaced by:

$$U^2 = \frac{2p_\infty}{3\rho}\left(\frac{R_o^3}{R^3} - 1\right) - \frac{2Q}{\rho}\frac{R_o^3}{R^3}\ln_o\frac{R_o}{R} \qquad (3-7)$$

For any real value of Q, the cavity will not collapse completely but

U will come to 0 for a finite value of R.

If Q is greater than p_∞, the first movement of the boundary

is outward. The limiting size of the cavity can be obtained by

setting U = O in equation (3-7) which gives:

$$p\frac{z-1}{z} - Q\ln z = 0 \qquad (3-8)$$

in which z denotes the ratios of the volumes R_o^3 / R^3. Equation

(3-8) indicates that the radius oscillates between the initial value

R_o and another which is determined by the ratio p_∞/Q from this

equation. If $p_{\infty}/Q > 1$, the limiting size is a minimum. (Buchanan describes $p_{\infty} = p_o, p_i = Q$ initial pressure of the bubble, but as far as the cavity is concerned Q is the initial pressure of the gas in the cavity.) When $p_i > p_o$ $(Q > p_{\infty})$ the expansion of the vapour bubble occurs, when the maximum bubble radius is reached due to sub-cooling bubble collapse and cavity moves towards the molten metal surface under the pressure difference $p_o - p_i$ $(p_{\infty} > Q)$. The total time taken for the bubble to expand and collapse is

$$t_b = t_g + t_c \qquad\qquad (3-9)$$

The expansion and collapse takes place adjacent to the fuel surface. Plesset and Chapman[43] have shown earlier that when an initially spherical cavity collapses adjacent to a solid wall the collapse produces a jet of liquid directed towards the wall.

In order to make a numerical simulation of this situation, Plesset and Chapman made the following assumptions.

a   the liquid is compressible

b   the flow is non-viscous

c   the vapour pressure is uniform throughout the bubble interior

d   the ambient pressure and vapour pressure are constant with
     time

e   bubble contains no permanent gas

f   surface tension effects are negligible.

Viscosity is unimportant for a spherical bubble collapsing in

water under atmospheric pressure if the initial radius is 10^{-3} cm or greater.

Plesset and Chapman specified the problem by the following conditions:

p   = ambient pressure

p_v = vapour pressure inside the bubble

R_o = initial radius of the bubble

b   = initial distance from the plane wall to the centre of

             the bubble

Because the flow is irrotational the velocity vector V can be written in terms of a velocity potential ϕ . Since incompressibility is assumed, ϕ must satisfy Laplace's equation throught the liquid.

The pressure boundary conditions can be re-stated in terms of ϕ and V with the aid of Bernoulli's equation. The equation of motion is

$$\rho \frac{Dv}{Dt} = -\nabla p - (\nabla \varsigma) + \rho g \qquad (3\text{-}10)$$

This form states that a small volume element moving with the fluid is accelerated because of the forces acting upon it. In other words this is a statement of Newton's second law of motion. Mass acceleration = sum of forces since viscous effects are negligible equation (3-10) becomes

$$\rho \frac{Dv}{Dt} = -\nabla p + \rho g \qquad (3\text{-}11)$$

Euler equation

$$\frac{Dv}{Dt} = -\nabla \frac{P}{\rho} + g \tag{3-12}$$

$$\frac{Dv}{Dt} = \frac{\partial v}{\partial t} + v \cdot \nabla v = -\nabla \frac{P}{\rho} + g \tag{3-13}$$

$$\frac{\partial v}{\partial t} + \tfrac{1}{2} \nabla (v^2) = g - \frac{1}{\rho} \nabla p \tag{3-14}$$

$$v = \nabla \phi \tag{3-15}$$

ϕ = velocity potential

$$\nabla \int \left(\frac{\partial \phi}{\partial t} + \tfrac{1}{2} v^2 + \frac{P}{\rho} \right) = Q \tag{3-16}$$

$$\frac{\partial \phi}{\partial t} + \tfrac{1}{2} v^2 + \frac{P}{\rho} = \text{constant} \tag{3-17}$$

Infinitely far from the bubble the velocity is zero, and the pressure is the ambient pressure. The velocity potential there is an arbitrary function of time only which can be taken as zero.

$$\lim_{|x| \to \infty} \phi(x,t) = 0 \tag{3-18}$$

Then on the free surface

$$\frac{\partial \phi}{\partial t} + \tfrac{1}{2} v^2 = P_\infty - P_v / \rho = \Delta p / \rho \tag{3-19}$$

The final boundary condition on the potential is that its normal

derivative must vanish at the solid wall. Initially potential is

uniformly zero.

As a result of the assumptions, the solutions are characterised

by the single parameter b/R_o. A solution for a particular value of

b/R_o can be scaled to bubbles of any initial size under any positive

collapsing pressure Δp. Velocities are independent of the size of

the bubble, and are scaled like $(\Delta p/\rho)^{1/2}$.

Plesset and Chapman[(43)] simulated the collapse of an initially

spherical bubble near a plane solid wall for two cases. In case 1

the parameter b/R_0 was unity–that is, the bubble boundary was in

contact with the solid wall and tangent to it. In case 2 b/R_0 was

1.5; the closest distance from the bubble boundary to the solid

wall was initially half the radius of the bubble. The solid wall

influences the bubble early in the collapse chiefly reducing the

upward motion of the lower portion of the bubble. As the bubble

gains kinetic energy, this energy is concentrated in the upper

portion of the bubble which eventually flatens and forms a jet.

Once the jet is formed, the speed of its tip remains fairly constant.

The behaviour of the upper portion of the bubble in both cases is not

very different. The overall shapes appear quite different, however,

because the bottom of the bubble must remain in contact with the

solid wall in case 1 but is allowed mobility in case 2. The jet

speed in case 2 (about 170 m/sec under atmospheric Δp) is larger

than the speed in case 1 (about 130 m/sec). When an initially

spherical bubble collapses while adjacent to a solid surface the

speed of the liquid jet will be smaller, if the same bubble will

collapse further away without actually touching the solid wall. This

behaviour is as expected since a bubble which is further from the

wall collapses to a smaller size and can concentrate its' energy

over a smaller volume. The jet in case 1 which strikes the wall

directly, seems the more capable of damage even though the jet

speed is lower. Apparently, cavitation bubbles must almost touch

the wall initially to be capable of damaging it.

A jet speed v directly striking a solid boundary produces an

initial pressure given by the water hammer equation, where the

L and s subscripts refer to the liquid and the solid respectively.

Usually $\rho_s c_s$ is large compared to $\rho_L c_L$ producing the

approximation

$$P_{WH} = \rho_L c_L v \qquad (3-21)$$

Hancox et al[44] have shown that multiple impact by water at a

speed of 90 m/sec can erode even stainless steel.

Benjamin and Ellis[45] present two series of photographs of

bubbles collapsing near a solid wall in figures 3 and 4 of their

article. The collapse illustrated in their figure 3 falls between

case 1 and case 2. They estimated the jet speed in their figure 3

to be about 10 m/sec under an ambient pressure of about 0.04 atm.

The vapour pressure of the water is very important at this reduced

pressure. Since they did not report the temperature of the water,

this pressure can not be determined directly. However, Δp can be

calculated from the total collapse time which they gave as 10 milli-

secs. The pressure difference for the collapse in figure 3 of

Benjamin and Ellis is approximately

$$\Delta p = P_\infty - P_v \approx 10^4 \text{ dynes/}cm^2 \qquad 0.01013 \text{ bar}$$

A vapour pressure of 0.03 atm corresponds to a temperature of

about $76^\circ F$. Speeds for one atmosphere pressure difference should

be increased by a factor of ten giving an estimated jet speed of

roughly 100 m/sec so that the experimental observation of

Benjamin and Ellis are compatible with the calculations of Plesset

and Chapman.

According to Plesset and Chapman, it is not clear that the

'water hammer' stress is the mechanism of damage to the solid.

For the case of spherical bubble initially in contact with the wall

and for $\Delta p = 1$ atm in water, the speed of jet $v \approx 130$ m/sec and

$c_L \approx 1500$ m/sec so that

$$PwH \approx 2.026 \times 10^3 \text{ bar}$$

This is a most impressive impact stress, it is not obvious that

it is the important damaging mechanism since the duration of this

stress is so short. The duration may be estimated as being no

longer than the time for the impact signal to traverse the radius of

the jet. For a bubble with an initial radius = 0.1cm, this time is

$\tau_{wH} \approx 10^{-7}$ sec. On the other hand the stagnation pressure

$$P_s \approx \frac{1}{2} v^2 \rho \approx 81 \text{ bars}$$

which will have a duration of the order of the length of the jet

divided by its velocity v. This pressure pulse may be the source

of the damage because its duration is an order of magnitude

greater.

Plesset and Chapman's final result shows that the jet velocity

scales as $(\Delta p/\rho_c)^{1/2}$ where Δp (=p_0 in this case). The final jet

dimensions scale as the initial cavity radius hence the dimensions

are determined by R_m.

The velocity, length and diameter of the jet when it strikes the

fuel surface are

$$V_o = V_c \left(\frac{\Delta p}{\rho_c}\right)^{1/2} \tag{3-22}$$

$$L_o = L_c \, R_m \tag{3-23}$$

$$d_o = d_c \, R_m \tag{3-24}$$

$$\left(\frac{\Delta p}{\rho}\right)^{1/2} = (10^6)^{1/2} = 10^3 \text{ cm/sec}$$

$$V = 130 \text{ m/sec (from Plesset and Chapman)}$$

$$130 \times 10^2 = V_c \times 10^3$$

For bubble collapse adjacent to a solid wall

$$V_c = 13 \tag{3-25}$$

$$L_c = 0.493 \tag{3-26}$$

$$d_c = 0.237 \tag{3-27}$$

If the adjacent layer is molten material then the collapse will still

be axisymetric (due to density difference and / or viscosity difference)

but the numerical values of the constants will be different. In addition

the values of constants will also be different if the bubble is not

tangential.

Stage 3

The jet of coolant now enters the molten material with velocity

V_o. Christiansen and Reynolds[46] have done a numerical

simulation of this situation. Their result demonstrates that the length

of the jet increases exponentially with a time constant proportional

to d_o / V_o

$$L = L_o e^{t/\mathcal{G}} \tag{3-28}$$

where

$$\mathcal{G} = f \, do/Vo \tag{3-29}$$

time (t) is measured from the moment the jet starts to get in the

molten material.

The result of Christiansen and Reynolds show that f has the

value 11/8, however, their method can only deal with the fluids of

equal density and it is obvious that f will be different value for

molten material, and coolant system. Taylor[47] results indicate

that $f = \frac{11}{8} (\frac{\int m}{\int c})^{1/2}$ where gm is the density of molten material.

Peckover[48] has explained Christianson and Reynolds's results by showing that the local vorticity increases exporentially. Batchelor[49] has investigated the effect of homogeneous turbulence on material lines and surfaces and he also finds that the length of a line increases exponentially. Further more, his results show that the area of material surfaces increases exponentially with a time constant double that for the length increase. Thus, the assumption made by Buchanan was that the surface area of contact between the fuel and the jet is given by

$$A = A_o e^{t/\tilde{G}} \qquad (3\text{-}30)$$

A_o is the initial surface area of the jet. While the jet remains liquid its volume is almost constant. As a result since the area increases exponentially the average distance, s, between molten material and the jet surfaces must decrease exponentially.

$$\tilde{G} = \frac{11}{4} \left(\frac{f_m}{f_c}\right)^{\frac{1}{2}} \frac{d_o}{v_o} \qquad (3\text{-}31)$$

$$s = s_o e^{-t/\tilde{G}} \qquad (3\text{-}32)$$

There are three factors limiting the area increase. Firstly, if the molten material surrounding the jet solidifies then no further increase in contact area can occur. Secondly, if the jet vapourises then the conditions will change. A high pressure bubble now exists and this blows out the surrounding molten material. Thirdly, the

minimum distance between surfaces may be obtained by a critical

Weber number. In this case surface tension limits the value of s.

S can be denoted s_m for its minimum value.

Stage 4

As the jet penetrates the molten material heat transfer occurs.
Buchanan[50] has discussed a variety of methods of treating the

problem of heat transfer across a hot-wall / liquid interface.

The heat transfer occurs between the coolant and surrounding

molten material. Thus the jet of coolant gets hotter.

Stage 5

When the jet of coolant has been heated to its saturation

temperature T_{sat}, the jet vapourises provided nucleation sites are

available. Since a finite mass of liquid is vapourised virtually

instantaneously the initial state after vapourisation is a high pressure

high density gas bubble which expands and sends a shock wave. The

rapid expansion of this bubble disperses the surrounding molten

material into the coolant. This bubble then collapses as a result of

condensation in the subcooled coolant and a new high velocity jet of

liquid coolant, directed towards the molten material is formed

again. This cyclic process continued until the final dispersal of

the molten material.

4.1 Experimental apparatus

The commonest method of investigation used in previous works has been to introduce a known quantity of molten metal into water without specifying geometry of the drops. To obtain metals in their molten state, it was necessary to design and build a suitable melting chamber. There are many types of melting apparatus given in the literature for the small-scale experiments including gas-fired furnaces, induction heated crucibles, etc.

The shape and size of the molten metal drop should remain reasonably constant. It is expected that the alteration in shape upon entry will also be reproducible. Experimental results obtained prove this to be the case. The interactions between molten metals and water are very rapid events. Therefore it is extremely difficult to obtain measurements without using high speed measurement techniques. The most common method for high speed recording is photography. Initially, still photography was not used but later it was found to be a very useful tool, and was extensively used. The interactions have been filmed by high speed camera and measurements have been made upon these films. By this method many useful quantitative results have been obtained. The violence of the interactions causes rapid pressure increases in the coolant (water). It was thought to be useful to measure these changes in pressure, therefore, a suitable instrument capable of picking up these pressure changes

was obtained. A hydrophone consisting of a tranducer whose capacitance varies with pressure changes resulting from under water explosions was used throughout the investigation. The Standard Measuring Hydrophone Type 8100 is a wide range under water transducer for making absolute sound measurements over the frequency range 0.1Hz to 200kHz with receiving sensitivity of 90dB relative 1 volt/1 Pascal (32 V per pascal ($1N/m^2$)). This hydrophone was supplied by Bruel and Kjaer of Copenhagen, Denmark. The hydrophone assembly employs lead zirconate titanate as the active sensing element and it can be operated over the temperature range of $-40^{\circ}C - +120^{\circ}C$. The temperatures of molten metals were measured by standard Chromel-Alumel thermocouple connected to a digital thermometer.

In the early stages, the metals were liquified by melting them in a crucible. Rather large and irregular drops were obtained when the molten metal was gradually poured into a square perspex container filled with water.

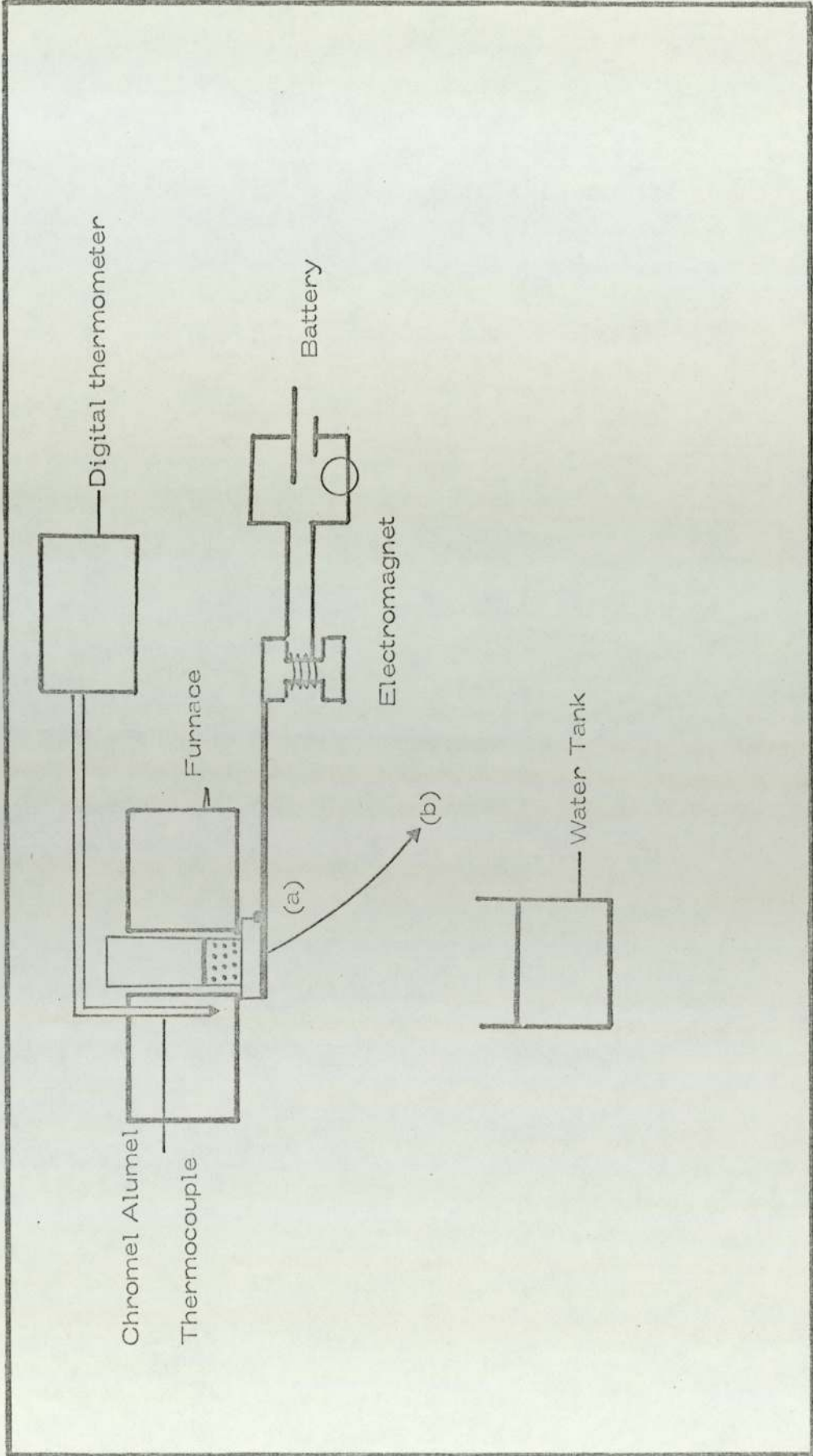To obtain geometrical reproducibility, the growth of a spherical drop at the end of a capillary tube was thought to be a useful method. It is very well known that the surface tension can sometimes be measured by determining the weight of a liquid drop falling from a tube. The simplest example of this kind of system is the laboratory burette which provides reproducible spherical drops. Consequently,

this principle was given consideration in obtaining a spherical molten metal drop falling from a tube. The only problem was the selection of appropriate material for the tube capable of withstanding very high temperatures. Whatever material was selected, it was found that it had a short lifetime. This tube was then placed in a furnace which can be set to any desired temperature.

In the early stages a silica glass tube of 2.54cm diameter was used as the melting chamber. It was placed in an electrically heated furnace. A variac was also connected to the furnace to supply different rates of heating. The outflow of the molten metal was controlled by a circular metal plate mounted on a metal rod. The flow of molten metal was stopped when this circular disc was in tight contact with the silica tube. As may be seen from figure 2a the other end of the metal rod was in contact with an electromagnet. When a discharge of the molten metal was required a switch in the electromagnetic circuit was opened and the rod was suddenly released from position (a) to position (b). Consequently the molten metal was allowed to drop into the water. The main problem with this set-up was to obtain a very tight fitting metal disc on to the silica tube and to prevent the leaking of molten metal. Furthermore spherical reproducibility was not obtained by this method.

Melting chambers and furnaces of various designs were tried out. A furnace consisting a reservoir and a capillary tube as an

Figure 2α

Chromel Alumel
Thermocouple

Furnace

Digital thermometer

Battery

Electromagnet

(a)

(b)

Water Tank

A schematic diagram of the early pouring method

outlet, was constructed using silica glass (figure 3). The basic

principle of this furnace was to push the molten metal from the

reservoir to the capillary tube where the drops to form by the

application of low nitrogen pressure. This furnace was also heated

electrically and was insulated by consecutive layers of asbestos and

aluminium cement. Numerous complications arose with this design

and only one or two spherical aluminium drops were obtained.

It should be noted that most of the earlier work done involved

pouring of molten aluminium into water with a crucible. Tin has

not been used in these furnaces. Since the type of furnace just

described did not give spherical reproducibility, a modified version

of this furnace was built. In this case, a plunge in the reservoir

was used instead of nitrogen pressure to push the molten metal

from the reservoir to the capillary tube. The main difficulty was

charging the metal in the furnace. However, it proved that a

spherical drop could be obtained by a suitable capillary tube design.

The problems with the previous models were due to the comp-

lexity of the nozzle design. As a result, a simple tube with a

nozzle at the end was made with a tap to regulate the flow of the

drops. Later desing excluded the tap as the pressure of the molten

metal in the tube was sufficient to push the molten metal through

the nozzle. By using this tube, it was possible to obtain reproducible

spherical drops. This tube was placed in a furnace with a temperature
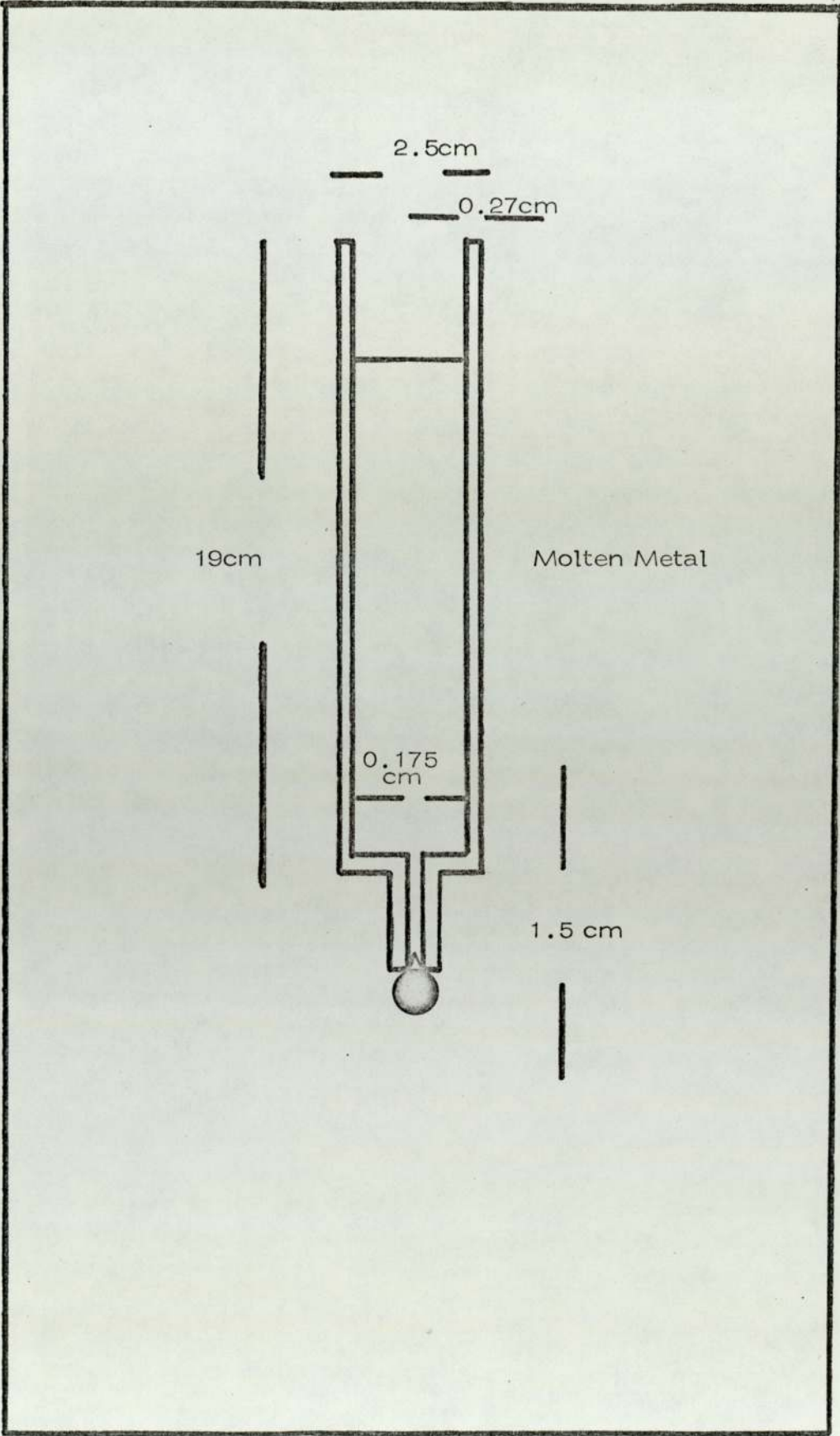
Figure 3

(a) Normal

(b) Modified
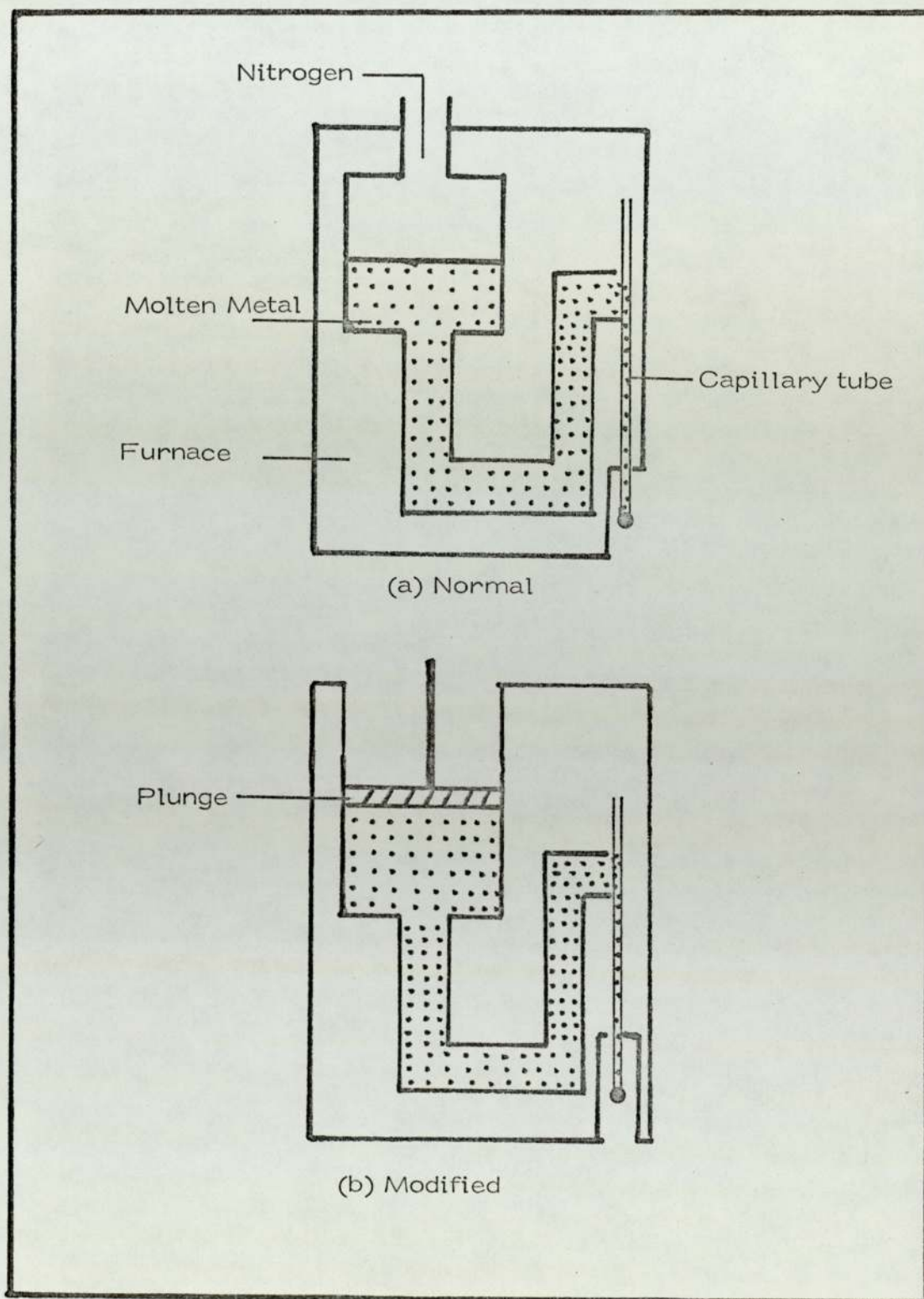
Capillary Furnaces

control circuit. Currents of up to 5A may be applied to the furnace

coils and the power was controlled by a variac attached to the

furnace.

The temperature could be set to any desired temperatures

ranging from room temperature to $1000^{\circ}C$. The temperatures

were estimated to be accurate to within $\mp5^{\circ}C$. Two separate

Chromel-Alumel thermocouples were used. One of them was used

to measure the temperature of molten metal in the tube and the

other one to supply a signal to the controller and placed just outside

the furnace windings. The former was directly connected to a

digital meter which gives the temperature of molten metal directly

in centigrades.

The tube which provides the spherical drops was made from

'Inconel' or 'graphite'. Ordinary steels oxidised excessively, and

were also severely attacked by molten metal. In fact, the oxidation

of graphite also occurs and after a short lifetime the tubes made from

graphite had to be replaced by new ones. However, the advantage

of using graphite tubes is that they are not attacked by molten metal.

A typical example of the tubes used is shown in figure 4 . The

size of spherical drops obtained from this kind of tube was reason-

ably constant. It should be noted, however, that the drops are

pear-shaped rather than complete spheres (figure 5). The drops

of molten tin obtained from these tubes weighed about 0.26 grams each.

Figure 4

The tube for reproducible metal drops

FIGURE 5.   A typical pear-like shape tin drop

0.2 cm

To demonstrate the reproducibility, 30 tin drops were weighed

individually and the corresponding histogram is shown in figure 6 .

The tin drops show a standard deviation in weight of less than 5%.

The distribution of the weight of these tin drops approximates the

normal curve. Similarly, 38 tin drops were measured in

diameter and corresponding histogram is shown in figure 7 . The

distribution of the results is negatively skewed. Most of the values

of the diameter of the drops are concentrated in the range of

0.356cm and 0.376cm. The average value for the diameter is

0.3707cm. It should be noted, however, that these measurements

were made on the drops which were obtained from the same tube.

Because the nozzle diameter is a very important factor on the

reproducibility of the drops. It is apparent that when different sizes

of nozzle are used, the measurements of weight and diameter would

be different. Although there is a limit for the nozzle diameter, above

which the continuous flow of molten metal occurs. Therefore, it is

not possible to obtain the individual drops by using considerably

large diameters.

Having ensured reproducibility of the molten metal drops, a

device was needed to trigger the high speed camera and the

oscilloscope. A photo-electric device was considered to be the

most suitable. This device consists of an electrical circuit which

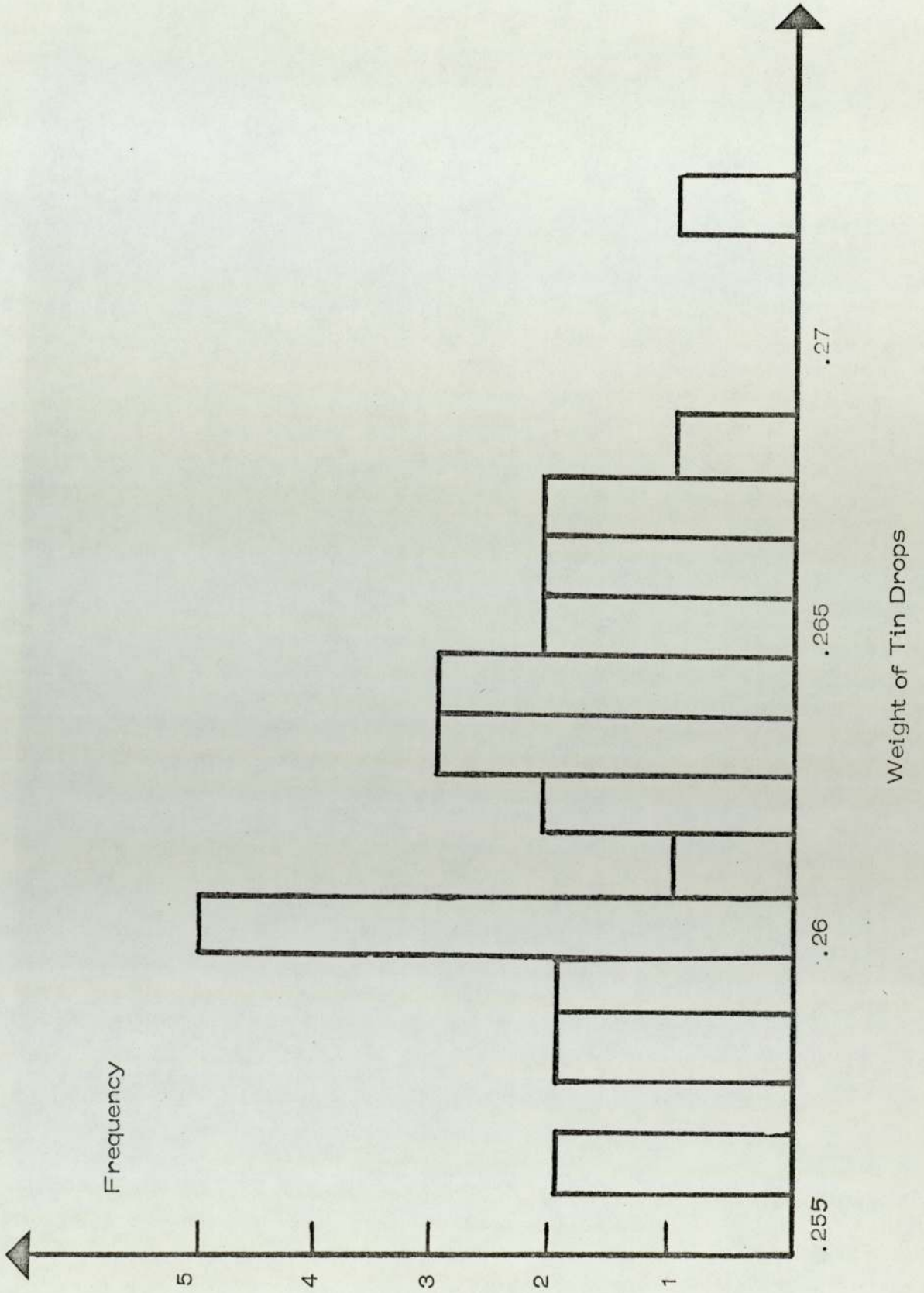can use the signal from a photo cell as a trigger pulse. The light

Figure 6

Frequency

Weight of Tin Drops

Figure 7

Frequency

12

10

8

6

4

2

.356   .361   .366   .371   .376   .381   .386   .391   .396

Diameter of Tin Drops
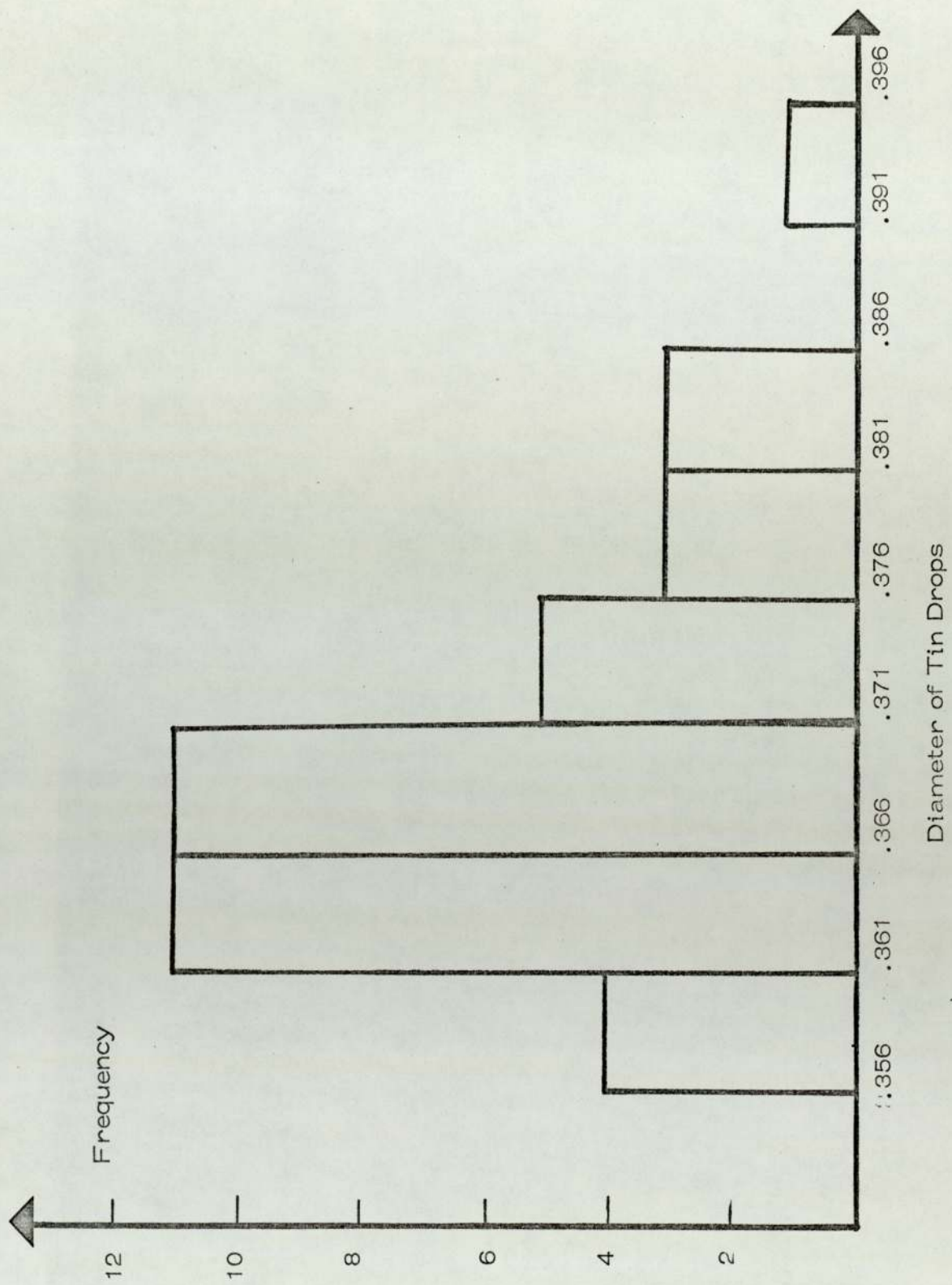
beam falling on the NLS 391 Mullard photo cell is interupted by the molten metal drop. To ensure that filming commences at the beginning of the event, it was necessary to apply the trigger pulse from the photo cell circuit to a suitable relay which would switch on the high speed camera. The interuption of the light beam produces a trigger pulse of 3 volts. This pulse is used for three different purposes.

The first application of the pulse was to trigger an oscilloscope (Textronix 4) with just sufficient oscilloscope delay to capture the signal from the hydrophone placed under water in the explosion region. The electrical circuit of the photo electric device is a simple one consisting of a singe Radio Spares BC 107 transistor which can take currents up to 100mA. The results show that if both traces of an oscilloscope are triggered at the same time, it is possible to time the event alongside the pressure histories of the explosion. Photographs of the oscilloscope display were taken by a polaroid camera which was operated at the fully open shutter position. Both traces can be clearly seen on the photographs, and accurate timing was established. The analysis of the pressure increases on these photographs is believed to be very dubious and did not yield in any conclusive results.

It was thought that trigger pulse should operate a suitable relay to switch on the high speed camera. Therefore, the second

application of the pulse produced by the interuption of the light

beam falling on a photo cell was to switch on the camera. The 3V

pulse was not capable of switching the camera on by itself without

amplification. Consequently, the circuit shown in figure 8 was

designed and constructed. This circuit is capable of amplifying the

pulse from 3V to 24V, the potential needed to operate the particular

relay in the circuit. The circuit which is used to amplify the signal

from the photo cell consists of an operational amplifier and a BC 107

transistor switch which can operate the relay at the instant when the

light beam is interupted. This 741 OPA operational amplifier is

a development of 709 OPA offering circuit simplification by employ-

ing internal frequency compensation. By this application the high

speed camera could be switched on and the event will be within the

frames of   30m long film.

It has been suggested by many workers that the collapse of

stable vapour blanket around the molten metal drops initiate the

thermal explosions. It is also suggested that the function of the

conventional triggering mechanism such as transition boiling is

to cause this initial perturbation. The onset of transition boiling

occurs spontaneously during the quenching of molten metal due to

collapse of stable vapour blanket. Board et al[51] carried out

experiments in which they applied mechanical disturbance to the

stable situation of a tin drop on a crucible under water at 80°C.

Figure 8
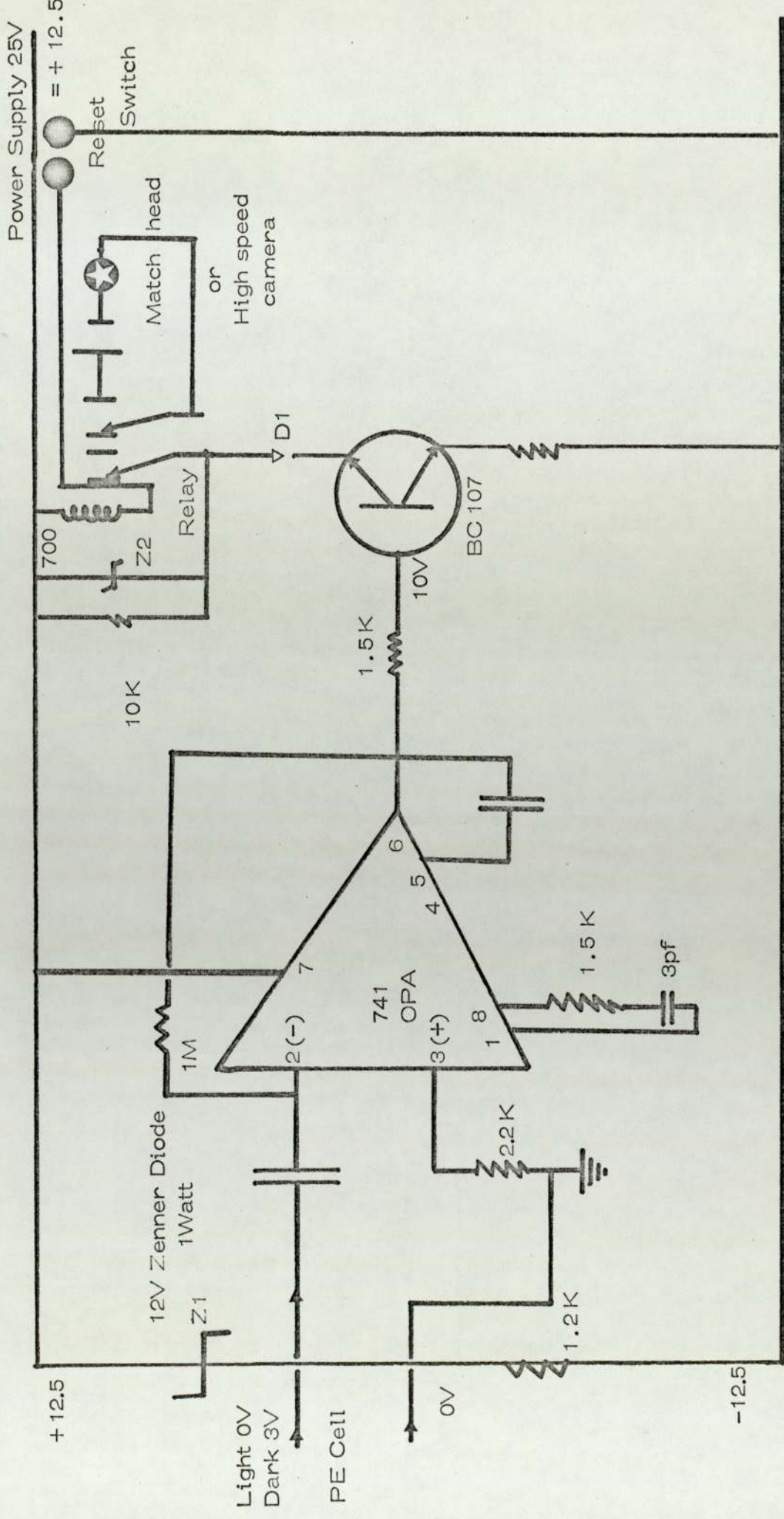
Circuit diagram of the triggering mechanism for the high spped camera and the match heads

Under these circumstances, stability of the vapour blanket has been disturbed. The collapse of the blanket initiates a minor interaction which produces a small vapour bubble which grows and collapes. This collapse initiates more substantial interaction which rapidly expanding hemi-spherical interaction region, and resulting in complete disintegration of the drop.

Cine-films of the explosive interaction of the tin drops show that when the molten drops entered the water one after another as several drops, fragmentation of a single drop was followed by fragmentation of the other drops. In one particular case, there were two drops involved, the late coming one fragmented, and set off the other one. There is little doubt that the first event initiated the other. Since no explosion between molten aluminium and the water was observed in laboratory scale experiments, it was. decided to force the stable vapour blanket to collapse around these molten aluminium drops by mechanical disturbance. Board[51] reports that the dynamic effects of the pressure increases from 100 torr to atmospheric pressure could initiate the explosion of molten tin. The resulting explosion was very violent. He also carried out experiments using aluminium and a similar, though less vigorous explosions were obtained. Small amounts of aluminium do not spontaneously explode in water. In the view of Board et al[51] the freezing point is well above the temperature for the onset of

transition boiling. These observations are in accordance with those which were stated in this work.

In an attempt to simulate premature vapour blanket collapse, an apparatus (figure 9) was constructed consisting of a piston at one end of which an explosive cap is detonated, pushing the piston sides against a solid support and sending a pressure wave down the piston and into the water at the same instant as a molten aluminium drop enters the water. The third application of the 3V pulse was used to detonate this explosive cap. The same circuit was used, but this time relay was used to switch on the power source to supply the necessary potential for the cap. However, no explosion has occurred.

There were several different attempts to obtain spherical reproducibility. A flame gun was used to obtain small aluminium spheres. This instrument is normally used in industry for coating of metal surfaces by other metals. The idea was that since the coating of metal surfaces was smooth and regular, the spheroids should be reproducible in sizes and may be in shape. The flame gun consists of a burner and a motor which feeds the aluminium rod into the flame. The motor is driven by compressed air. The speed at which the metal rod enters the flame was such that when the aluminium melts, pressure from another air inlet drags the molten particles away from the flame and deposits them on a metal

Figure 9
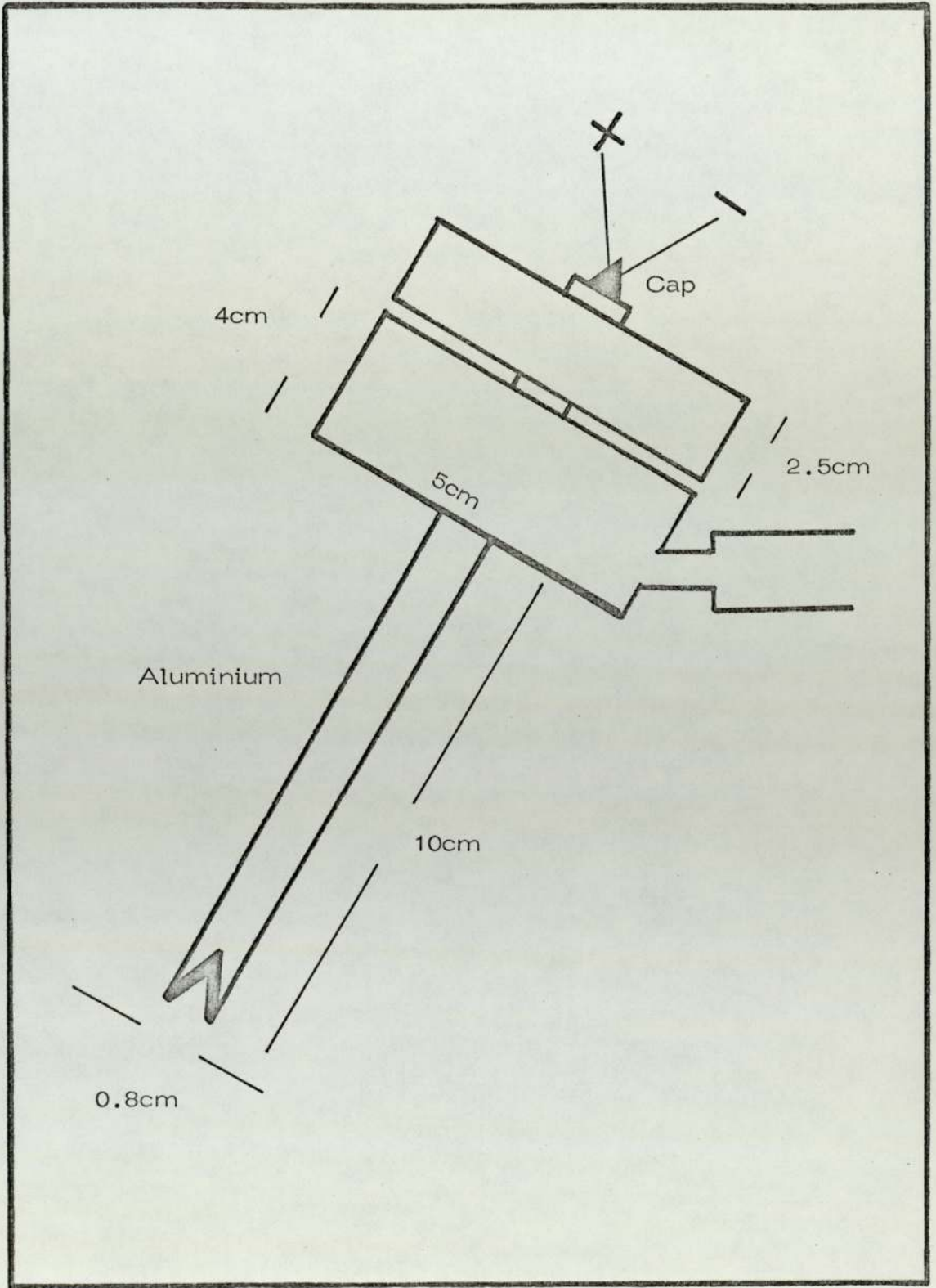
Detonator and Hammer mechanism

surface for coating purposes. By using the same system, molten

aluminium spheres were allowed to fall into water and their

behaviour was observed. Under these circumstances, no interactions

between the molten aluminium and water occurred. It should be

noted, however, that very small spherical aluminium particles were

obtained.

It was found that the best method of obtaining spherical drops

of molten metals was to use the tubes which are shown in figure 4 .

The application of nitrogen pressure was found to be unnecessary

since the pressure of the molten metal in the tube was sufficient

enough to push the metal though the nozzle where the molten metal

drops are formed. As the level of the molten metal increases in

the tube, the number of drops falling into the water increases

proportionally. The overall experimental arrangement is shown

in figure 2b.

4.2 High speed photography

In the common motion picture camera the film drive includes an

escapement mechanism that provides an intermittent movement. By

this means the film is held at rest during exposure in the shutter open

period and sharp images can be recorded. However, the mechanical

arrangements severely limit the possible framing rate. There are

three basic systems for cameras which overcome this limitation and

allow pictures to be taken at very high framing rates.

1   Moving optical system cameras whereby the image formed by

the main lens is held stationary with respect to the moving

film. Shuttering is operated mechanically. By using a

camera which uses this system, it is possible to obtain

framing rates between 18-15000 frames per second. The

Fastax camera is an example of the moving optical system

type. In the early stages, high speed film recording was done

by Fastax cameras.

2   Multi flash-light systems whereby motion is stopped by the

short duration of repeated illumination flashes.

3   A combination of a moving optical system and a stationary loop

of film inside a drum.

Moving optical system cameras use rotating lenses, mirrors

or prisms which are located between the main lens and the film.

The work of Edgerton et al[52,53] using the stroboscopic light

system in the 1930's was a major influence on modern high speed

photography. This included the improvement of short duration flashing

lights and their use for stroboscopic recording by photographs. In

this system the motion was stopped by the short duration of the

illuminating flash. The camera was shutterless and the light

flashing rate determined the number of exposures per second. This

system has several advantages, including simplicity. It has an

inherent possibility of a high framing rate without image distortion

problems of the moving optics arrangement.

The third system, the use of moving optics and a stationary film loop inside a drum has proved to provide the highest framing rates. Using this system, Ellis[54] made a significant development in high speed filming. He used a Kerr cell as a shutter and used continuous high intensity illumination. The Kerr cell consists of a liquid which is polarised for light transmission when placed in a suitable electric field. When combined with polaroid plates, the cell becomes a shutter to transmitted light if an alternating current is applied across the electrodes. Thus, the Kerr cell converts by a pulsing mode, a steady light source into a stroscopic light. The camera of Ellis consisted of a stationary 2.29m long strip of film forming a closed circular loop along the inside wall of the drum. At the center of the circle a mirror was mounted so as to rotate at high speed about the axis of the drum. The mirror surface was set at 45° to the rotation axis. Images of events illuminated by the Kerr cell light system were transmitted by the axially mounted lens system to the mirror and reflected onto the film. With this unit framing rates of 10^6 pictures per second at exposure times of under 10^{-7} seconds were achieved in 1955[55].

The explosions between molten metals and water were initially filmed by a Fastax camera. Standard 30m rolls of 16mm film are pulled past the shutter and lens arrangement. The limitations of

this type of arrangement are the ability to move the film at such high translatory velocity (and acceleration) without tearing and to obtain a sufficiently fast mechanical shutter arrangement. The quality of the image obtained is reduced because of the unavoidable small displacements of the film normal to the plane of the image as a result of vibrations.

With the very short exposure times provided with such high speed cameras, difficulty may be encountered in obtaining enough light (with non-luminous events) to expose adequately even the fastest films. Since molten metal water interactions are non-luminous events, it is necessary to provide enough lighting for the right exposure. The lighting techniques may seem simple to apply but in practice, considerable difficulties were encountered. There are basically two kinds of lighting techniques for high speed photography.

Front lighting can be applied for illuminating molten metal water interactions. However, back lighting was found to be more convenient once initial difficulties were resolved. It was found necessary to place a diffusing screen between the object and the light source. The illuminating power of 2.5kW to 7.5kW was found to be adequate for filming at very high framing rates up to 10000 frames per second. In the later stages, high speed photography was also carried out using another camera similar to the one mentioned above.

This camera, called 'Hyspeed' had half height framing arrangements. The normal frame of a 16mm film consisted of two half frames. Consequently, the framing rate is doubled. The speed of the 'Hyspeed' camera was between 20 and 20000 frames per second. It had inter-changeable and readily detachable optical units. The speed of the camera was controlled by a solid state electronic frame rate controller to plus or minus 1% in all speed ranges.

Experimental procedure and experimental results

The transient behaviour of molten metal-water interactions is a

limiting factor in obtaining suitable experimental results.

Consequently, theoretical approaches do not yield any comprehensive

solution to the problem. The general difficulty arises from the

absence of a criterion to evaluate the degree of interaction. The

problem was partly resolved when a method for producing metal

drops of known size and shape was found. This reproducibility of

metal drops of fixed geometry made it possible to quantitatise the

study for statistical analysis.

A variety of metals were used in the experiments and included lead

aluminium, tin, thallium, indium, gallium and bismuth. Except

for aluminium, all the other metals mentioned explode under certain

conditions. At first, molten aluminium drops were obtained when

a heated crucible was slowly emptied by hand into a small perspex

tank filled with water. The temperature of the molten metal was

varied from $700^{\circ}C$ to $850^{\circ}C$. At any fixed temperature, several

runs were made. The amount of aluminium used in these

experiments was varied from 5 to 40 grams. The results show

that after the quenching of molten aluminium, solidified masses

were almost spherical and that there were tiny holes on the surface

of each solid metal drop. The manually dropped molten aluminium

does not explode in the same way as molten tin. When molten tin

explodes the resulting debris is finely divided and is a spongy mass.

This kind of debris can not be obtained from aluminium-water

explosions under the stated conditions. However, it was found that

partial disintegration of the drops of molten aluminium does occur.

These types of fragments are not finely divided nor are they a

spongy mass. In fact, they are only parts of the solidified crust

which is loosely held on to the surface of the partially disintegrated

drop (figure 10). Upon entering the water, the aluminium drop

forms a mushroom-like shape. The nose of the drop spreads

horizontally forming a hemi-spherical front. The tail of the drop

meeting no resistance continues its downward course at approximately

the same velocity as that upon entry, thus penetrating the horizontally

flattened nose section. Before disappearing into the bulk of the

molten metal, the tail of the drop forms the stem of the mushroom.

The same behaviour occurs in the case of molten tin drops entering the

water (figure 11).

With molten aluminium, not a single violent explosion was

recorded when it was manually poured into water. The reproducible

aluminium drops from the graphite tube were 9mm in diameter.

There was no explosion when these spherical aluminium drops

fall into water either. The main observation was the violent

boiling around these molten drops causing them to shift to other

parts of the container floor from the point where they originally
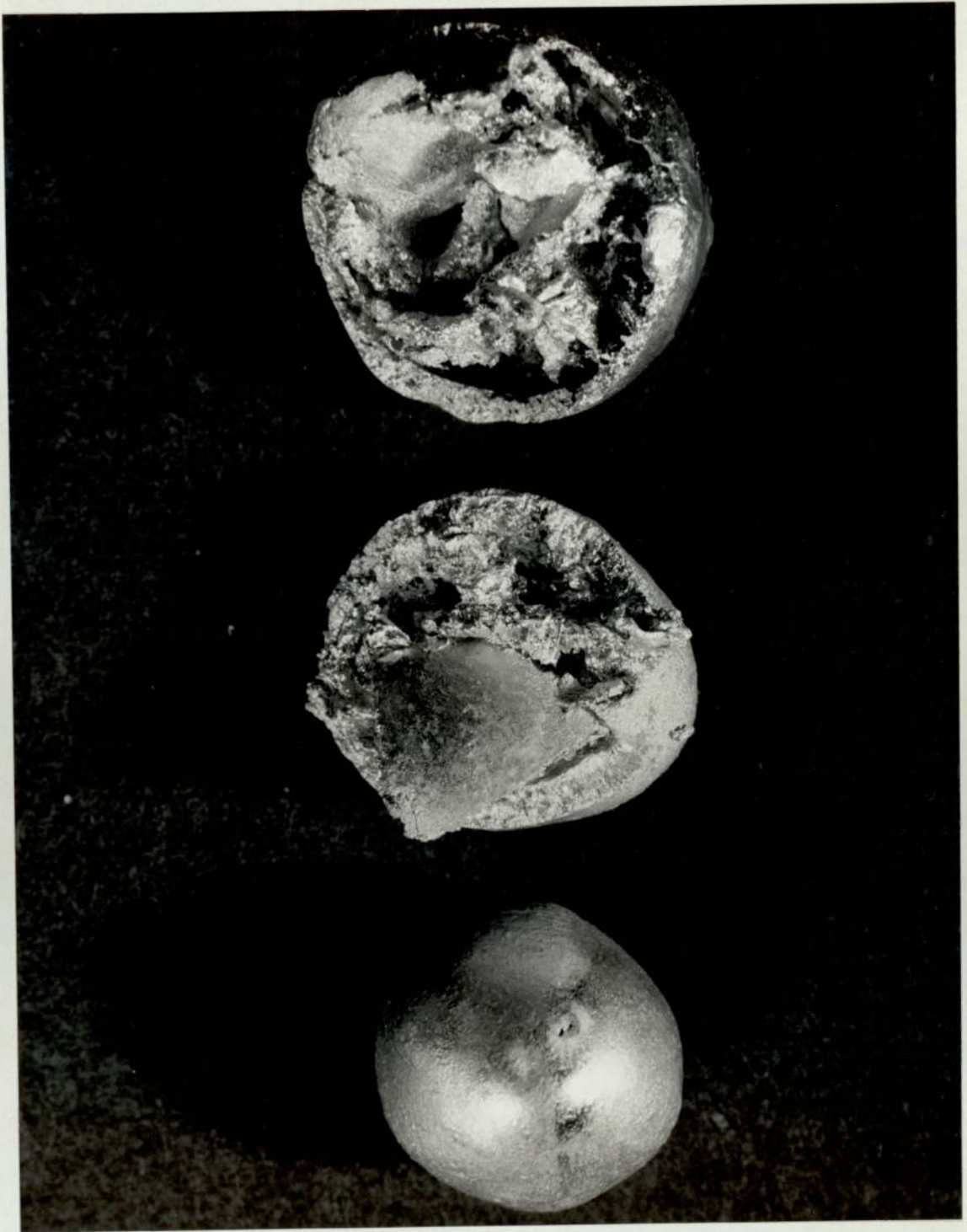
FIGURE 10.   Aluminium Drops after Quenching in Water

      a) Partially Disintigrated Aluminium Drop
      b)   "   "   "   "   "
      c) Floating Aluminium Drop (Completely spherical)

       ← 0.7 cm →
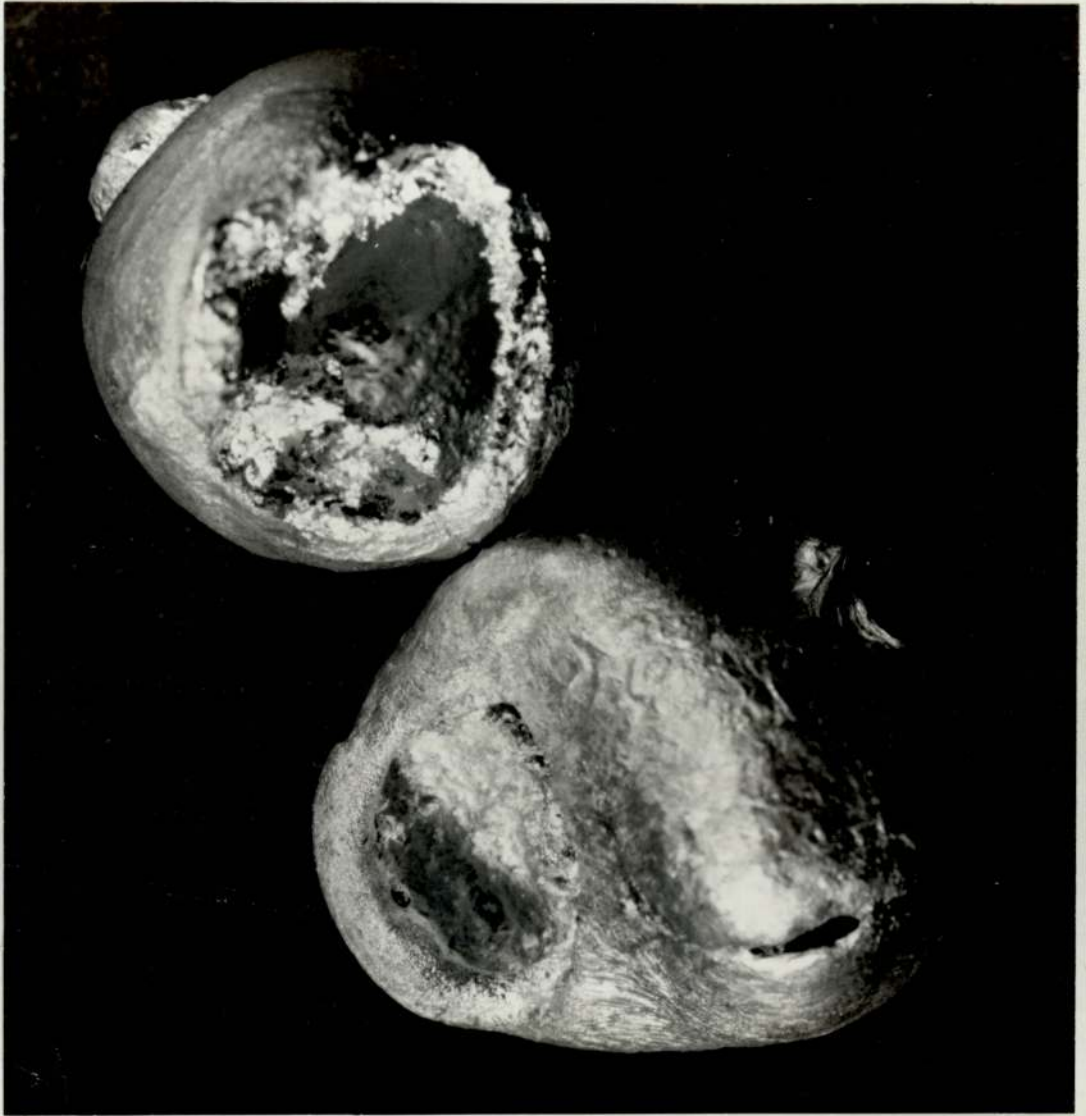
FIGURE 10. Aluminium drops after quenching.

d) Drops bursting outwards

0.75 cm

12ms

20ms
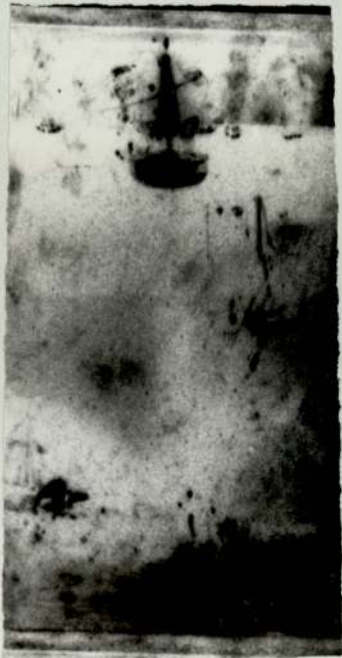
24ms
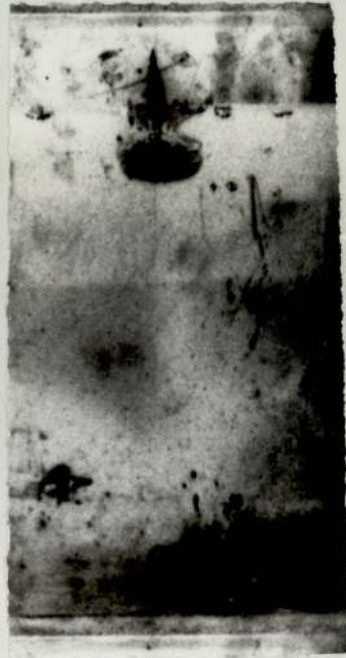
29ms

FIGURE 11.   High-speed photographs of the aluminium drops at 700°C
developing a mushroom-like shape upon entering the
water at room temperature.

41ms

48ms

63ms

80ms

FIGURE 11.

landed. It is generally accepted that when the molten aluminium drop

enters the water a vapour blanket establishes around it. The result

demonstrates that this vapour blanket can clearly be seen around

these molten aluminium drops. This blanket remains stable until

the drop cools down to a temperature at which such a blanket can

no longer be sustained. When this point is reached the vapour

blanket collapses with considerable violence causing the whole

mass to shift. Cine-films of this phenomenon show the collapse

and the resulting effects very clearly. It was observed from these

films that until the collapse the system is hydrodynamically stable.

However, when this stability is upset by the collapse, a new boiling

regime is established in which some part of the drop's surface is in

direct contact with the water. The collapse of the stable vapour

blanket does not lead to its total disappearance but what remains is

an irregular unstable vapour film which continuously break up and

is reformed. It must be noted that the drop begins to shift its

position at the bottom of the tank when the stable vapour blanket

collapses. As the temperature of the drop decreases, the vapour

film disappears and the whole body is in contact with the water.

Cine-films reveal information about the growth and the collapse of

the vapour bubbles forming the unstable film around the drop. The

time taken for these bubbles to collapse was taken from these films

and they are between 1 and 5 milli seconds.

The manually obtained molten aluminium drops have a characteristic appearance. During their quenching in water, large solid bubbles resulted. Some of these bubbles were completely spherical. On opening these hollow spheres, water was found inside them. No observations by high speed filming have been made which show how the water was entrapped. Some of the aluminium bubbles that had burst outwards ejected a stream of vapour that had either condensed or had been absorbed by the quench liquid (water in this case) before reaching the surface of the quench liquid. Some aluminium bubbles collapsed instead of bursting outwards. It was also observed that the drops of molten aluminium upon entering the water, developed a mushroom-like shape as described earlier, changing to a spherical geometry later in the fall. These were the hollow spherical drops which contained water inside them. Some drops rose to the surface of the water after travelling almost half-way down the tank, and some even rose from the bottom of the container. It was observed that from a small hole vapour had ejected and it seems that this ejection gave the upward thrust to the drop. The distance travelled by these drops was about 8cm. Upon opening the floating spherical drops, no water was found inside them. Some of the drops that had travelled upwards to the surface of the water had suddenly burst open violently and audibly. One particular cine-film shows the upward motion of a molten aluminium

drop during the quenching. The drop developed a mushroom-like

shape upon entering the water and when reaching the bottom of the

tank, it was almost a sphere, but the expansion continued until a

complete sphere was formed. The spherical drop then travelled

up the tank to the surface where it floated (figure 10). It had a very

thin wall and was found to be completely hollow. The floating drops

were observed many times during the quenching of molten

aluminium in water.

These observations are in accordance with those made by Flory

et al [5] and Brauer[4]. The existance of water inside those

spherical drops, and that some had burst outwards indicates that a

small quantity of the quenching liquid (water) was trapped inside

these drops. The trapped liquid is rapidly vapourised producing

a large internal pressure causing the weakest point of the metal

shell to give way. The fragments of these partially exploded

drops or those drops which had burst outwards with some fragmen-

tation can be put together to form the original bubbles. This

observation was consistent with all those aluminium bubbles that

had burst outwards. It seems likely that these drops had burst

open after solidification, a considerable pressure must have built

up for fragmentation to occur. All of these observations were made

with drops of molten aluminium obtained from a heated crucible

emptied by hand. Some of the aluminium drops obtained from a

tube with a nozzle, fell into a tank from a height of 10cm. The
initial temperature of these drops was $885^{\circ}C$. Hollow spheres 2cm
in diameter, were formed similar to those obtained in experiments
where the molten metal was poured from acrucible. On opening
these spheres it was occasionally found that some fragmentation
had occurred on the inner surface. This indicates that the water
is trapped inside the drops and because of the large heat content,
the water vapourises causing the pressure inside the drop to rise
sharply. If the pressure is high enough the bubbles burst outwards
with some fragmentation occurring.

There are grounds for believing that the entrapment theory
could explain these experimental results to a certain extent.
However, the theory cannot propose any mechanism explaining
how the quench liquid (water) is entrapped in the molten metal
drops. Cine-films of the molten aluminium drops provided some
evidence on which a mechanism of the entrapment of water can be
proposed. The entrapment of water could occur when the drop of
molten metal forms the mushroom-like shape upon entry. It is a
well known fact that when a liquid is introduced into another liquid
of similar density, 'vortex rings' formation occurs. These vortex
rings' while they are growing entrap some of the liquid around them.
The essential requirement for the production of a vortex ring is that
linear momentum should be imparted to the fluid with axial symmetry.

After entry the injected liquid develops a mushroom-like shape and later the edges of the hemi-spherical front zone rolls up of a vortex ring. Each ring winds up and as it does so it generates alternate layers of liquid which is around it. After entry, the molten aluminium drops could form such vortex rings while developing the mushroom-like shape. By doing so, some of the quenching liquid becomes entrapped. This first stage may be called 'entrapment'. Entrapment causes intimate mixing of molten metal and water. The next stage is for the interface area to increase to a point where rapid heat transfer can take place. Consequently, the instantaneous vapourisation of the water causes the fragmentation of the molten metal drop.

The experimental results obtained from the molten aluminium water interactions are insufficient for a quantitative analysis of explosive metal water interactions under the conditions previously described. For this, a suitable metal was necessary as experiments showed that the probability of a violent interaction between aluminium and water was very small.

A metal with a low melting point was chosen so as to allow for a wide range of liquid metal temperatures. It also had to disintegrate extensively in the presence of a quenching media. This media was water for most of the time. Tin and lead were both found to be very suitable. Consequently, experiments similar to those carried out with aluminium were performed using these metals. With molten

tin, violent exposions occurred resulting in extensive fragmentation. The fragments were spongy and finely divided. Initially, molten tin drops were obtained by gradually pouring the molten metal from a heated crucible into water. Fragmentation of molten tin always occurred under these circumstances over a wide range of metal temperatures. The violence of the interaction was found to increase as larger quantities of molten tin were used. The force of the interaction was sometimes sufficient enough to break the water container (1 lt glass beaker). Cine-films of molten tin water interactions clearly show the very violent nature of the resulting explosions (figure 12). The sequences from these cine-films show that the interaction and the dispersion of molten tin is a very rapid phenomenon and it is in the order of 1 to 3 milli seconds (figure 12).

The results show that the explosive interactions between molten tin and water commonly involve the occurrence of several distinct interactions in the same mass of material and each interaction in one region of molten metal triggers the next region and eventually the whole molten tin fragments. It should be noted, however, that the local interaction which sets off the other regions within the molten material starts to interact after an elapsed time. That is, the interaction between molten tin and water proceeds when such a time has been elapsed. The results demonstrate that as the

Molten Tin Drop
is above the
surface of the
water

0 ms
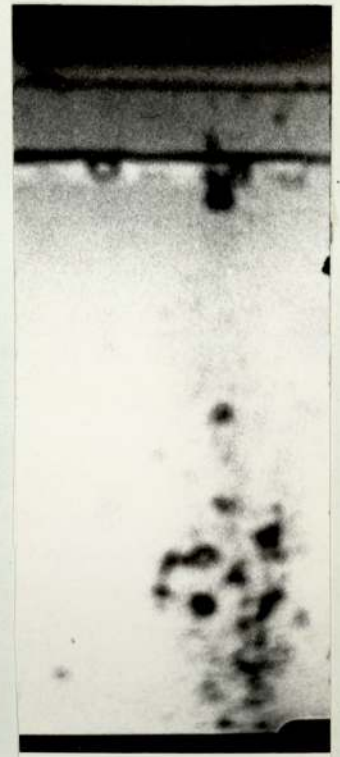
10.35 ms

12.33 ms

14.60 ms
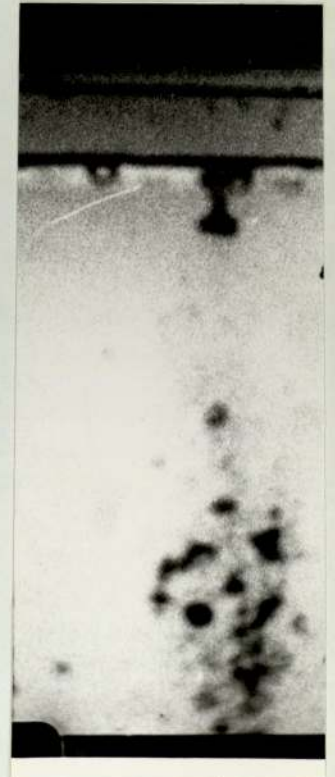
15.96 ms

FIGURE 12. High speed Photographs of the Explosion between
Molten Tin and Water.
Initial Molten Tin Temperature is 536°C and
Water 47°C. The distance between the water
surface and the furnace is 4 cm.
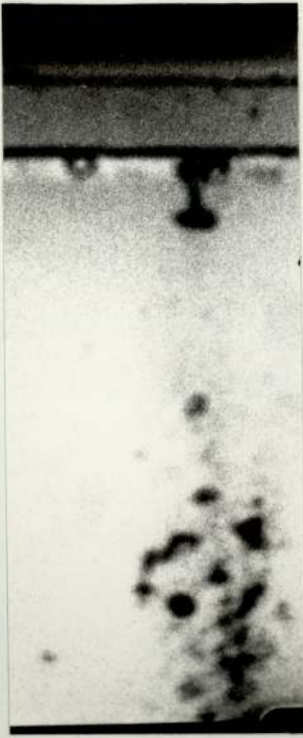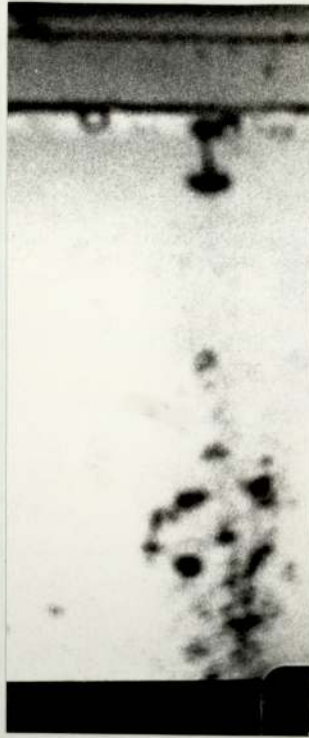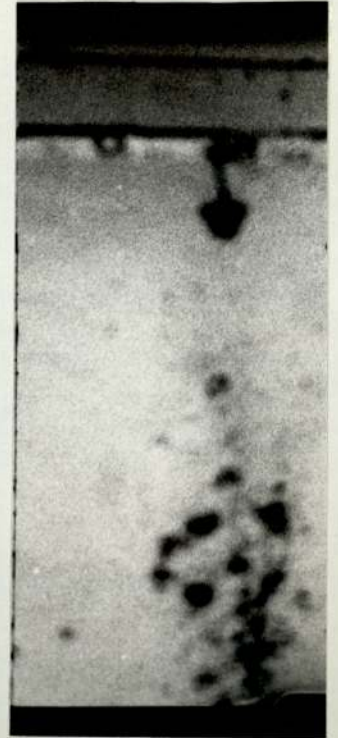
17.96 ms   18.03 ms   19.92 ms

20.25 ms   20.415 ms   20.745 ms

FIGURE 12.
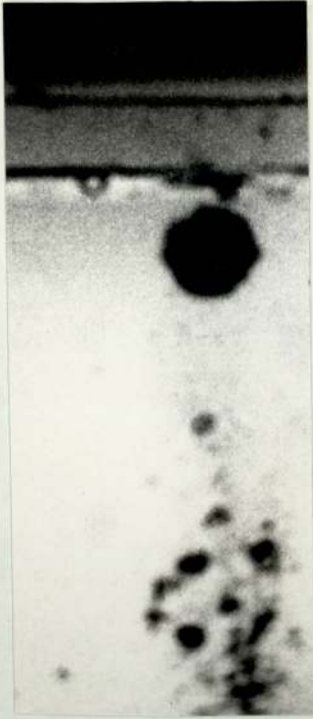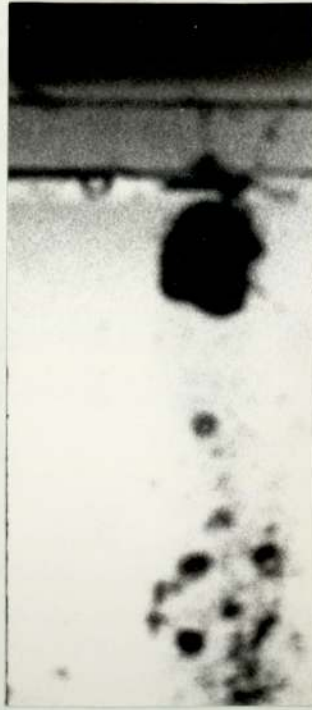
21.075 ms   21.9 ms   22.23 ms

22.89 ms   23.385 ms   24.21 ms

FIGURE 12.

25.2 ms

26.19 ms

30.48 ms

33.73 ms

FIGURE 12.

coolant temperature increases, the explosive interaction can be

delayed. Similarly, as the initial metal temperature increases this

elapsed time increases proportionally. Cine-films of molten tin

and water show that after the elapsed time the interaction starts and

proceeds as a series of cycles. A small interaction within lumps of

molten tin escalate in this manner in several growth and collapse

cycles into a violent explosion. During the interaction phase,

contact surface area between molten tin and water increases.

Witte et al[7] have shown that in the case of molten metal-water

explosions heat transfer rates are three orders of magnitude

greater than those occurring during boiling processes are required.

This result implies that the contact area increases by a factor of

10^3. Many films of molten tin and water explosions were taken at

different initial conditions. The findings demonstrated that every

individual interaction occurs exactly in the same manner as the

previous one, hence tin was chosen for further investigation and

detail analysis of the observed interactions was pursued. In the

early films, molten tin was poured manually when the required

metal temperature monitored by a thermo couple was reached.

When molten tin and the other metals were dropped into

liquid nitrogen, no explosive interaction occurred.

Molten tin was also dropped into boiling water. There was no

explosion under these conditions. This experimental evidence

suggests that the explosive interactions can be prevented by using

volatile liquids. Similarly, no explosions were observed when

acetone, alcohol and carbon tetra chloride were used as coolants.

These facts show that the volatability of the coolant is an important

parameter in determining an explosive interaction.

Since molten tin and other metals explode at lower water

temperatures and do not at higher temperatures, a cut-off point

must exist above which no explosive interaction would occur. The

results show that such a temperature for water exists. This

threshold temperature was found to be different for the various

metals used. Values are listed in table 2.

5.1 Measurement of percentage disintegration

Having developed a method of obtaining reproducible molten metal

drops, the next step was to observe closely the fragmentation of

these drops in water. Tin and lead drops were the subject of such

a study. Their history after entering the water is determined by

the temperatures of the two media and also by the purity and

surface tension of the water. When the metal drops disintegrate,

they form fine spherical globules (radius less than $100\,\mu$) which

may sinter into extended open structures.

The degree of disintegration may be assessed subjectively by

collecting the debris from a number of drops and separating it into

parts which have disintegrated and those which have not. Such an

Table 2

Threshold temperatures for different metals

Metal	Critical Threshold Temp of Water (^{o}C)
Aluminium	–
Tin	65
Thallium	40
Indium	60
Bismuth	70

assessment is less dubious than appears at first sight, since it seems

that disintegration is a statistical phenomenon with drops either

disintegrating completely or not at all. However, this may be

rationalised by postulating that an event may occur with a probability

per unit time and unit area depending on the temperature.

Drops which have disintegrated either produce a finely divided

debris or the fragmented parts are loosely attached to the remains

of metal drop. The degree of fragmentation is defined as the ratio

of the weight of the drops which have exploded to the total weight of

metal used. This ratio may be called 'percentage disintegration'

and is mathematically expressed as,

$$PD = \frac{M_E}{M_T} \times 100 \qquad\qquad (5-1-1)$$

where PD is the percentage disintegration, M_E is the weight of the

disintegrated drops and M_T is the total weight of the drops.

Three variables which to a very large extent control the degree

of disintegration are the metal and water temperatures and the

latter's surface tension. There are other factors causing

disintegration, but the three stated above seem to exert the most

influence. A study was therefore made to get some indication of

the relationship between these three variables and percentage

disintegration.

In the experiments carried out, the number of molten metal drops falling into the water was kept constant. Values of percentage disintegration have been calculated for different coolant temperatures at a constant metal temperature. Similar results have also been obtained for different metal temperatures and a fixed water temperature. The results have been treated in two different ways. Each drop was considered individually, separating the exploded fragments from those which had not. The second method was to count the number of molten metal drops falling into the water and noting the ones which had exploded. This method does not take into consideration disintegration where the fragmented parts are loosely attached to the remains of the metal drop. It assumes that the disintegration of the drops is 100% if there is significant deformation and fragmentation (figures 13a and 14 show this difference). Consequently in some plots there is a difference in the percentage disintegration values at points where the degree of disintegration should be the same. The values obtained from the analysis of individual drops are expected to be smaller than those obtained by recording the number of drops exploded regardless of the nature of fragmentation.

It was mentioned earlier that there exists a threshold temperature for water above which no explosion takes place. Since these cut off temperatures, mark the beginning of non-explosive regions,

Figure 13a

Percentage Disintegration

Water Temperature 20°C

Initial Molten Tin Temperatures °C

Figure 14

Percentage disintegration

Water Temperature = 35°C

Initial Molten Tin Temperature
°C
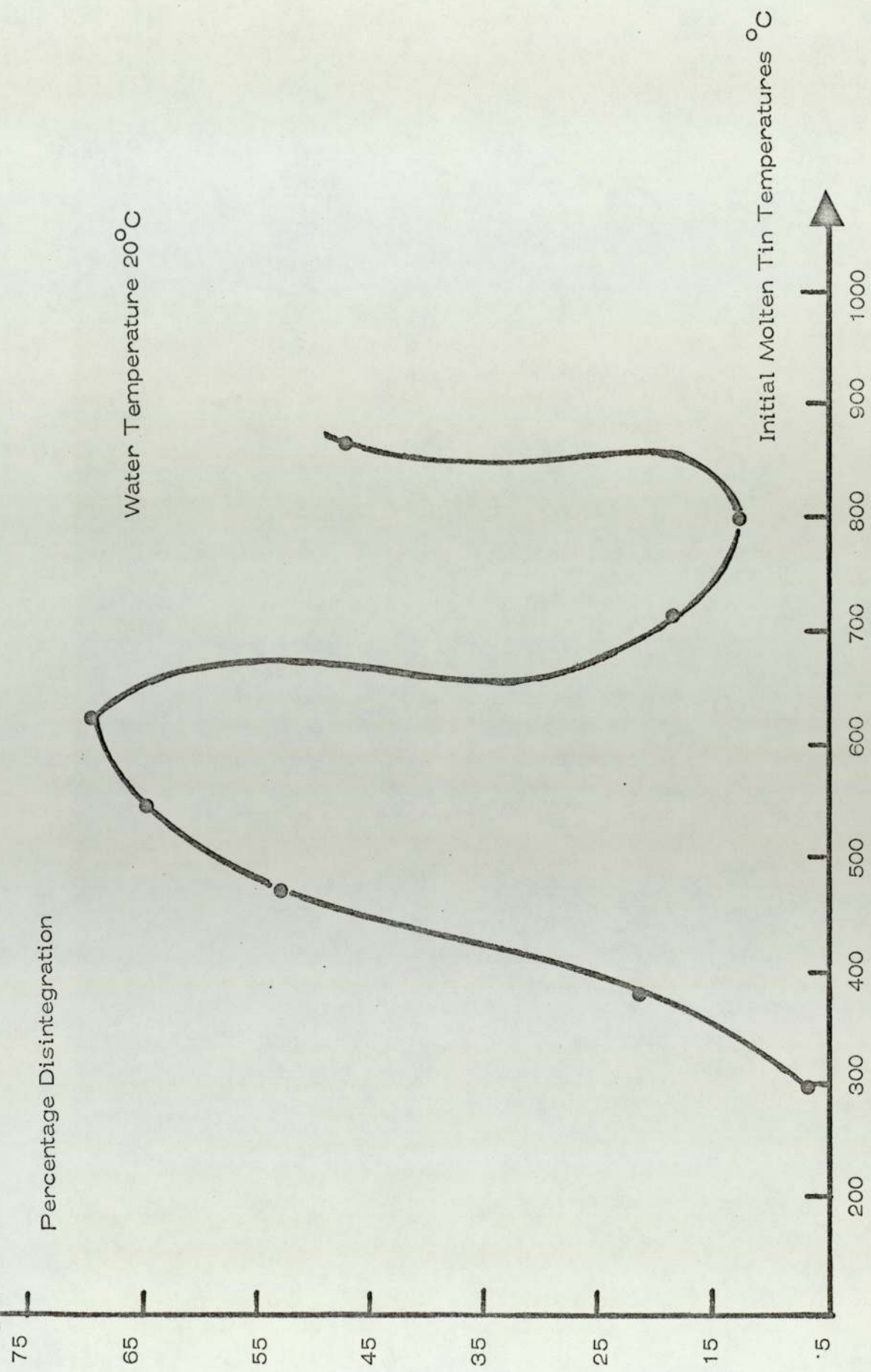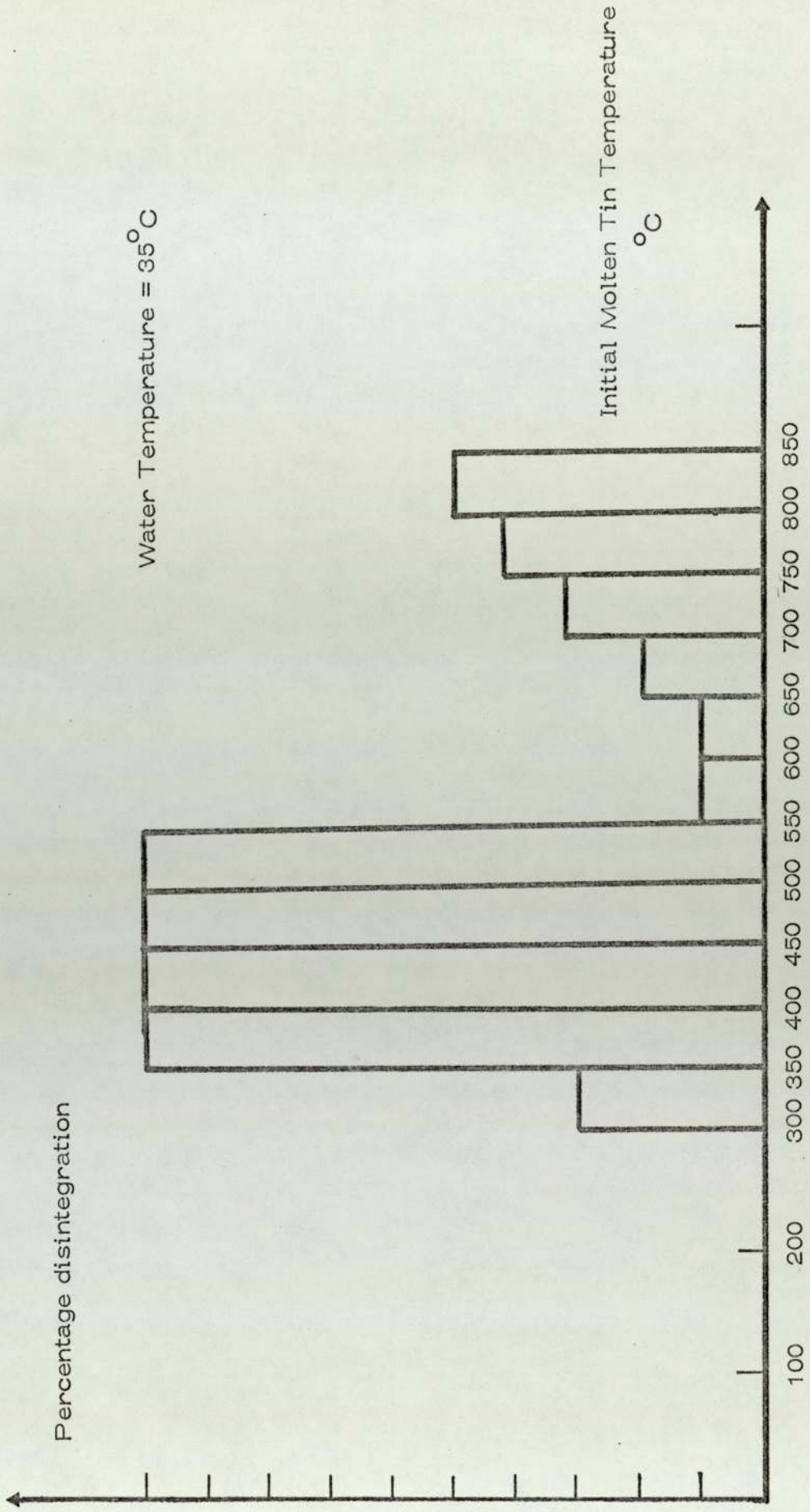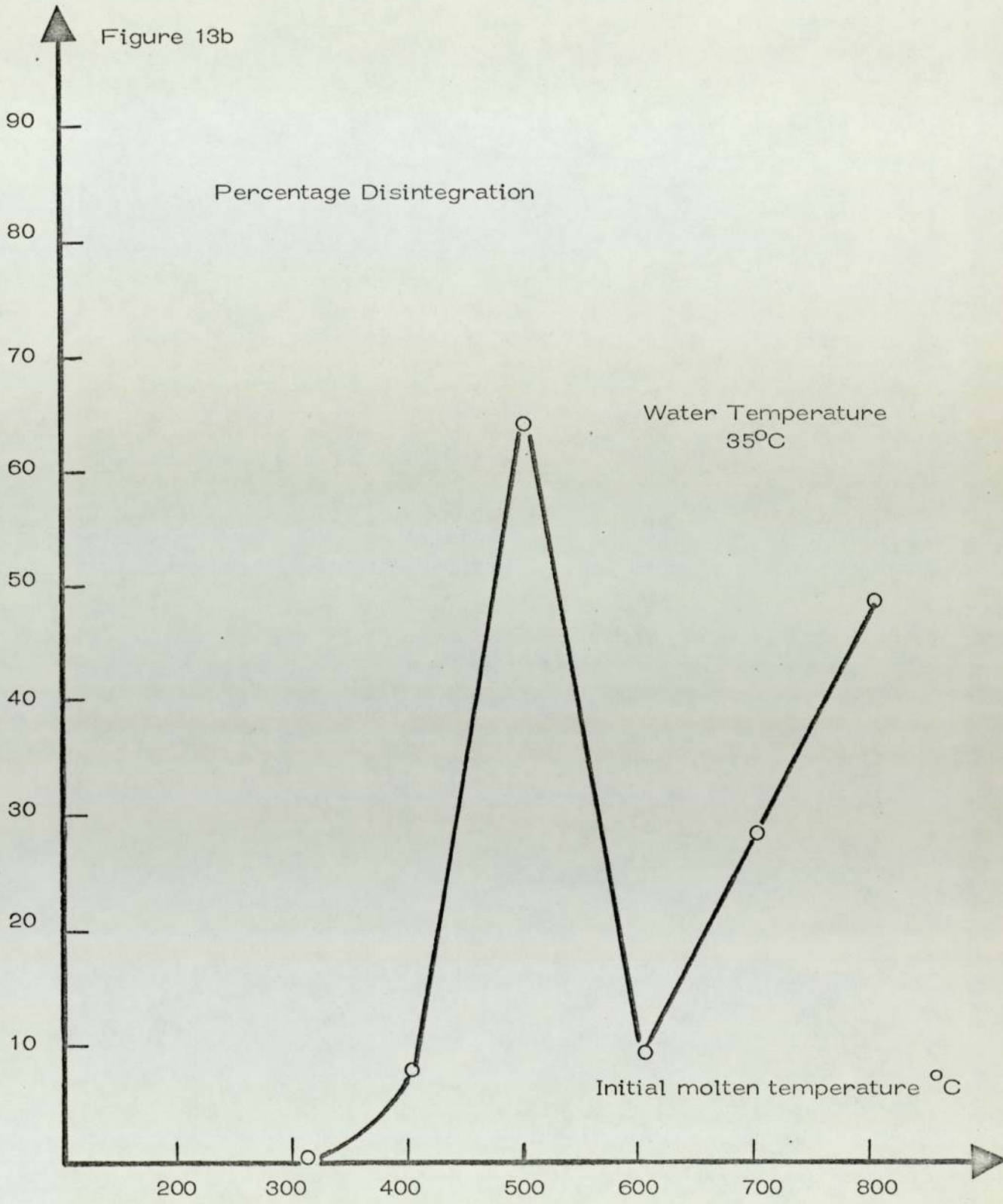
Figure 13b

Figure 13c

Percentage Disintegration

Water Temperature 50°C

Initial Molten Tin Temperature °C
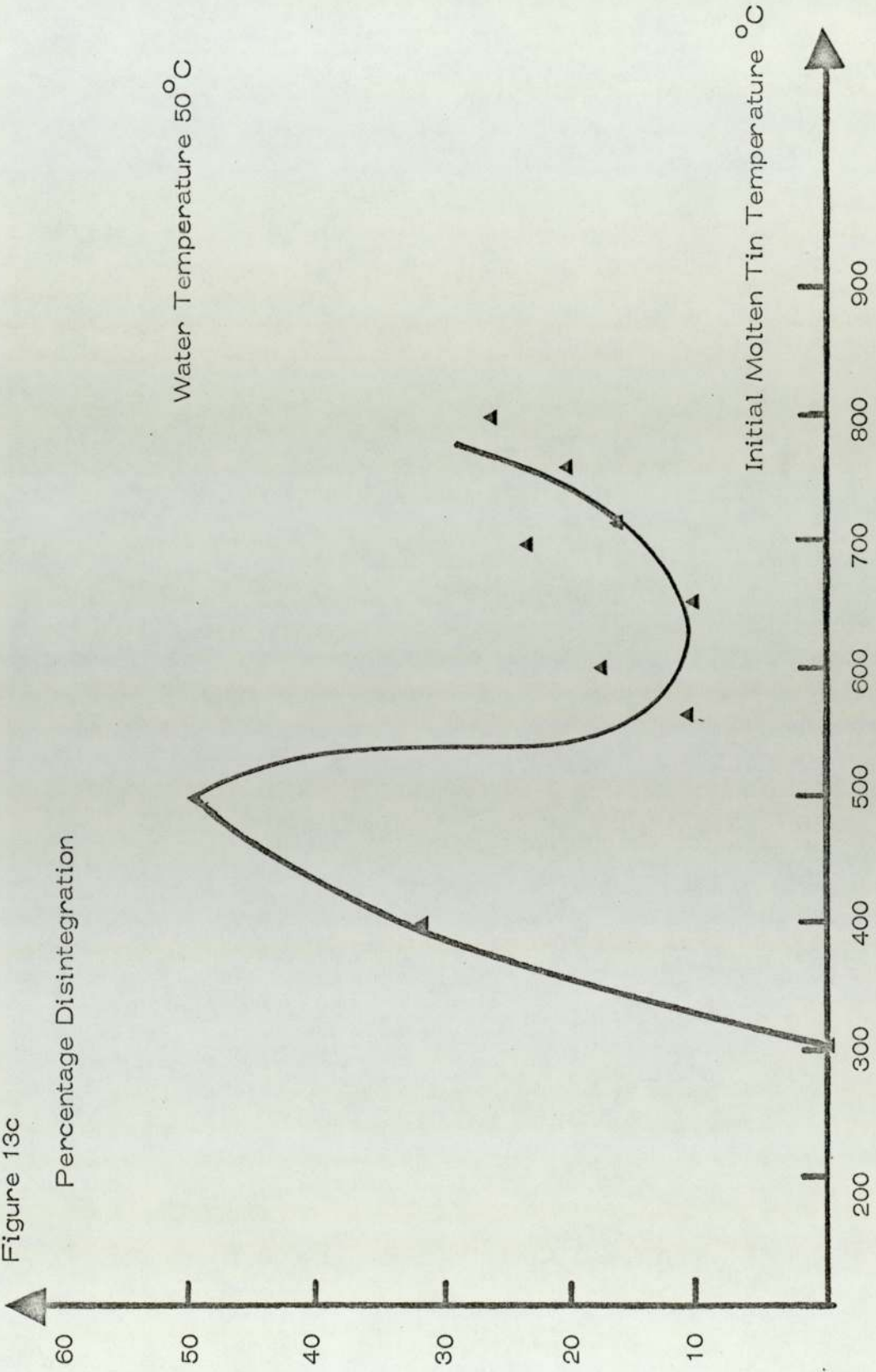
at these temperatures the percentage disintegration values are
zero. The results show that initially the percentage disintegration
is almost constant or decreasing slightly with an increase in coolant
temperatures. However, a further increase in the coolant
temperature causes the percentage disintegration to decrease
sharply, reaching zero at the cut off coolant temperature. The
curves of percentage disintegration (at fixed metal temperatures) as
a function of coolant temperatures are shown in figure 15. The most
important result is that the shift in threshold temperatures as the
initial metal temperatures change. If on the the other hand,
percentage disintegration is plotted against the initial metal
temperatures, a different relationship is obtained. The plots of
percentage disintegration increases with increasing initial metal
temperatures up to a certain value then decreasing suddenly with
further increases in metal temperature. However, it increases
again at higher metal temperatures, but never exceeds the values
obtained at lower metal temperatures. A typical example of this
relation is shown in figure 14. As the metal temperature was
increased from $310^{\circ}C$, explosions occurred, but at about $550^{\circ}C$
the percentage of drops exploding fell from a 100% to 10% as the
metal temperature increased to about $600^{\circ}C$. The degree of
disintegration then gradually increased again until the maximum
temperature of $850^{\circ}C$ was reached.

Figure 15

Percentage Disintegration

○ $T_{initial}$ 560°C
● $T_{initial}$ 650°C
▼ $T_{initial}$ 472°C

Percentage disintegration for fixed molten tin temperature

Coolant (water) Temperature
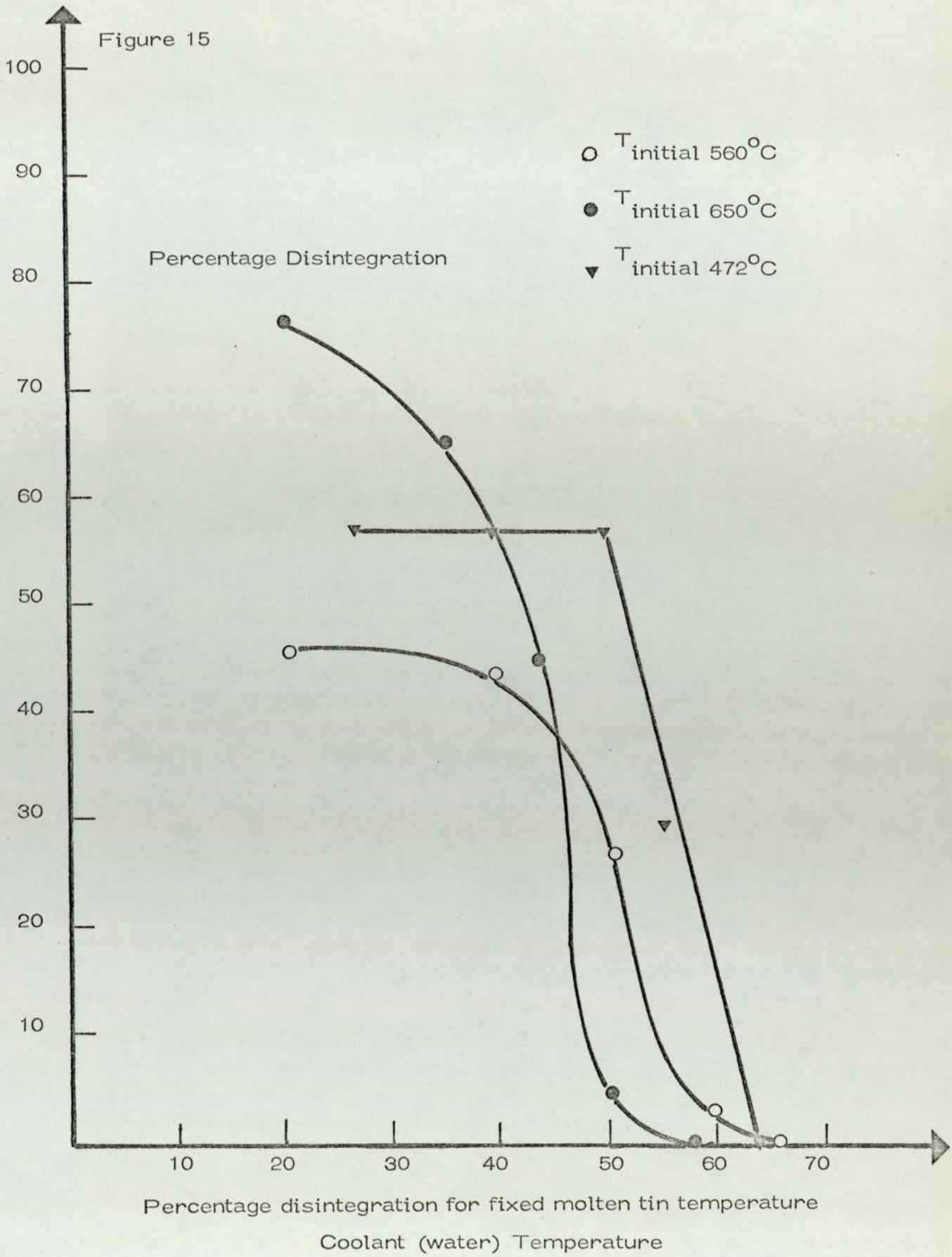
The plots of percentage disintegration for coolants which have

surface active properties show a different behaviour. Addition of

surface active materials changes the interfacial tension between

the molten metal and the coolant. Consequently, the percentage

disintegration and threshold temperature values are expected to

alter as well. Experimental results prove this to be the case. The

results show that molten tin drops at higher initial temperatures

yield higher percentage disintegration values in solution of

detergent and alkalis. As can be seen from figure 16 drops initially

at 850°C falling into aqueous solutions of teepol and sodium hydroxide

exploded violently. The concentration of the sodium hydroxide was

10% by weight. Teepol solution of two different concentrations,

one and two percent by weight, were used in these experiments.

The maximum percentage disintegration was nearly 75% in all

cases. However, this maximum value occurred at different

coolant temperatures. These are 25°C for 2% teepol, 30°C for 1%

and 40°C for sodium hydroxide solution. The percentage disintegration

values at 850°C for boiled distilled water reaches a maximum of 45%

and this maximum value occurred at 1°C of coolant temperature.

The percentage disintegration curves resulting from tin at an

initial temperature of 472°C falling into water are shown in figure 17.

In addition, the results also show that threshold temperatures are

altered by the addition of teepol and sodium hydroxide. Although,

Figure 16
Percentage Disintegration

Legend:
- ● 10% Sodium Hydroxide
- ○ 1% Teepol
- ▦ Distilled Water
- ☐ 2% Teepol

$T_{initial} = 850°C$ (Tin)

Coolant Temperature °C
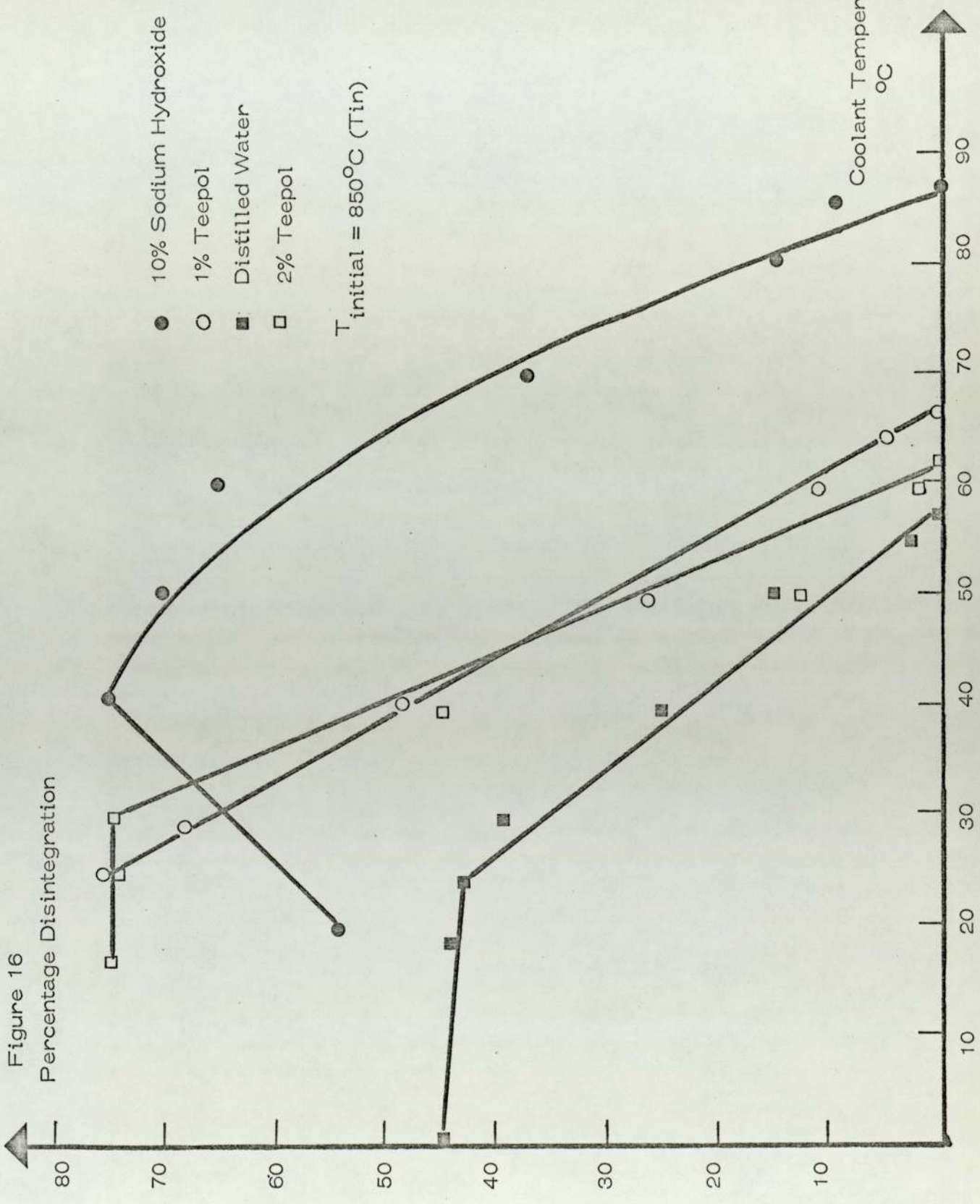
Figure 17

$T_{initial} = 472°C$ (Tin)

Percentage Disintegration

○	1% Teepol
□	2% Teepol
▼	Distilled Water
●	10% Sodium Hydroxide

Coolent Temperature °C
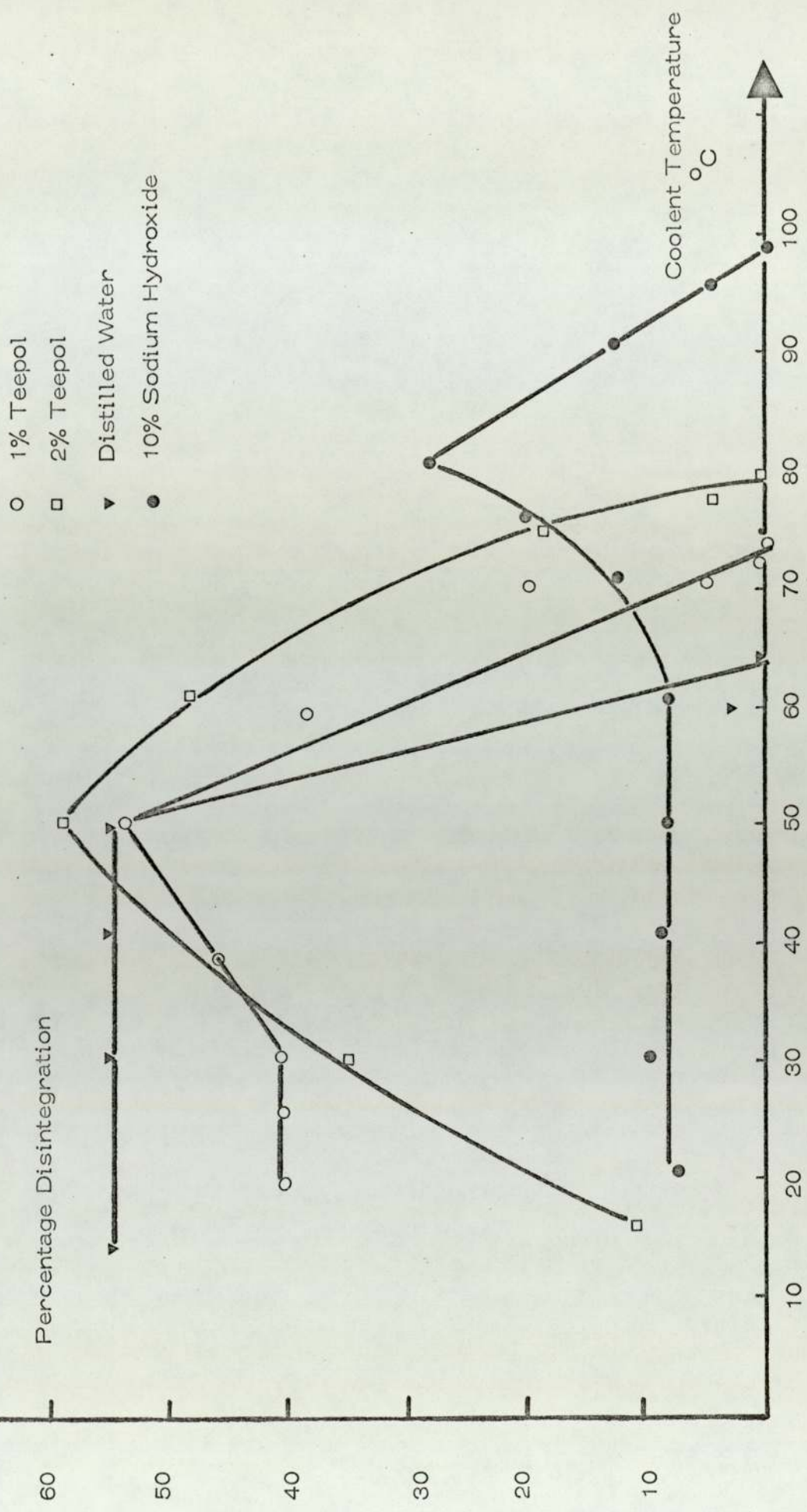
these two additives have opposite effects on the surface tension of the water, both raise the threshold temperatures. These results are only in partial agreement with those of Long[3] who found that sodium chloride solution (brine) raised the threshold temperature for aluminium water interactions, but that various soluble oils decreased it.

Experiments have been carried out by Paschkis[35] to obtain boiling curves from a 5cm diameter sphere immersed in a solution of sodium hydroxide. The addition of sodium hydroxide to water replaced film boiling by transition boiling at higher body temperatures. The boiling regime changed because sodium hydroxide was deposited on to the surface of the metal sphere as water evaporated at the interface. The surface on which boiling took place was therefore one of sodium hydroxide. The relatively poor thermal conductivity of sodium hydroxide meant that the surface on which boiling occurred was cooler than the body temperatures. It has been proposed by many workers that the onset of transition boiling can initiate the explosive interactions, there-fore, the premature onset of transition boiling around molten tin drops when they are quenched in sodium hydroxide solutions provide some evidence why the cut off temperature for the sodium hydroxide solution is the highest. The values of the cut off temperatures for these coolants are shown in figures 16 and 17.

Percentage disintegration values for lead, bismuth and tin have been calculated from experimental results obtained with these metals. The degree of disintegration of molten tin drops is higher than that of molten lead and bismuth. Figures 18 and 19 show the variation in the degree of disintegration with coolant temperatures for lead and bismuth. However, only water was used as a coolant for these experiments involving lead and bismuth. The results show that the cut off temperatures for lead and bismuth are lowered when high initial metal temperatures are used. This result is in accordance with the one obtained for tin. When the initial metal temperature is 850°C, the threshold temperature for bismuth is 55°C (figure 19) but this temperature is 83°C when the initial metal temperature is 472°C. Similar results were obtained for lead as well. As shown in figure 18 , the measure of the degree of disintegration has proved to be a useful method for comparing interactions occurring under different initial conditions.

5.2 Boiling around the falling tin drops

It has been shown earlier that for a specific metal, there exists a temperature for water above which no explosions occur. The existence of such a temperature has been reported by Board et al[23] and also by Brauer[4]. The results demonstrate that a violent interaction between the molten metal and water can be triggered automatically if the coolant temperature is below the threshold value.

Figure 18
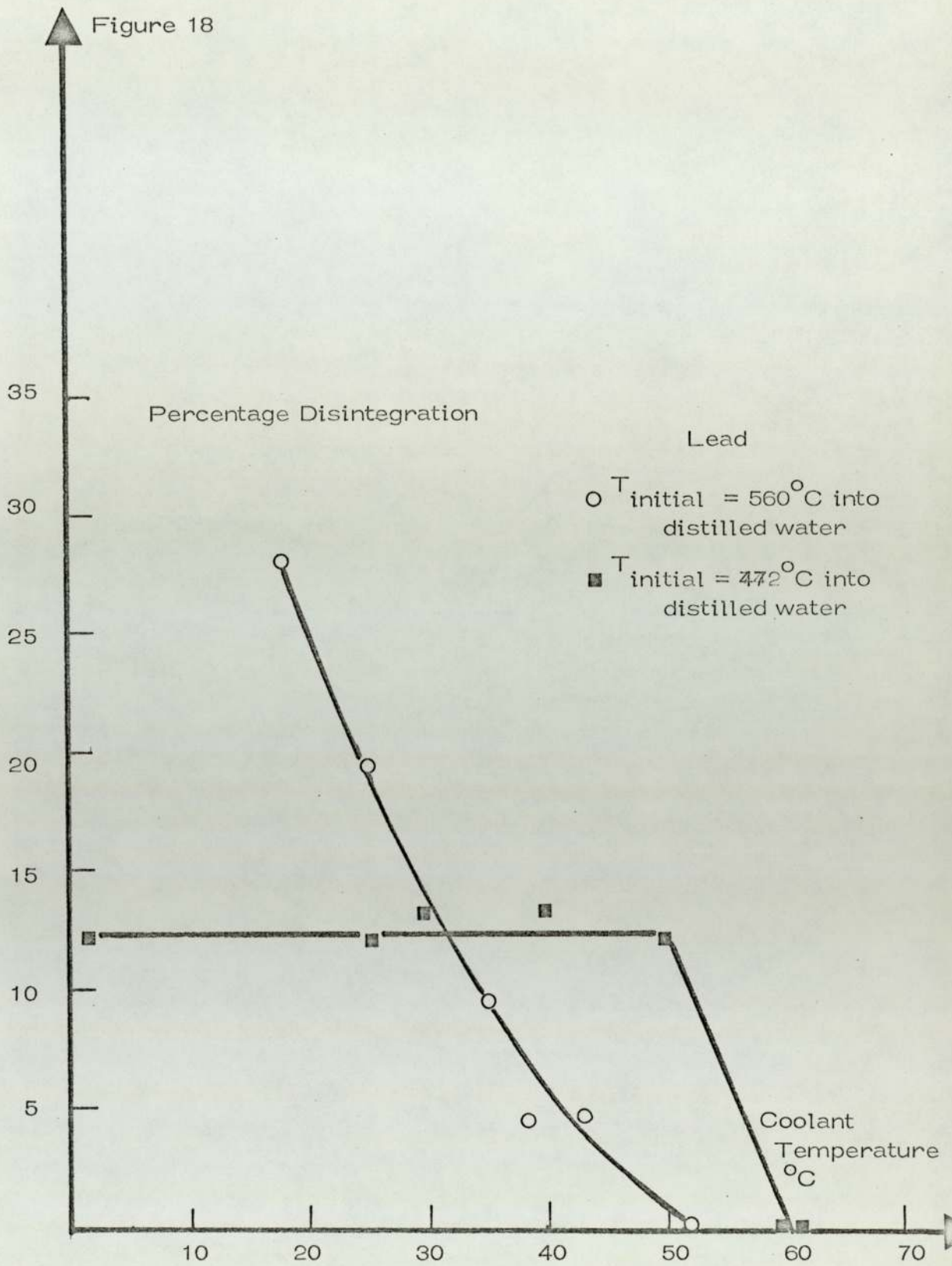
Percentage Disintegration

Lead

O $T_{initial}$ = 560°C into distilled water

■ $T_{initial}$ = 472°C into distilled water

Coolant Temperature °C

Figure 19

Percentage Disintegration

Bismuth

$T_{initial} = 950^{\circ}C$ into distilled water

$T_{initial} = 450^{\circ}C$ into distilled water

Coolant Temperature $^{\circ}C$
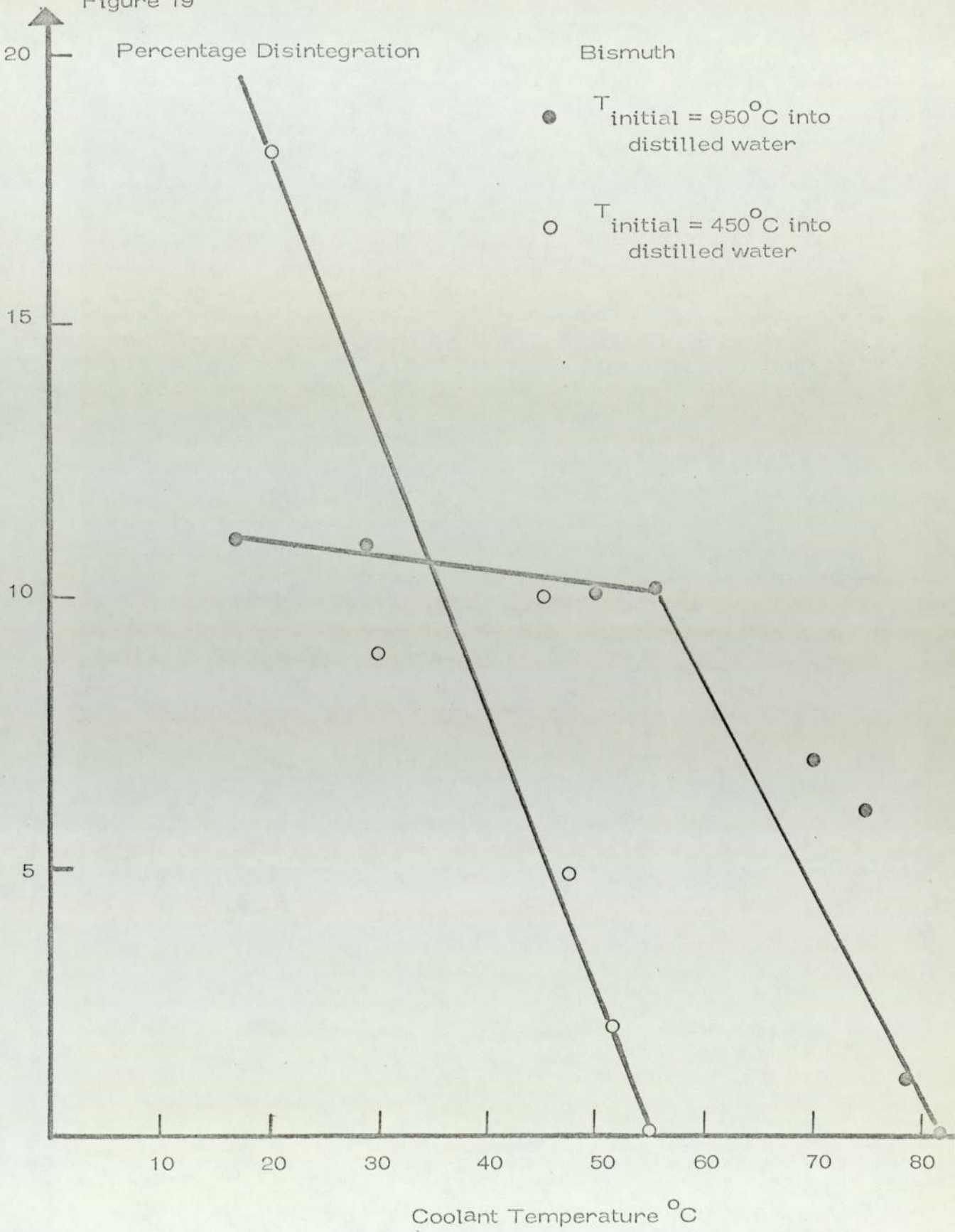
However, a mechanical disturbance, as Board et al[51] found can also trigger an interaction well above the threshold temperature.

The threshold temperatures can be explained in terms of the factors governing the conventional boiling curve. When a molten metal drop is introduced into water, it will undergo a quenching procedure. The quenching process can be illustrated in terms of the conventional boiling curve. At the beginning of the quenching process the heat transfer mechanism is film boiling. During film boiling, the molten metal is completely surrounded by a vapour film. As the temperature of the molten metal decreases, the vapour film becomes unstable and collapses upon the surface of the molten metal. However the molten metal is still well above the boiling point of the liquid and the film re-established. This transition regime continues until the nucleate boiling regime attained. The transition can be very violent hydrodynamically. Bradfield[56,57] observed explosive vapour formation when quenching a porous graphite cylinder in water. he nucleate boiling regime is somewhat turbulent due to the growth and collapse of bubbles adjacent to the surface of molten metal. In an earlier study, Stevens and Witte[58] investigated transient film and transition boiling from a 1.9cm diameter silver plated copper sphere for initial temperatures up to $246^{\circ}C$. They reported observing a pulsation boiling phenomenon, associated with transition boiling in which the liquid vapour interface oscillates with

a rhythmic expansion and contraction normal to the sphere's surface.

Bradfield[56] has reported a similar phenomenon for transient

boiling from a 6cm diameter chrome plated copper sphere. Bradfield

also observed that for a very smooth surface, the resulting hydro-

dynamics disturbance could be detected by loud bumping sounds.

These hydrodynamics disturbances are presumed to result from

flash evaporation of the liquid as it comes in contact with a large

surface area of the sphere. Walford[59] investigated transient

heat transfer from a 6.35mm diameter nickel sphere moving

through water. Using high speed photography, Walford studied the

rapidly changing modes of boiling during quenching. In slightly

subcooled water at $80^{o}C$ and $95^{o}C$, he observed an 'Expansion

Cavity' phenomenon where large spherical shell was produced around

the sphere. The sphere progressed through this cavity until it

contacted the liquid-vapour interface. At this point, a new cavity

of equal size was formed. Walford reports that this cycle was

repeated with a period of 5-10 milli seconds. Board et al[60]

experimentally investigated transiet film boiling from a metal foil,

6mm diameter and 0.01mm thick, which was heated under water by

pulsed ruby laser. They reported having observed an oscillating

vapour blanket boiling mode for foil temperatures below $450^{o}C$ over

a wide range of subcooling. The frequency of oscillation increased

linearly from 5 to 15kHz as the subcooling was varied from $25^{o}C$ to

75°C. For temperatures above 400°C, and moderate subcooling, Board describes a thin vapour blanket with rapidly moving irregularities on the interface. As the level of subcooling was decreased further, a 'stable thick blanket' was observed.

A small number of films were taken at 3000 frames per second in which explosions can be seen involving molten tin drops beneath the surface of the water. In these films, the cross-sectional area of the explosive region in the plane of the film is seen to expand and contract. The explosion takes about 1.5 milli seconds but in the preceding few milli seconds an oscillation of the area of period about 0.5 milli seconds was measured. It could be that this oscillation of the visible area surrounding the drop prior to the explosion plays a part in a possible triggering mechanism. The rhythmic nature of an actual explosion has a period a similar magnitude to that of the preliminary oscillations. These films are examined frame by frame (in fact there are two images per frame due to half framing arrangement of the high speed camera) and areas of activity surrounding the tin drops measured with a planimeter. The change in this area with time can then be plotted. An example of the graphs obtained is shown in figure 20 . It is possible that the area measured is the extent of a rhymically contracting and expanding vapour blanket which eventually contracts onto the molten metal at a point, and initiates a fragmentation process. Also it needs

Figure 20

Area of Explosive
Region, mm

● – drop (a) explodes shortly
after drop (b)

▲ – drop (b)

Initial tin temperature = 745°C

Water temperature = 47°C

Time ms

Area of explosive region versus time for molten tin explosion
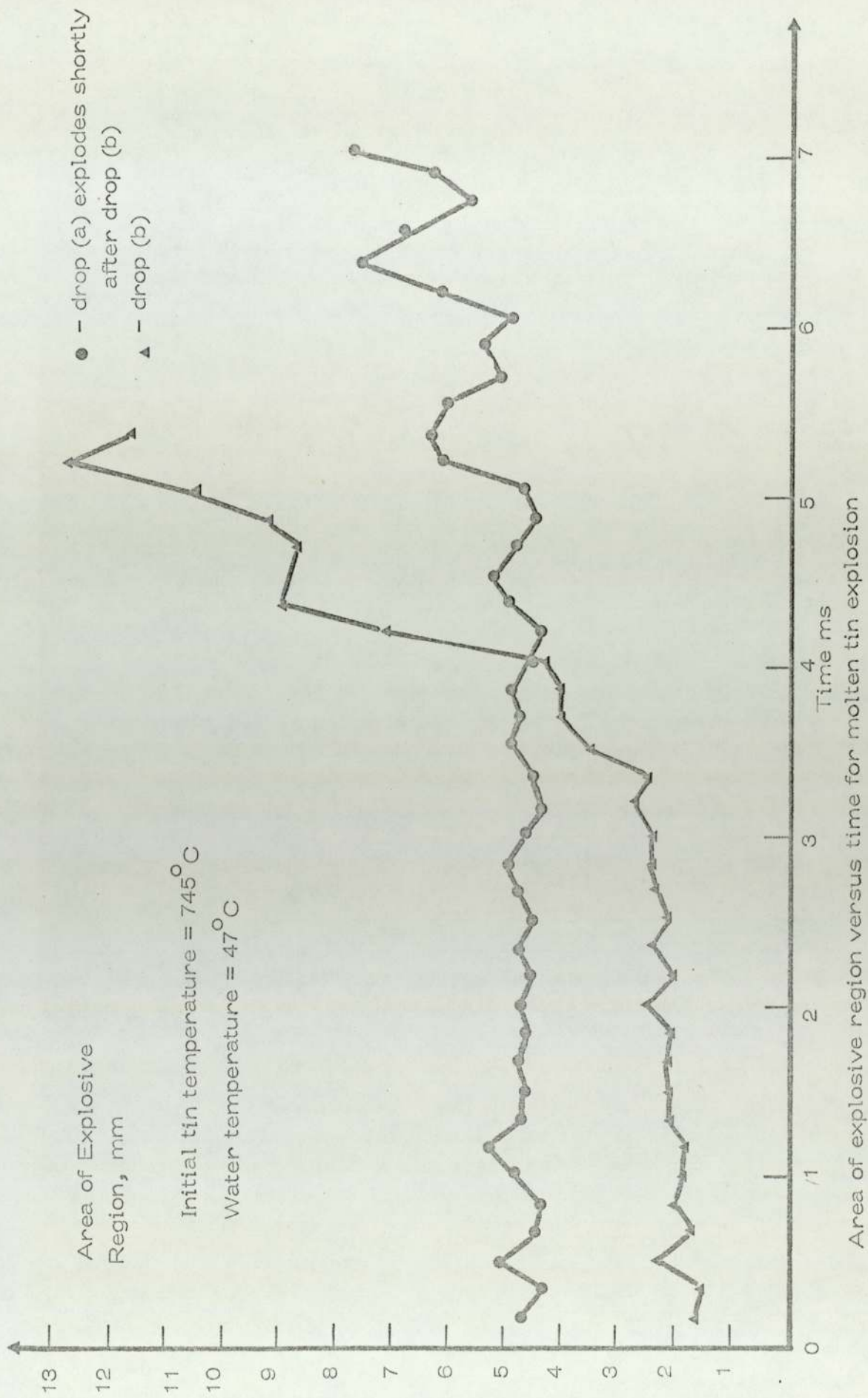
to be decided whether the pulsations if present are a boiling

phenomenon alone or are connected with the oscillations of the

liquid metal drop. From Lamb's[61] work on oscillating drops the

natural frequency of molten tin drops would be about 1 sec^{-1}. The

Reynold's number for these drops is about 2000, and consequently

wake eddies will form, however, the frequency of their formation

will be no higher than 20 sec^{-1}. Hence an oscillation of 2000 sec^{-1}

as seems to occur cannot be explained in hydrodynamic terms

alone, but must be considered a boiling phenomenon.

From the area of measurements it is possible to estimate the

change in thickness of the vapour film during a single contraction.

The values obtained were about 0.02cm which is of the same order as

the thin film thickness reported in quenching experiments by Stevens

and Witte[58]. The authors also found that a precipitous collapse of

this thin film took place in less than 0.25 milli seconds which is of

the same order as the time for the contractions obtained from high

speed films. Also the figure for the pulsation frequency 2000 sec^{-1}

compares Witte's statement that a form of pulsation boiling occurred

around a solid sphere quenched in water with a frequency in excess

of 2000 sec^{-1}.

These results indicate that the boiling around molten metal drops

just before their fragmentation is important. In addition, the exist-

ence of threshold temperatures, also indicates the importance of the

boiling around the molten metal drops.

5.3 Boiling heat transfer from a heated solid sphere

It is extremely difficult to obtain any quantitative measurement for liquid particles quenched in water. There is an additional difficulty in the case of molten metal, because of their interactions with water. Therefore, experiments were carried out to investigate transient and transition boiling, from a 2.54cm diameter stainless steel sphere for initial temperatures up to $950^{\circ}C$. The sphere, whose cross-section is shown in figure 21 was made from stainless steel. Chromel-alumel thermocouple was placed in the centre of this sphere and the thermocouple wires from the junction were encased in an Inconel sheath. The sphere was heated in a furnace kept under a Helium atmosphere in order to reduce surface oxidation.

When the desired temperature was reached, the sphere was then quenched in water. Other liquids were also used, and included the detergent solutions and the liquid nitrogen.

As would be expected, the type of stable vapour blanket that was generated around the sphere upon entering the water was dependent upon the initial sphere temperature and the level of sub-cooling of the quenching liquid. There was little heat loss from the sphere prior to its entry into the water and the temperature recorded by the thermocouple was assumed to be the average throughout the sphere. The output of the sphere thermocouple was used for two purposes in

Figure 21

Chromel–Alumel

Thermocouple

Inconel sheath

Thermocouple Junction

2.54cm
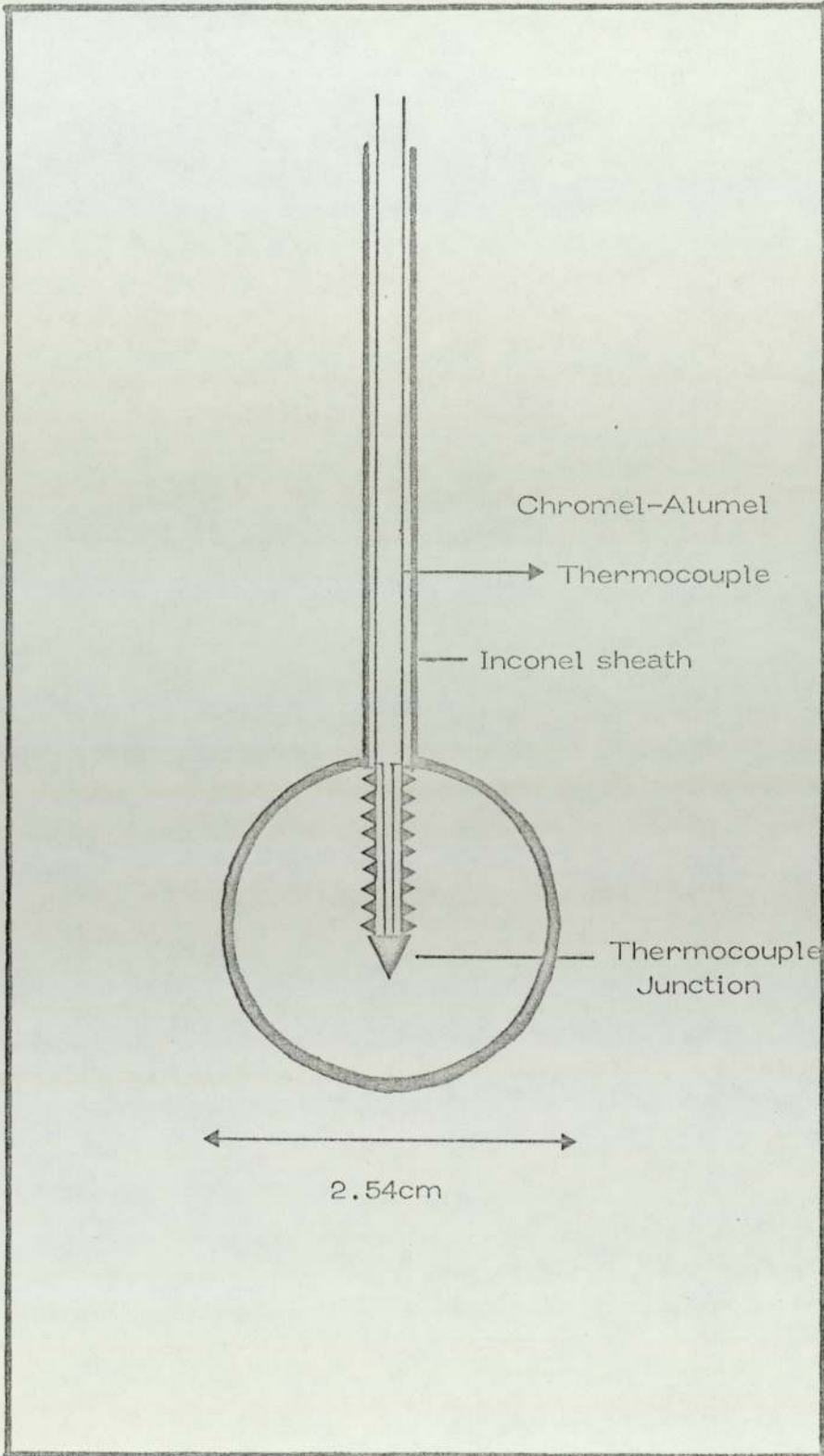
Cross-section of the solid sphere

order to get the cooling rates. The temperature of the sphere was

displayed on the 'Y' axis of an ordinary 'X-Y' plotter. Another lead

from the sphere thermocouple was used as an imput signal for a

device called 'differentiator'. This device was constructed by the

electronic workshop of the Department of Metallurgy of the University

of Aston in Birmingham and it is used to differentiate the temperature

values with respect to time in heating and cooling processes.

Consequently, it gives the instantaneous cooling or heating rates.

Two different types of this instrument were used and their output

calibration was $0.2\,C^{o}sec^{-1}$ per mv for the first one and $0.138\,C^{o}sec^{-1}$

per mv for the second one. The output from this instrument was

then displayed on the 'X' axis of the recorder. Details of the

experimetal arrangement is shown in figure 22.

Experiments were performed with distilled water as the quenching

medium. Temperature was varied from $30^{o}C$ to $85^{o}C$. The initial

sphere temperatures were held constant when different values of sub-

cooling were used. Instantaneous heat trasfer data was obtained

from the experimentally obtained temperature cooling rate traces.

The heat transfer rates have been calculated on the assumption

that the sphere cooled uniformly. Heat transfer rates can be

calculated by using a model based on the assumption that an isothermal

sphere exists at any instant in time.

$$Q = \rho \frac{V}{A} \; C_p \; \frac{dT}{dt} \qquad\qquad (5\text{-}2\text{-}1)$$

Figure 22

X-Y Plotter

Differentiator

Connector

Thermocouple leads

Solid sphere

Water Tank
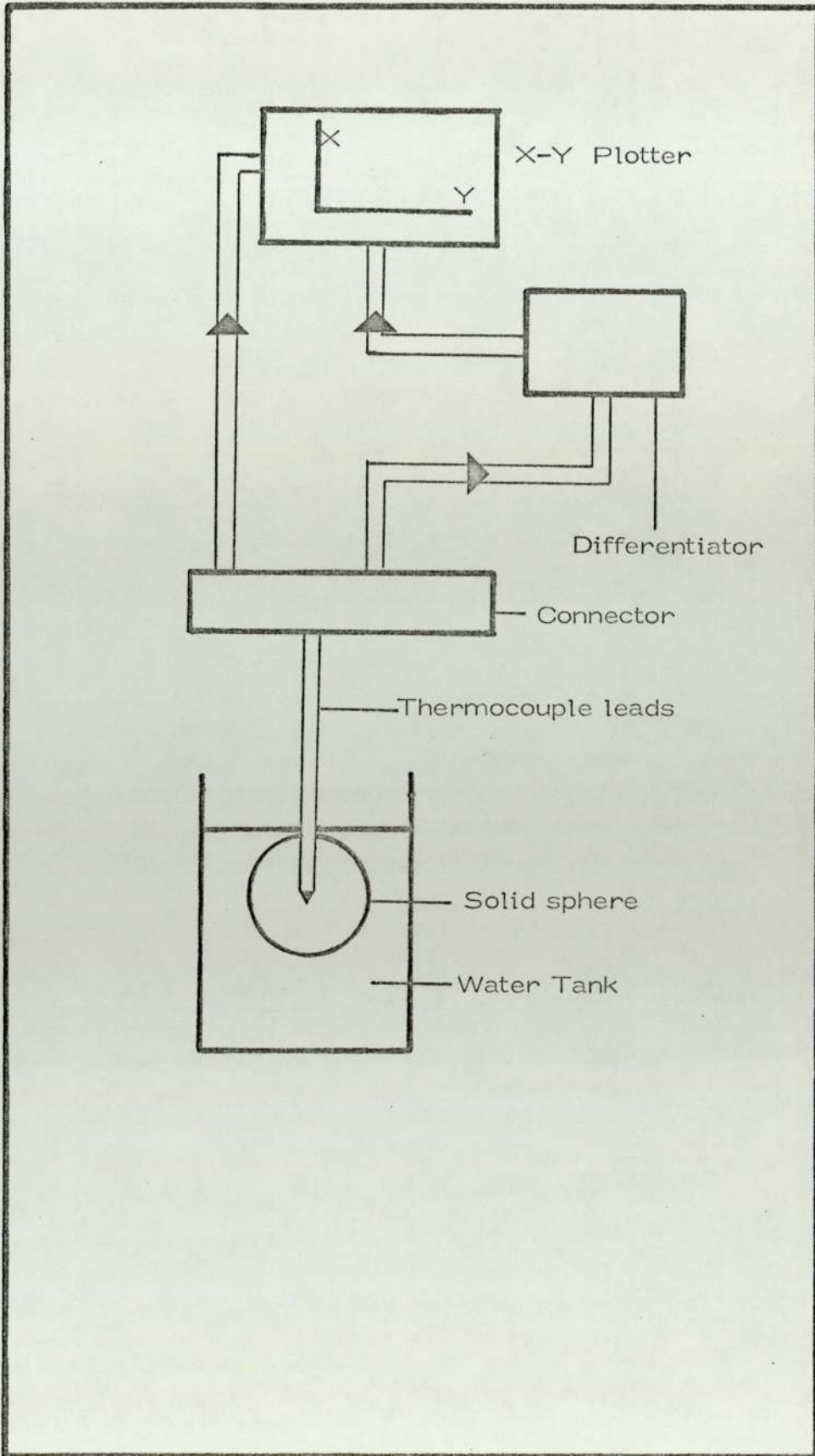
Experimental arrangement for quenching
experiments

Where ρ (grcm^{-3}) is the metal density, $\frac{dT}{dt}$ is the cooling rate at

any instant in time (C^{o}sec^{-1}), V(cm^3) and A(cm^2) are the volume

and surface area of the sphere respectively. The advantage of

using a device like a differentiator is that it eliminates the need to

calculate accurately the slopes of the temperature-time curves. The

existence of temperature gradients within the sphere introduces some

error in the heat transfer rates. This is, however, within the limits

oflthe experimental error.

The instantaneous heat transfer (cooling rates) results for

quenching at different values of subcooling are presented in figures

23, 24 and 25. As the level of subcooling was decreased the cooling

rates decreased likewise. At the same time the curve shifted to

the right to lower values of super heat. Both the maximum and the

minimum of the cooling rates are lowered as the level of subcooling

is decreased. The temperatures of the sphere corresponding to the

end of the stable film boiling regimes are lowered as the temperature

of the coolant is increased (figure 26). This results from the fact

that vapour formation is enhanced at higher water temperatures. A

smaller fraction of the energy leaving the sphere is required to

bring the water up to its saturation temperature at the liquid vapour

interface. The instantaneous cooling rates resulting from the

quenching of a 2.54cm stainless steel sphere in water is higher than

in the detergent solutions. Teepol solutions and cetyl pyridinium

Figure 23
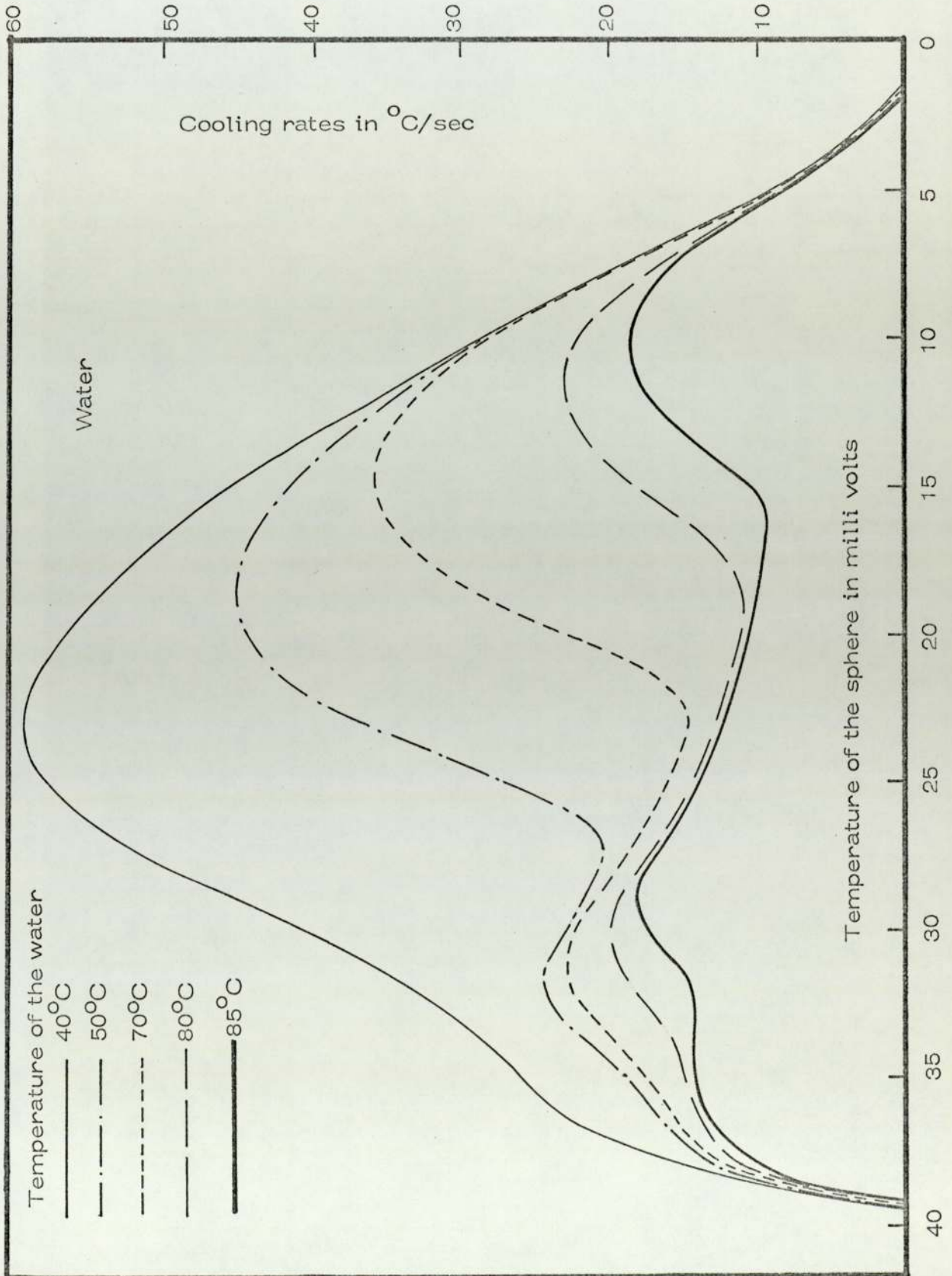
Instantaneous cooling rates of the solid sphere in water at different
levels of subcooling

Figure 24

Teepol solution 1% by weight

Cooling rates in °C/sec

Temperature of the sphere in milli volts

30°C
40°C
50°C
60°C
70°C
80°C
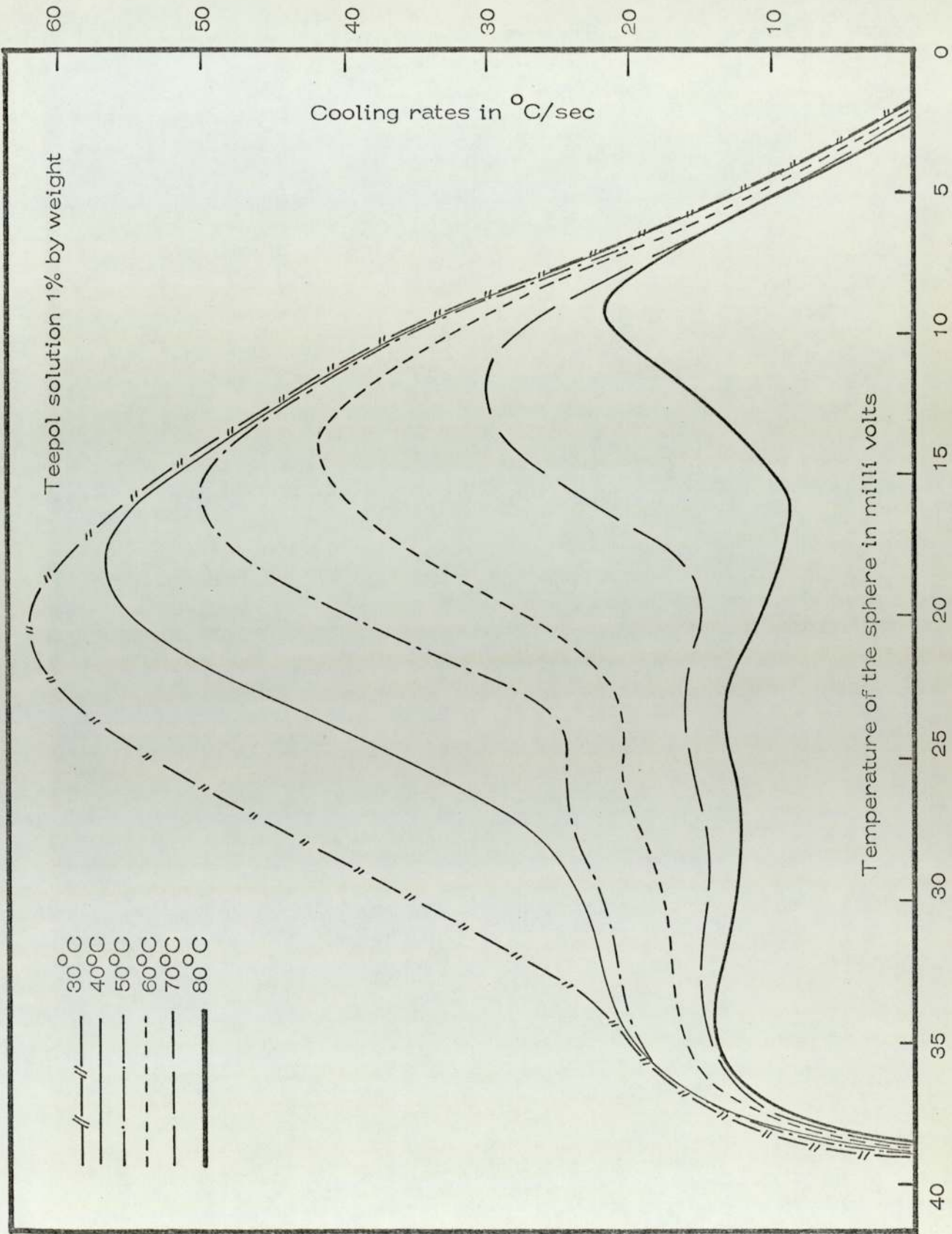
Instantaneous cooling rates of the sphere in teepol solution
1% by weight

Figure 25
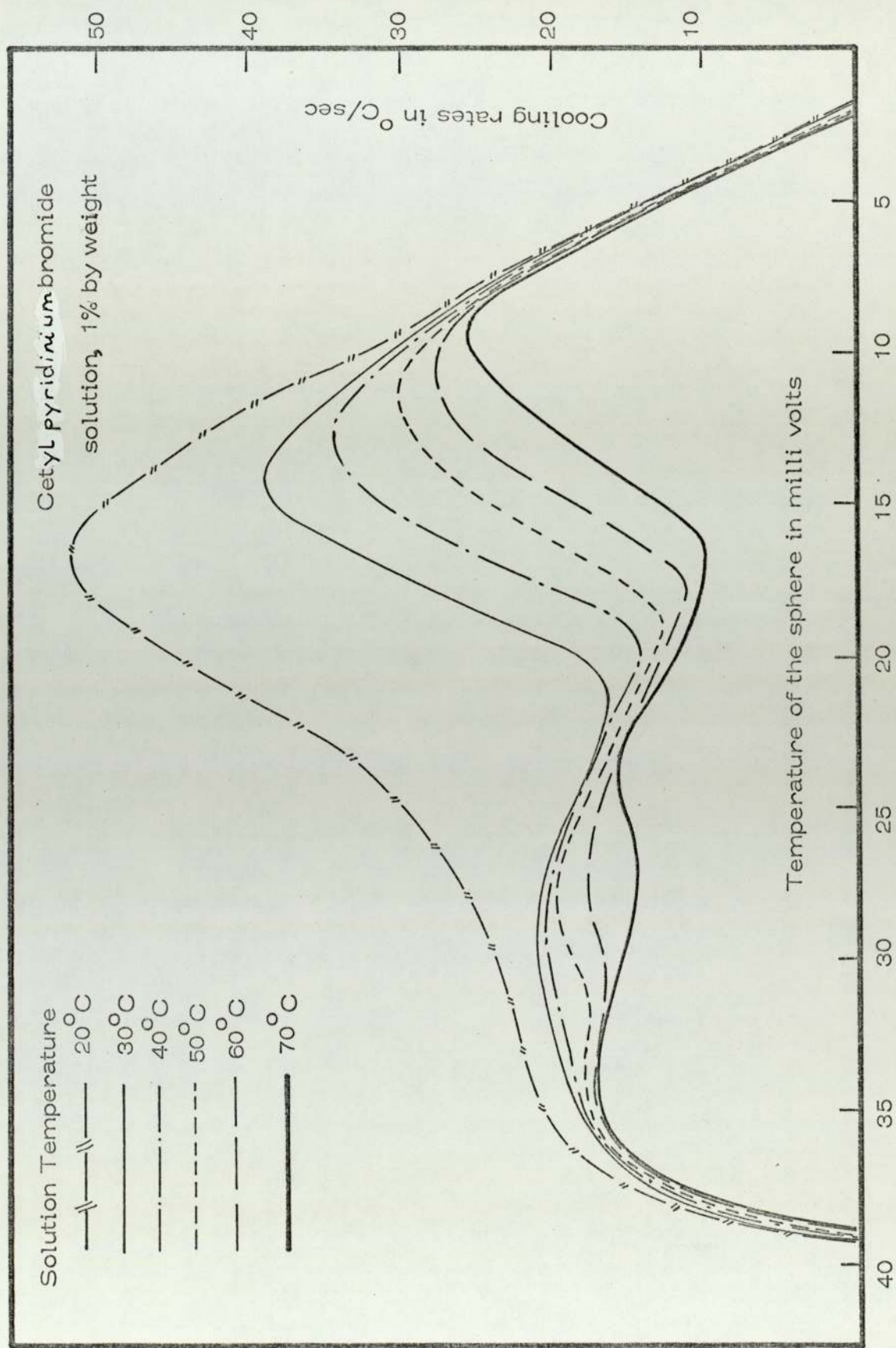
Instantaneous cooling rates of the solid sphere of cethyl primidine bromide solution, 1% by weight

Figure 26

Temperature of the hot sphere
where the stable film boiling ends in (mV)

○   Teepol 2%

●   Cethyl Prymidine Biomide 1%

■   Water

Coolant temperature °C
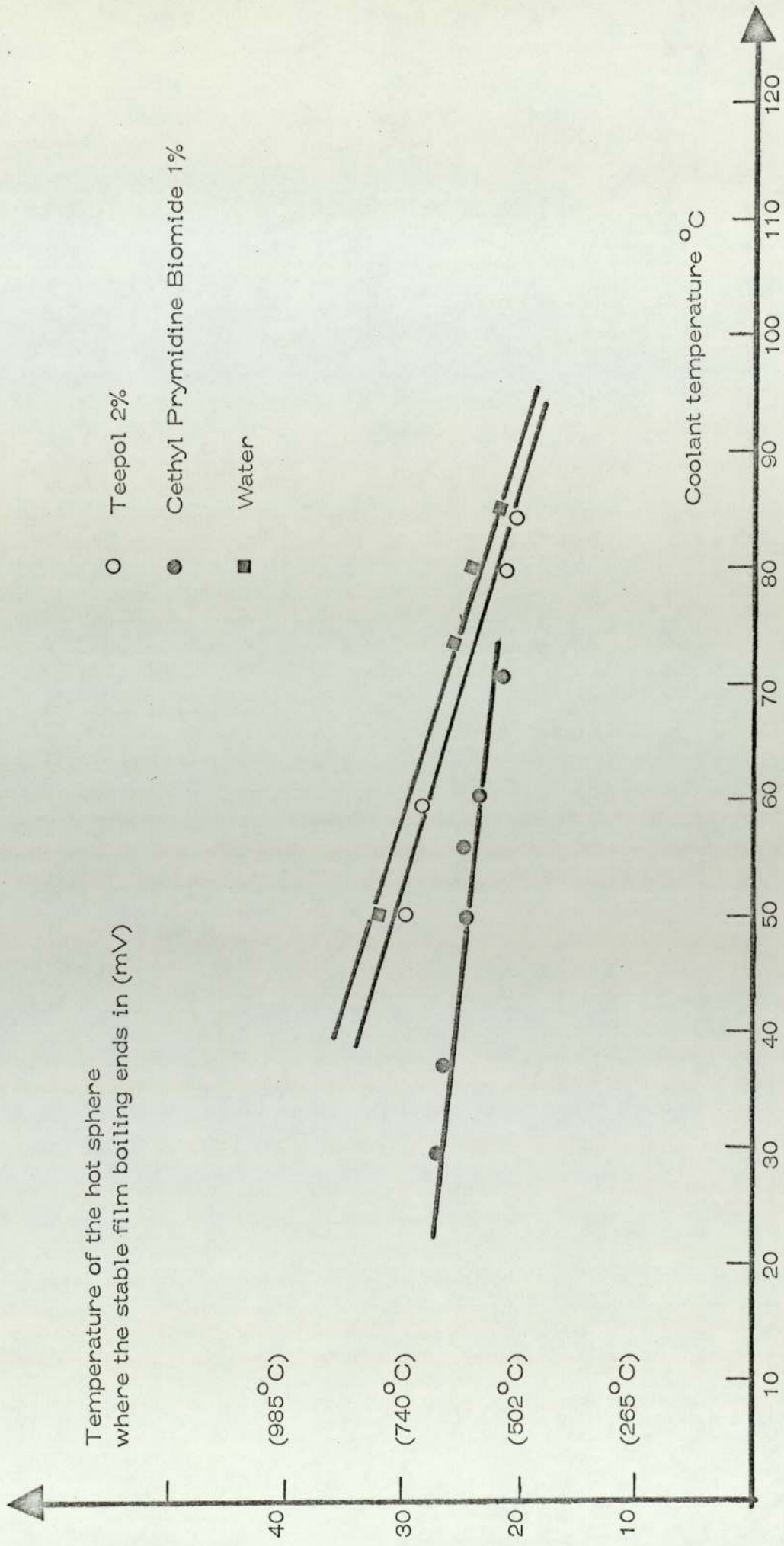
Dependence of the stable film boiling to the subcooling of the coolant

(985°C)

(740°C)

(502°C)

(265°C)

bromide solution of 1% by weight were used as detergent

solutions.

These experimental values of heat flux are comparable with

those of Witte et al[58]. It should be noted, however, that these

spheres used by Witte were quenched under a velocity field,

therefore the instantaneous heat flux values should be higher than

those obtained for stationary spheres. The difference between

the specific heats of silver and stainless steel should also be taken

into consideration. The results obtained by Witte and by the

present investigation are shown in table 3 . These results show

that the heat flux increases by a factor of 10 for a silver sphere

moving with a velocity of 152cm sec^{-1} in comparison with a

stationary stainless steel sphere immersed in water.

It was mentioned earlier that no explosions were observed when

molten metal falls into liquid nitrogen and this was explained by the

existence of a continuous stable nitrogen vapour blanket between the

molten metal and liquid nitrogen. Under these conditions, the heat

flux values are expected to be very low, the results have proved this

to be the case, when the same hot solid sphere was immersed in

liquid nitrogen. The range of initial sphere temperature was from

700°C to 900°C. The resulting cooling curves of the sphere in

liquid nitrogen are shown in figure 27. The results show that the

heat flux from a sphere quenched in liquid nitrogen is very low and

Table 3

Water Temperature °C	Maximum Heat Flux KWatts / cm²	Minimum Heat Flux KWatts / cm²	Source of Information
24	0.950	0.400	Witte et al [58]
60	0.700	0.250	Witte et al
77	0.380	0.070	Witte et al
20	0.148	–	Present investigation
30	0.121	–	"
70	0.060	0.025	"
80	0.038	0.016	"

Figure 27

Cooling Rates C°/sec

Sphere temperature in mV
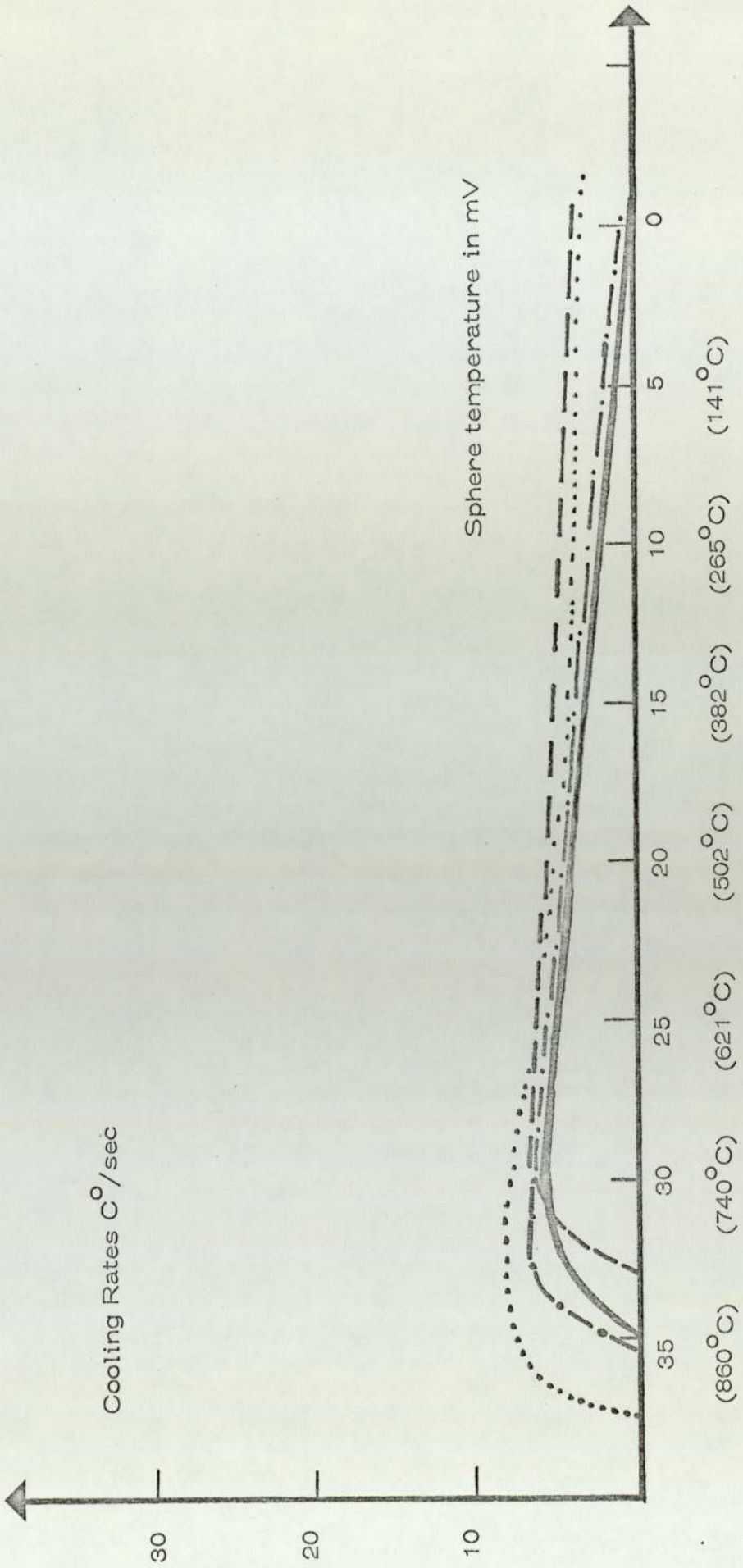
Cooling of the solid sphere in Liquid Nitrogen

the average cooling rate for this range of initial sphere temperature

is $7.75C^{o}/sec$ and the corresponding heat flux is $0.012 kW/cm^{2}$.

5.4 Boiling heat transfer from a crucible filled with molten tin

Experiments were carried out with molten tin to determine the heat

transfer rates in water. The apparatus used was the same as that

used for the solid spheres. Molten tin placed in a container to which

a chromel-alumel thermocouple was attached. The small container

was made of stainless steel and its dimensions were 2.54cm in

diameter and 1.27cm in depth. Same amount of molten tin was used

in all runs. The weight of molten tin was 43 grams. Boiled-

distilled water and liquid nitrogen were both used as quenching media

in these experiments. Since explosive interaction occurs between

molten tin and water below the threshold temperatures, the water

was always kept above these cut-off values. Results were obtained

at six different initial metal temperatures. These experiments were

carried out under quasi-static conditions, but the actual heat transfer

mechanism from the pear shaped tin drops to water occurs in the

presence of a fluid velocity field. Consequently, the values of

instantaneous heat flux should be converted to values which could be

achieved during the fall of metal drop in the water. The results -

obtained from quenching solid spheres in water show that the values of

heat flux increases by a factor of 10 when the velocity field is present.

The instantaneous cooling rates and heat flux from a crucible filled

with molten tin immersed in water are shown in table 4. These
results show that the rates of heat transfer are in accordance with
those achieved in boiling processes around submerged hot bodies.
They are about $10^3 - 10^4$ Watts cm^{-2}. The instantaneous cooling
rates for quenching a crucible filled by molten tin at different levels
of subcooling are presented in figure 28a. The effects of subcooling
on the heat flux is graphically illustrated by the six curves of
figure 28b. The results show that as the level of subcooling was
decreased, the heat flux decreased likewise. The heat transfer
results obtained for a given tin temperature are plotted as a function
of subcooling and show a linear relation which could be used to predict
heat transfer values at lower water temperatures (figure 29). Figure
28^{b}also illustrates the heat transfer values obtained when a crucible
filled with molten tin quenched in liquid nitrogen. The values of heat
flux varies from 0.01 to 0.012 kW/cm^2. It should be remembered
that exactly the same value was obtained when a hot solid sphere was
quenched in liquid nitrogen.

5.5 Threshold temperatures

Results obtained show that the values of threshold temperatures could
be altered by changing the initial metal temperature. It was shown
earlier that cut-off temperatures are lowered when initially higher
metal temperatures are used. In fact, the relationship between
initial metal temperatures and the cut-off temperatures is graphically

Table 4

Initial Temperature of Molten Tin °C	Cooling Rates C° / sec	Maximum Heat Flux kWatt / cm²	Coolant Temperature °C
695	119.37	0.256	65
695	21.39	0.046	100
655	105.57	0.227	69
655	21.39	0.046	100
602	112.47	0.242	66
602	21.39	0.046	100
501	82.11	0.176	79
501	24.15	0.052	100
421	77.28	0.166	75
421	26.22	0.056	100
365	63.43	0.136	74
365	20.70	0.044	100

Figure 28a

1mV Cooling rate output is 0.138°C/sec

Titan Thermocouples (Chromel-Alumel)
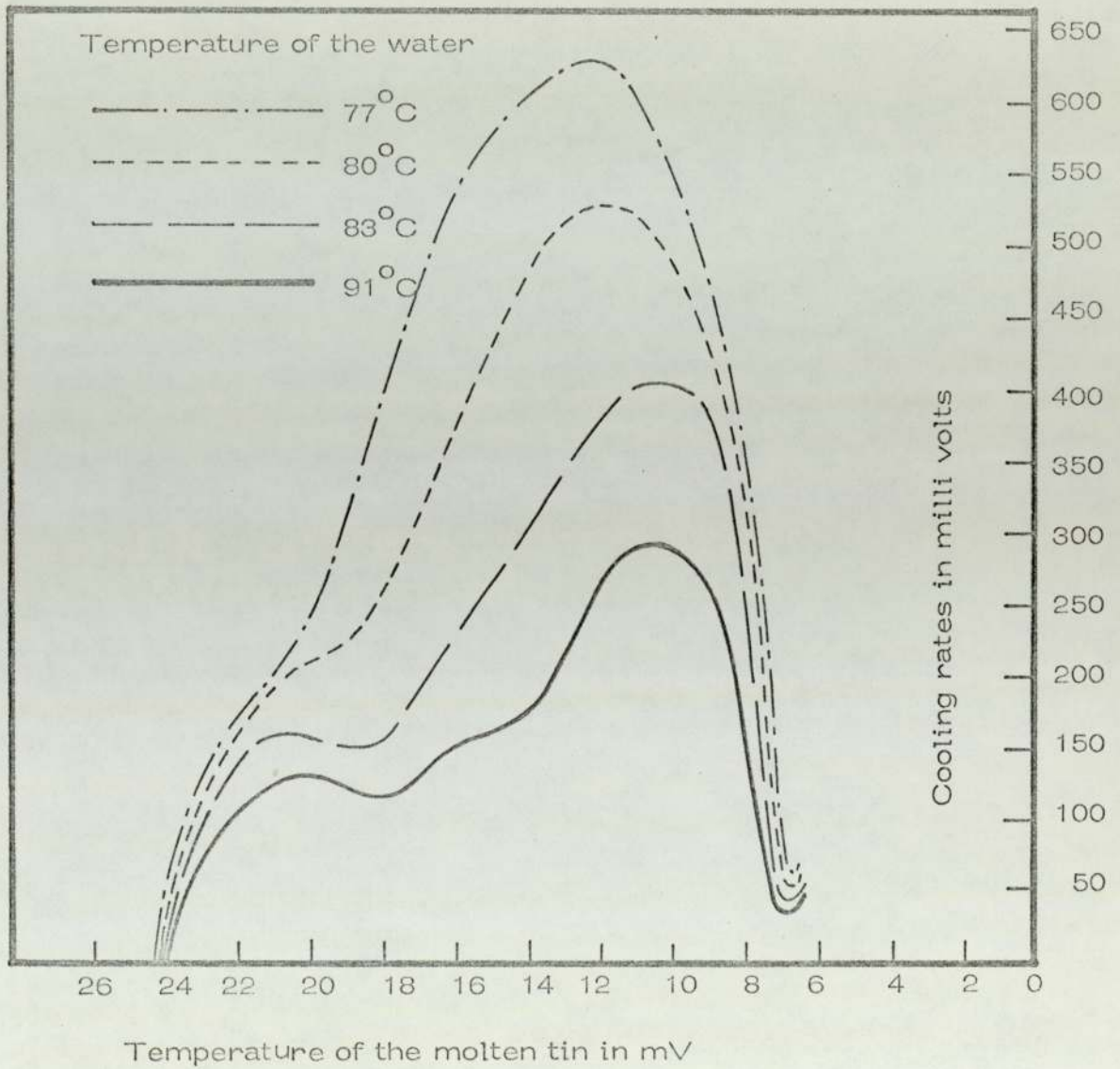
Instantaneous cooling rates for quenching a crucible filled with molten
tin

Figure 28b

Heat Flux, kWatts cm^{-2}

$T_{water} = 70^{o}C$

$T_{water} = 78^{o}C$

$T_{water} = 80^{o}C$

$T_{water} = 85^{o}C$

$T_{water} = 90^{o}C$

$T_{water} = 100^{o}C$

Liquid nitrogen

Molten Tin Temperature ^{o}C
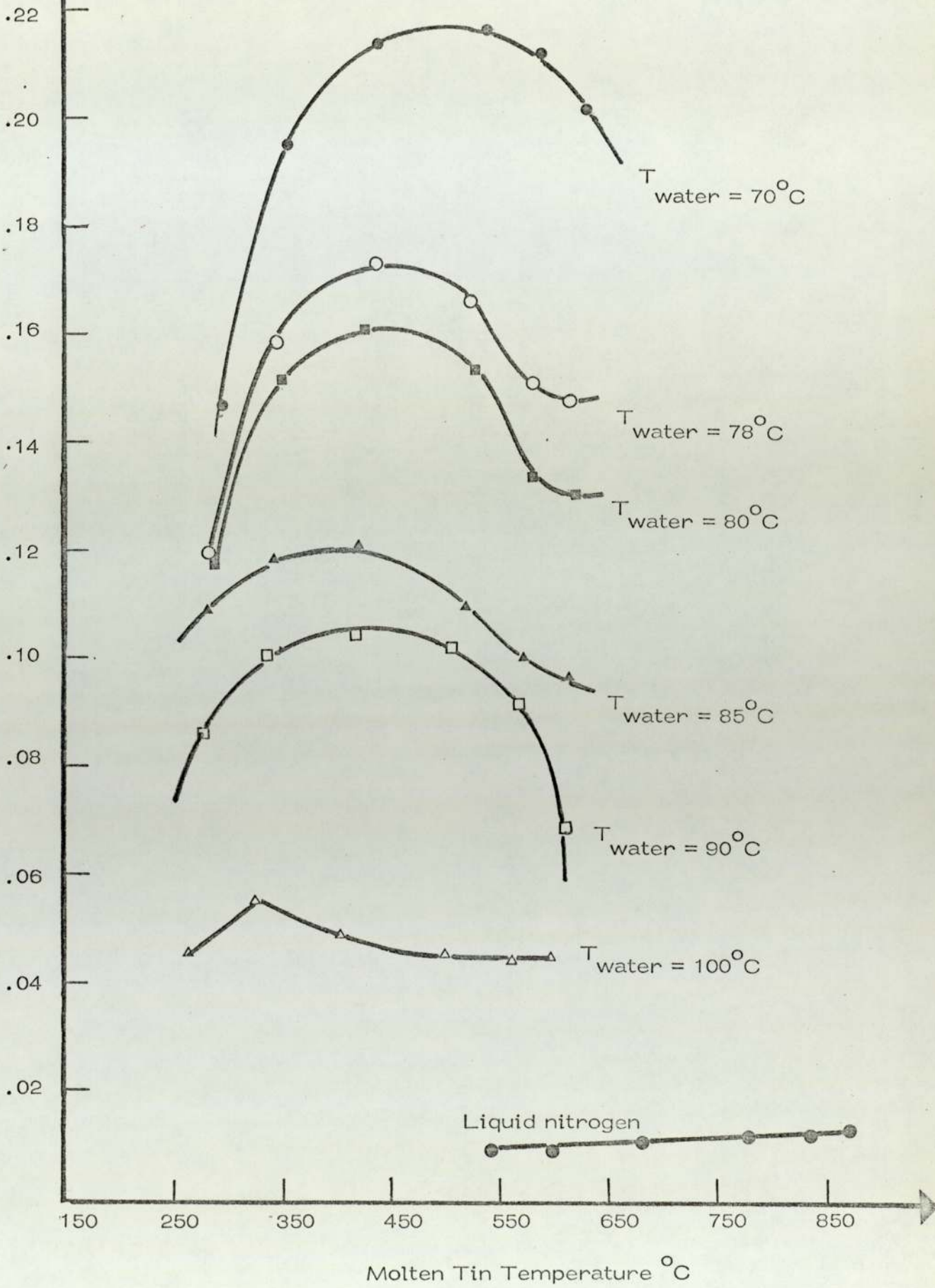
Instantaneous heat transfer results for the crucible filled with molten tin
at six different levels of subcooling and in liquid nitrogen

Figure 29

Heat Flux kWatt cm^{-2}

421°C Initial Molten Tin Temperature

Subcooling   θ = (ts-tc)°C
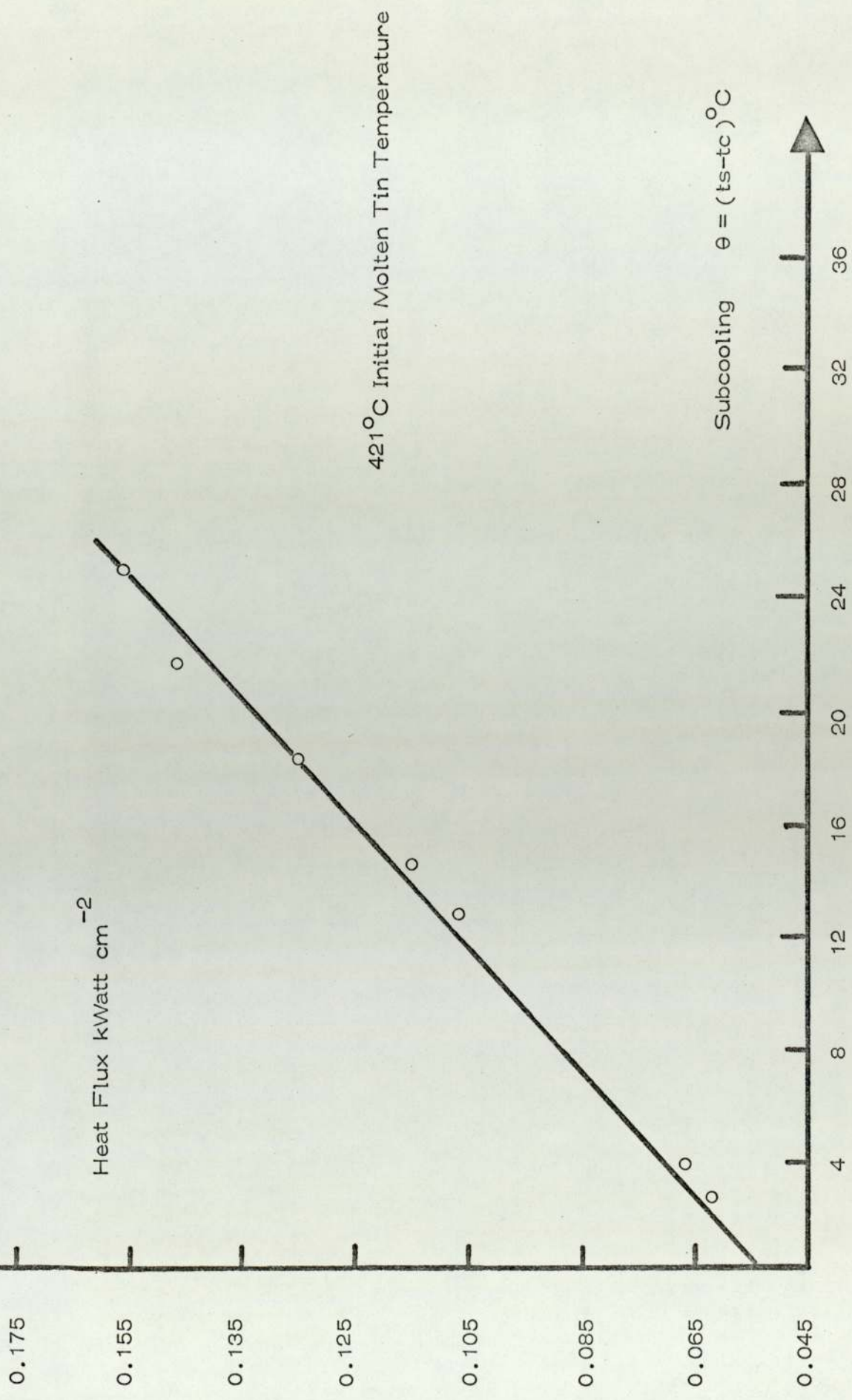
Instantaneous heat transfer as a function of subcooling for the crucible filled with molten tin

90

illustrated by the two curves of figure 30. These curves were

obtained for water and 1% teepol solution. The values of cut-off

temperatures for 1% detergent solution are higher than those for

water. They lie between 63°C and 93°C while for water the range

is 53°C to 74°C. The rather large increase in temperature can be

explained by the existence of a better interfacial contact between

molten tin and the coolant due to a reduction in surface tension.

The collapse of the stable film around the hot solid spheres when

they are quenched in 1% detergent (teepol) solution is much more

violent than a similar collapse occuring in water.

The relationship between the cut-off temperatures and the initial

metal temperatures clearly demonstrate that the threshold is lowered

by higher metal temperatures. However, there are three distinct

regions on these curves. The first region lies between 330°C and

405°C of initial tin temperatures. In this region, the cut-off temp-

erature increases as the metal temperatures increase. Upon reaching

a maximum at about 408°C the threshold temperatures then begin to

decrease as the metal temperatures are further increased. These

two regions are exactly similar for both coolants. However, in the

third region, there is a very slight increase in the threshold temperatures

for water as the metal temperature increase further but the threshold

temperatures slightly decreases for 1% teepol solution.

It was shown earlier that the relationships between the heat

Figure 30

Coolant temperature °C

● Boiled Distilled Water

■ 1% Teepol Solution

Initial Molten Tin Temperature

Initial metal temperature as a function of cut-off temperatures
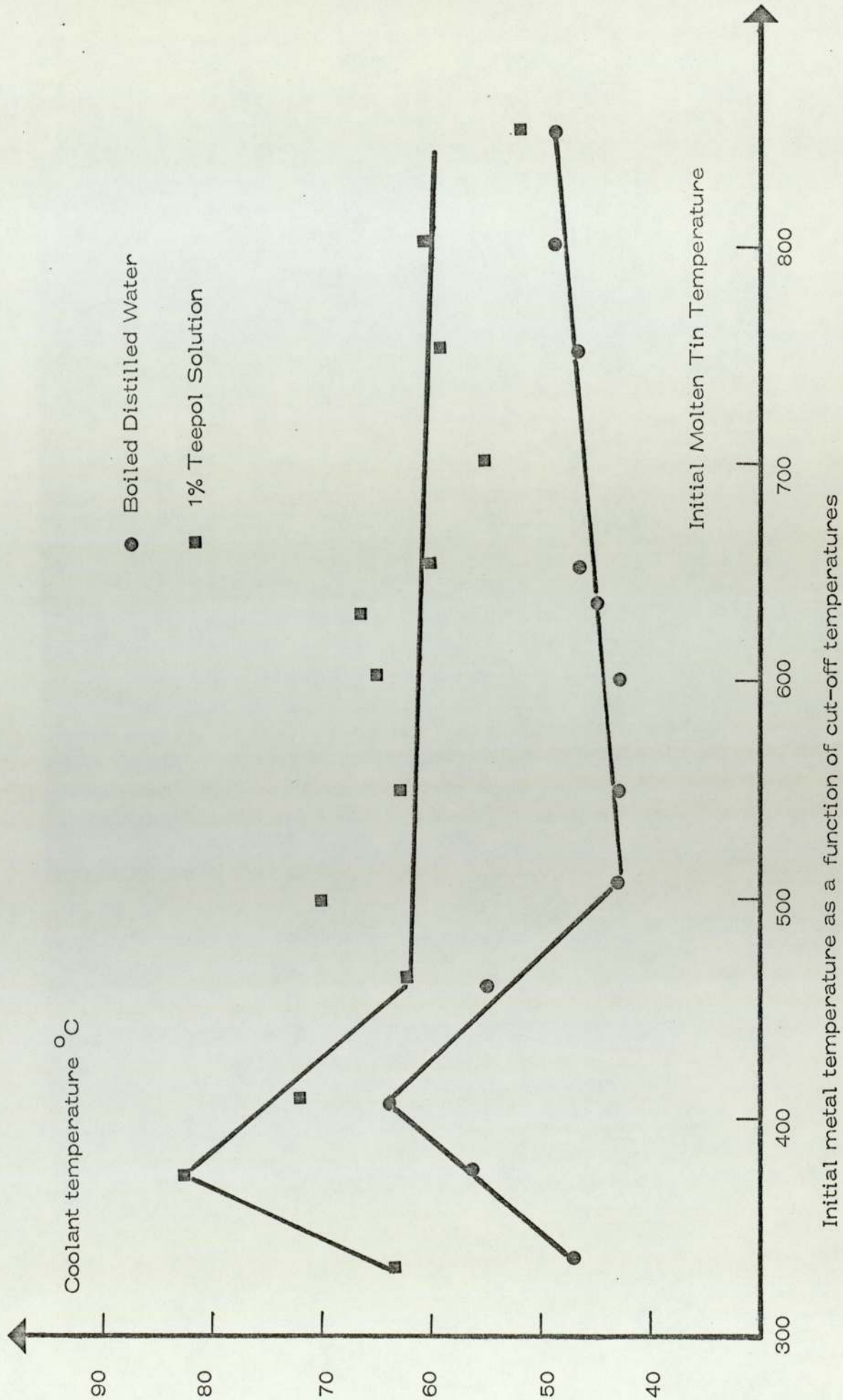
transfer rates and the temperature difference between the initial

metal temperature and the coolant also gave similar peaks in the

initial metal temperature range of $350^{\circ}C$ and $500^{\circ}C$. Furthermore

similar peaks are also obtained in the percentage disintegration curves

when the percentage disintegration is plotted as a function of the

initial metal temperature. These findings demonstrate that there

is a critical range of initial metal temperatures for molten tin. The

heat transfer rates, the percentage disintegration and the cut-off

temperatures tend to reach their maximum values within this range.

As a result, it is possible to conclude that these three variables are

inter related. Experimental evidence strongly suggests the

existence of a relationship between the explosive interaction and the

rates of heat transfer from the molten metal drop to the coolant.

During the course of cooling of the molten metal drops, there

exists a temperature and a critical heat flux where interaction will

take place. It is generally believed that this temperature and the

corresponding critical heat flux is in the region of transition boiling.

The results obtained by quenching a crucible filled by molten tin

indicate that this is the case for water temperatures just below the

threshold values. The explosive interactions will not proceed

instantaneously upon entering the water which its temperature near

to the threshold values. Therefore, it was possible to determine the

cooling rates of molten tin until the explosions occurred. These results

indicate that the explosions always occurred while cooling rates were increasing towards a maximum which marks the end of transition boiling.

Witte et al[7] have summarised the violent boiling theory of molten metal water interactions. This theory asserts that if the molten metal enters the transition boiling regime then violent boiling tears the molten metal apart and causes an explosion. However, the experimental results indicate that the transition boiling occurs around molten metals when they are quenched in water above threshold values but causes no explosion. It was shown earlier that as the water temperature increased, the boiling curve shifted to the left and the maximum was lowered. This indicates that when molten metal quenched in water at or above threshold values, either the critical heat flux during the transition boiling regime was not attained or when this flux is attained the molten metal had already solidified. Board et al[51] have initiated an explosive interaction above the cut-off temperature by disturbing the system with a pressure pulse which was propagated several seconds after the molten metal had come into contact with the water. The explanation generally accepted is that the pulse collapses the vapour blanket around the molten metal causing enriched heat transfer and hence allowing the critical heat flux to be obtained. It was found that the temperature for the onset of transition boiling occurring when a crucible filled

with molten tin is immersed in water decreases as the water

temperature increases. However, this temperature was found to

be higher than the melting point of tin. Similarly, those temperatures

occurring during the transition boiling were also found to be higher

than the solidification point of tin. This result indicates that transition

boiling occurs around the molten tin even above the threshold coolant

temperature. As the heat flux in this region cannot reach its

critical value, an explosive interaction does not occur. Their

grounds for believing that the onset of transition boiling do not

necessarily cause an explosion. However, it could initiate the

explosive interaction when it occurs around molten metals. For inter-

actions at low subcoolings and at subcoolings corresponding to the

threshold values it was found that the interaction was less violent

or does not occur at all. According to the 'jet penetration hypothesis'

such a behaviour would be expected. Since the jet velocity scales as

$(P_\infty - P_V)^{\frac{1}{2}}$, the mixing time scale increases and the probability of

an interaction is diminished. However, the lack of spontaneous

explosions above the threshold values of $74^\circ C$ and $53^\circ C$ for initial

metal temperatures of $400^\circ C$ and $500^\circ C$ is unlikely to be due to

an insufficiently rapid collapse. In fact, the impulse initiated

explosions at $80^\circ C$ and the explosions of one or two individual drops

of molten tin above the threshold values confirm that the $74^\circ C$ to

$53^\circ C$ range is a threshold for the trigger mechanism only and that the

collapsing bubble in this range is still sufficiently energetic to

initiate further escalation. This trigger mechanism is the onset

of transition boiling. The role of the various triggering mechanisms

suggested, in initiating thermal explosions, seems to be that of

disturbing the stable liquid - liquid film boiling occurring between

the molten metal and the water.

Chapter 6 ## Fall of liquid metal into water

6.1 Introduction

There is a possibility of explosions occurring under a wide range of conditions[3 - 9] when liquids are rapidly mixed. When molten tin is poured from a crucible into water in defined conditions, a rapid explosive interaction takes place producing a sponge-like mass of debris[4 -23]. Similar experiments were carried out using an apparatus which provides small (0.25g) and reproducible single drops of molten tin, and it was possible to determine quantitatively the dynamics of the interaction by a photographic technique. Using a metal temperature of $300^{\circ}C$ and water at room temperature, metal drops were produced which entered the water in a straight vertical line but were then observed to deviate suddenly and sharply from their course without losing their pear-like shape. This metal temperature was just below that necessary to produce explosive interactions for the given water temperature.

6.2 Photographic technique

The photographs of the fall of liquid metal drops into water were taken by an ordinary camera using stroboscopic illumination. Minolta SRT 303, single lens reflex camera was used in these experiments. The whole experimental procedure was carried out in total darkness. A stroboscope which can be operated at different flashing speeds was used. The range of the flashing speed of this

stroboscope was between 10 to 15000 flashes per minute. The total

time for the tin drops to travel from the water level to the bottom of

the water container (20cms) was about 264 milli seconds.

Consequently, the number of images required of a single tin drop

during the fall in the water can be calculated. The results show

that if the flashing speeds of 4000 and 9500 flashes per minute are

used, the number of images obtained of the single tin drop was

adequate to obtain the necessary measurements. Therefore, two

flashing speeds were used throughout these experiments and they

were 5000 and 9500 respectively flashes per minute for tin and lead

drops.

The location of the stroboscope with respect to the rest of the

apparatus was found to be an important factor in determining the

quality of the photographs. The optimum conditions for its location

were that it should be placed 20cm away from the water container

at an angle of 30° to the front wall. This experimental arrangement

is shown in figure 31 . The exposure time was another important

factor in obtaining good quality photographs. When all the images

of the single drop are required during the fall, the exposure time

was always set above 264 milli seconds to ensure that the drop had

sufficient time to reach the bottom of the container. The shutter of

the camera was operated manually (corresponding to the 'B' position

on the camera) to obtain longer exposure times. It was found necessary

Figure 31
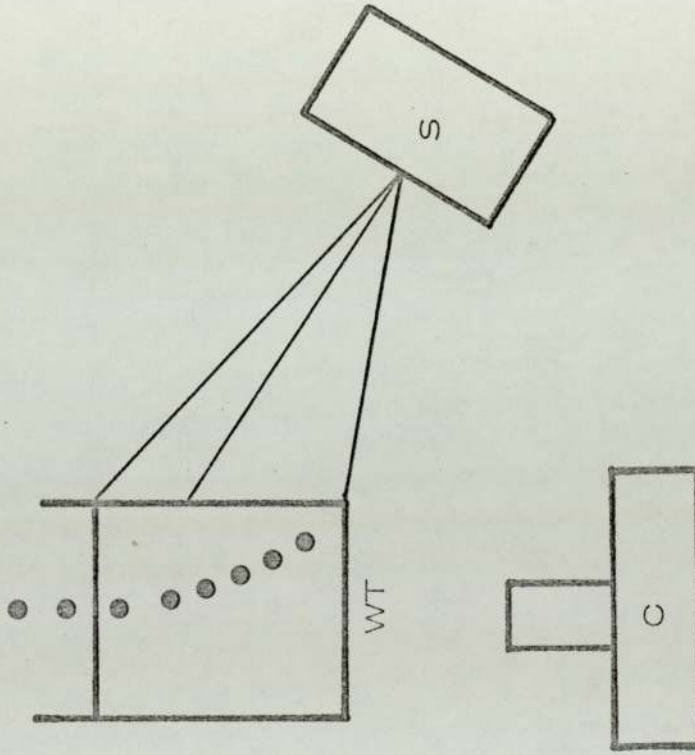
Key

S = Stroboscope
C = Camera
WT = Water Tank

Experimental arrangement for stroboscopic photography

to operate the camera in the 'B' while taking a picture of a moving

drop when illuminated by a stroboscopic light. The distance between

the furnace and the water level was altered. However, the range was

not sufficiently comprehensive to obtain conclusive results. The

furnace was situated at 4, 7.8, 8, 20 and 23cm above the water level.

The results show that the film speed used is also an important factor

in obtaining good quality pictures. Two different kinds of film were

used. Kodak Tri-X and Ilford HP4, and their speeds were 400 and

500 ASA respectively. The faster one was found to be more suitable.

No other films were used. The quality of images may improve if a

faster film was used than the ones mentioned above.

6.3 Impulse and Momentum

It has been suggested[23-40] that the fragmentation of molten tin is

linked with the collapse of a vapour blanket surrounding the molten

metal during the change from stable film boiling to transition boiling.

Using a model for the collapse of a vapour bubble, developed by

Plesset and Chapman[43], Buchanan and Dullforce[40] predict the

velocity and the dimensions of a slug of water resulting from the

collapse of a bubble of initial radius R_m, which then penetrates

the liquid metal initiating the first cycle of a fragmentation process.

From the photographs of the deviating drops and using simple particle

dynamics, it is possible to find the direction and magnitude of momentum

imparted to the tin drop. Assuming that this momentum results from

the collapse of a single vapour bubble adjacent to the tin drop, the initial radius of the vapour bubble, R_m, can be evaluated.

Starting from Newton's Law of Motion it is possible to evaluate the momentum and its direction. Newton's Law of Motion states that a particle will remain in its uniform motion (at constant speed) along a straight line unless compelled by some force to change that state. The rate of change of the product of l the mass and velocity of a particle is proportional to the force acting on the particle. The product of the mass, m, and the velocity, V, is the linear momentum I.

$$F = \frac{d(mV)}{dt} = \frac{dI}{dt} \qquad (6\text{-}3\text{-}1)$$

if m is constant then the above equation becomes

$$F = m\frac{dV}{dt} = ma \qquad (6\text{-}3\text{-}2)$$

The vector sum of the external forces acting on a particle is equated to the rate of change of the linear momentum.

$$\sum F = \frac{d(mV)}{dt} = \frac{dI}{dt} \qquad (6\text{-}3\text{-}3)$$

which may be integrated as

$$\int_{t_1}^{t_2} \sum F\, dt = \int_{I_1}^{I_2} dI = I_2 - I_1 = mV_2 - mV_1 \qquad (6\text{-}3\text{-}4)$$

The integral on the left hand side is the linear impulse acting in the

time interval from t_1 to t_2. Thus, this linear impulse is equal to the change in the linear momentum.

Conservation of linear momentum in a given direction occurs if the sum of the external forces in that direction is zero. By resolving this principle's vertical and horizontal components, it is possible to determine the magnitude and the direction of the impulse imparted on to the molten metal drops. The diagram below illustrates the position of the drop before and after the impact.

Before impact   After impact
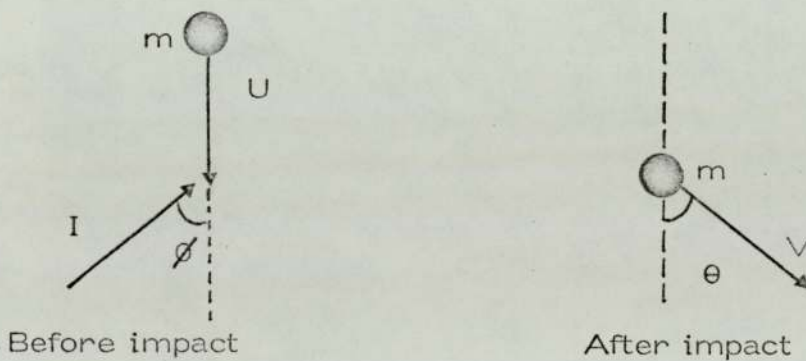
The vertical component is

$$mU - I\cos\phi = mV\cos\theta \qquad\qquad (6\text{-}3\text{-}5)$$

and resolving horizontally gives

$$I\sin\phi = mV\sin\theta \qquad\qquad (6\text{-}3\text{-}6)$$

where U and V are the velocities of the drop before and after the impact, θ is the angle of deviation of the drop, ϕ is the angle at which the impulse I is applied. Solving equation 6-3-5 and equation 6-3-6

for $\emptyset$ and I

$$\tan \emptyset = \frac{V \sin \theta}{U - V \cos \theta} \qquad (6-3-7)$$

and

$$I = \frac{mV \sin \theta}{\sin \emptyset} \qquad (6-3-8)$$

Assuming that this momentum results from a slug of water hitting

the metal drop, then

$$I = mV \quad \frac{gr - cm}{sec} \qquad (6-3-9)$$

can be written.

Plesset and Chapman[43] scale velocities as

$$\left(\frac{\Delta p}{\rho}\right)^{\frac{1}{2}} \qquad (6-3-10$$

when p is atmospheric pressure and the density , he found the

velocity of the slug of water on impact was 130m/sec. Thus, the

corresponding mass of water can be found, and so R_m the maximum

size of bubble radius causing the jet of water to be formed can be

calculated. Since m is known, it is possible to evaluate the

dimensions of the jet, assuming a cylindrical geometry.

$$V = m = \frac{1}{4} \pi L_o d_o^2 \qquad (6-3-11)$$

The length and diameter of the jet when it strikes the drop surface

are

$$L_o = L_c R_m \qquad (a)$$

$$\qquad (6-3-12)$$

$$d_o = d_c R_m \qquad (b)$$

where $L_c = 0.493$ and $d_c = 0.237$, so

$$\frac{L_o}{d_o} = \frac{L_c}{d_c} \tag{6-3-13}$$

$$L_o = \frac{0.493}{0.237} d_o \tag{6-3-14}$$

Upon substituting this value of L_o in equation 6-3-11, d_o can be calculated, and from equation 6-3-12b R_m, the maximum radius of the bubble causing the jetting phenomenon, is easily obtained.

6.4 Experimental procedure and results

Photographs of the fall of molten tin drops at $300^{\circ}C$, and molten lead at $410^{\circ}C$ as well as mercury and carbon tetra chloride at room temperature, into water at $20^{\circ}C - 25^{\circ}C$ were taken using stroboscopic illumination. The path of a falling drop is clearly visible, both in air and below the water and velocity may be determined from the image spacing. Although mercury and carbon tetra chloride fall in vertical straight lines to the first order (figure 32), molten tin drops (figures 33a and 33b) initially fall in vertical straight lines, but after a few centimetres in the water deviate from this straight line by up to $\frac{1}{3}$ radians.

As the photographs taken correspond to a fixed plane of vision, those tracks which featured the greatest deflections were considered as these were most likely to have occurred in the plane of the photograph.
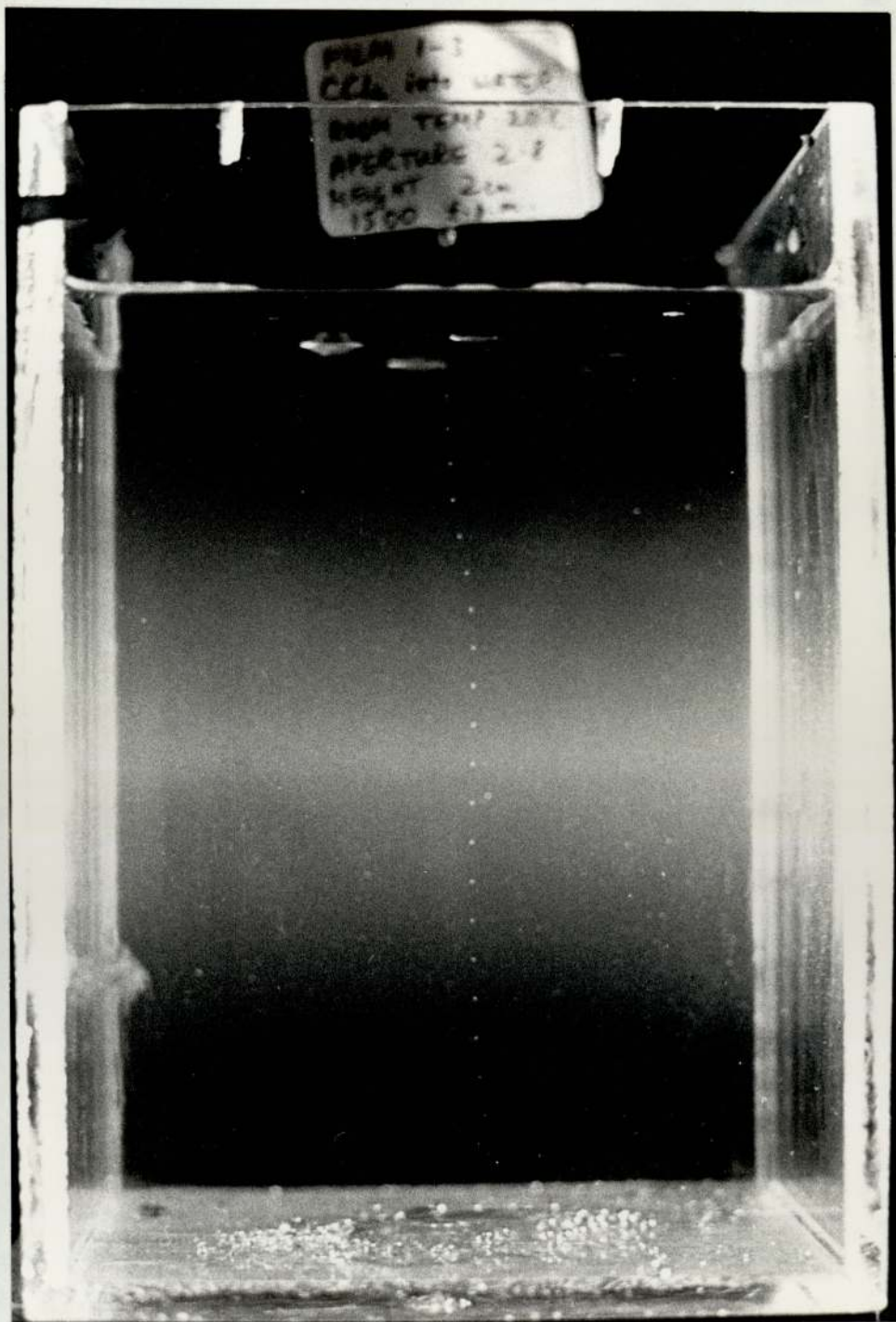
FIGURE 32. A carbon tetrachloride drop falling from a
height of 2 cm into water. Both liquids at
20° C, and the drop was photographed in a
stroboscopic light at 1500 flashes per minute.

FIGURE 33a. Molten tin drops at 300°C falling from a height
of 23 cm into distilled water at 20°C. The drops
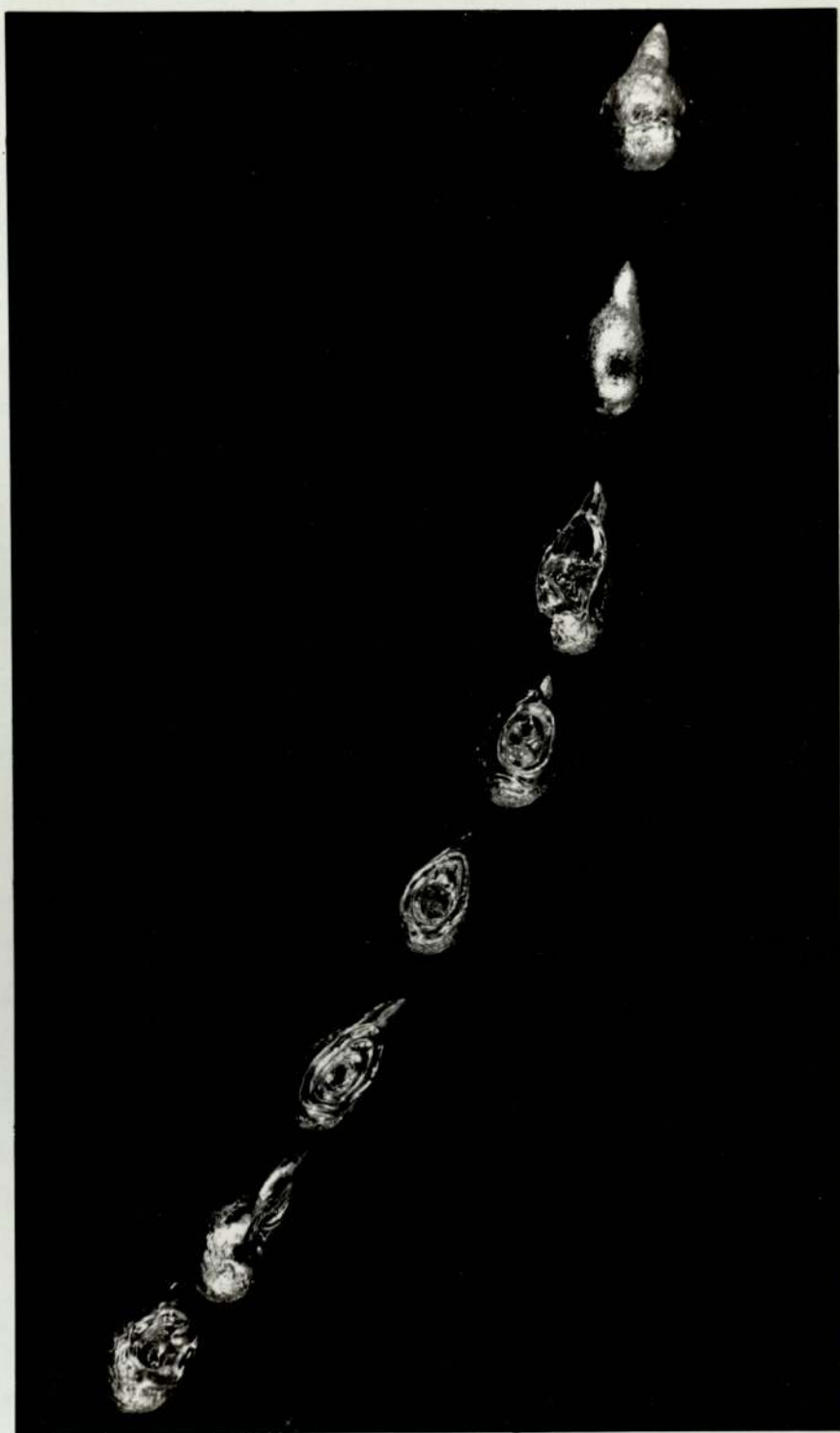were photographed in a stroboscopic light at 9500
flashes per minute.

FIGURE 33b. Simulation photograph of the deviating tin drops.

Data obtained from the projected nagatives is shown in table 5.
Assuming that this momentum results from the collapse of a single
vapour bubble adjacent to the tin drop, R_m can be evaluated. Values
of momentum lay between 1.9 and 12 g cm s^{-1}, and the momentum
was directed upwards at angles to the vertical, between 0.9, and 1.22
radians.   These seem too large for single bubble collapse to be
a complete explanation for an initiation of the fragmentation
process, at least for molten tin drops of radius 0.15 to 0.175cm.

Work has been carried out[58] on quenching hot solid metal
spheres by moving them at a constant speed (of a similar value to
that of the tin drops). A phenomenon, termed 'transplosion' is
described which takes place between stable film boiling and
transition boiling. In less than 0.25 milli seconds the vapour shell
is explosively destroyed giving rise to a regime of boiling described
as pulsation boiling which consists of a thin oscillating vapour film.
This progressively changes to nucleate boiling from the front of the
sphere to the rear with a pulsating vapour ring separating the
nucleate boiling zone from the remaining thin vapour film. The
sphere temperatures which correspond to the transition phenomenon
are plotted against the water temperature and the results show that
the transplosion mechanism occurs at a metal sphere temperature
of 300°C for a water temperature of 20°C. This combination of
metal and water temperatures is exactly the same as those

Table 5

Picture	h cm	θ °	cm	d cm	w cm	x cm	y cm	z cm	Metal	Metal T °C	Water °C	φ °	I grcm/sec	Rm cm.
1	4.0	8.0	16.1	1.6	0.9	0.9	0.9	0.7	Tin	280	19	86	2.33	0.201
2	4.0	9.0	15.4	1.9	1.0	1.0	1.0	0.7	Tin	300	19	85	3.04	0.220
3	4.0	8.0	15.4	2.4	1.0	1.0	1.0	0.8	Tin	285	20	84	2.71	0.212
4	4.0	10.5	–	1.0	0.6	0.6	0.5	0.4	Tin	300	20	51	2.71	0.212
5	4.0	10.0	16.5	1.9	0.9	0.9	0.9	0.8	Tin	300	19	84	2.84	0.215
6	4.0	9.0	12.5	1.8	0.6	0.6	0.6	0.5	Tin	300	20	85	2.25	0.199
7	4.0	7.5	12.5	1.8	0.6	0.6	0.6	0.5	Tin	300	20	86	1.87	0.189
8	7.8	8.0	–	5.1	1.13	1.11	1.01	0.75	Tin	300	22	52	4.08	0.243
9	20.0	16.0	–	4.9	1.5	1.1	9.9	8.1	Tin	300	22	73	6.71	0.287
10	23.0	25.0	–	5.4	1.4	1.1	9.0	5.5	Tin	300	22	58	12.62	0.354

h   height of drop from furnace to water

θ   angle of deviation

A   apparent width of perspex beaker

d   apparent distance travelled before impact below water

w   apparent distance travelled in 1 flash upon entering water

x   apparent distance travelled in 1 flash before impact

y   apparent distance travelled in 1 flash after impact

z   apparent distance travelled in 1 flash near bottom of tank

φ   angle of momentum application

I   Impulsive momentum

Rm   Maximum radius of collapsing vapour bubble

temperatures for deviating tin drops in water. If the transplosions and the resulting pulsating vapour rings occur in a similar fashion on the molten tin drops, they could perhaps provide an explanation for the considerable momentum found to be imparted during the quenching process.

When close-up photography was used, an association was observed between the deviation and the rotational motion of the metal drop. Upon a vertical entry into the water, the drops of molten tin and lead are found to rotate while falling further in the tank (figure 34).

This behaviour of the drops occurs after a few centimetres below the water surface. A careful analysis of the photographs show that the first and the second images of the single drop are not clear as the latter ones. In fact, a cloud of water vapour can be seen around these drops and is responsible for the obscurity. The image after these two is always associated with rotation. Since the angular velocity of the rotating drops can be measured from these picturesthe impulsive couple causing this rotational motion can be easily obtained. However, the impulsive momentum can only be evaluated if the point at which the momentum was imparted to the drop is known. It is obvious that momentum was applied along the length of the drop but it is necessary to determine the exact position of this point with respect to the centre of gravity of the metal drop.
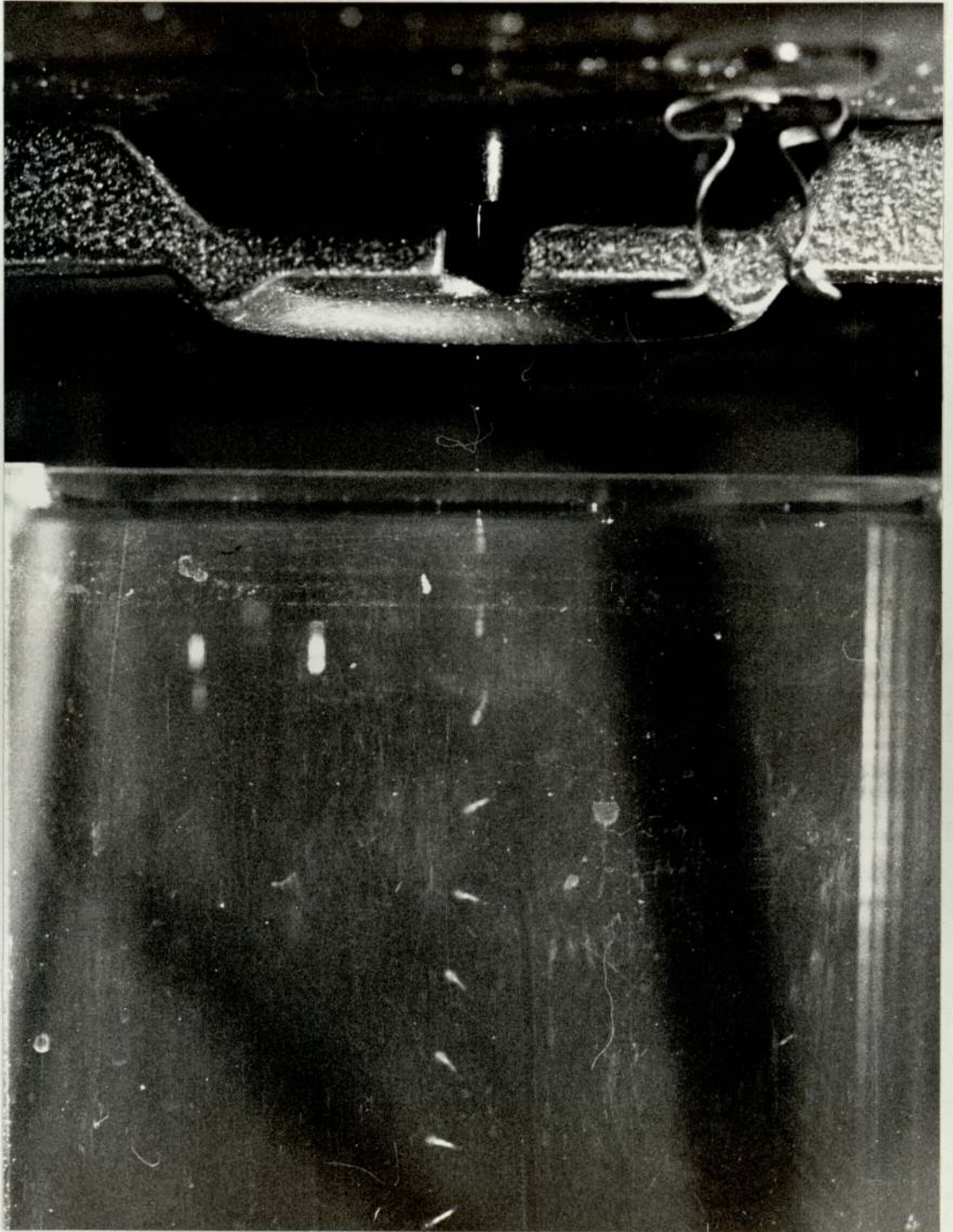
FIGURE 34.   Rotational Motion of the Metal Drops in Water.
The Photograph was taken using Stroboscopic
illumination, 5000 Flashes per minute.

First the impulsive couple was calculated. It is obtained by taking

the product of the change in angular velocity and the moment of

inertia of the metal drop. The pear-like shape of the drops of the

tin and lead was considered to be a combination of a hemisphere and

a cone. The moment of inertia of this body about an axis through its

centre of gravity can be evaluated, if the whole body is resolved in

terms of the above two geometries. The sum of the two moments,

gives the moment of inertia for the drop as a whole. The centre of

gravity of the pear-like tin and lead drops was found to be within

the cone section of the drop and is given by

$$X = \frac{3l^2 + 3a^2 + 8al}{4(2a + l)} \qquad (6-4-1)$$

where X is the position of the centre of gravity from the apex of the

cone; l is the height of the cone and a is the radius of the hemisphere.

Two different sizes were distinguished for the drops generally and

were 0.872 and 0.650cm in length and 0.385 and 0.350cm in

diameter respectively. Results obtained from 37 photographs of lead

and 13 pictures of tin drops.

The photographs were taken under stroboscopic illumination with

the speed kept constant at 5000 flashes per minute for all pictures.

Since the moment of inertia of the drops were known, the impulsive

couple was calculated using the formula given below.

Impulsive couple $= I \times \Delta W$ gr-cm^{2}sec^{-1} $\qquad\qquad$ (6-4-2)

where I is the moment of inertia and   W is the change in the

angular velocity.

Estimates of the impulsive momentum can be made by dividing

the impusive couple by arbitrary distances from the centre gravity

for both metals. A typical example of this relation is shown in

figure 35.

In fact this type of relation is expected. As it was mentioned

earlier, the impulsive momentum can only be obtained if the point

at which the momentum is applied is known. However, the order of

impulsive momentum should be similar to that obtained from the

deviating drops. The angular velocities of the tin drops are between

2 and 5.5, whereas these values for the lead drops are between 2

and 6.7. Since two different sizes of metal drops were obtained

impulsive couples were calculated for both of these drop sizes. The

moments of inertia and the corresponding centres of gravity of the

drops are shown in table 6 . One representative value of angular

velocity for the tin drops and one for lead was selected in order to

calculate the corresponding impulsive couple $(C = \text{grcm}^2\text{sec}^{-1})$.

The impulsive momentum for the deviating tin drops lay between 2

and 12 grcmsec^{-1}. From this the distance between the point at which

the impulse momentum was applied and the centre of gravity was

calculated. The results are shown in table 7 . Results were only

Figure 35

Impulse Momentum
grcm/sec

I = Moment of Inertia of the drop = 3.70×10^{-3} grcm^2

W = Angular Velocity = 2.136

Impulsive Couple = I × W

Impulsive Couple: d_H = Impulsive Momentum

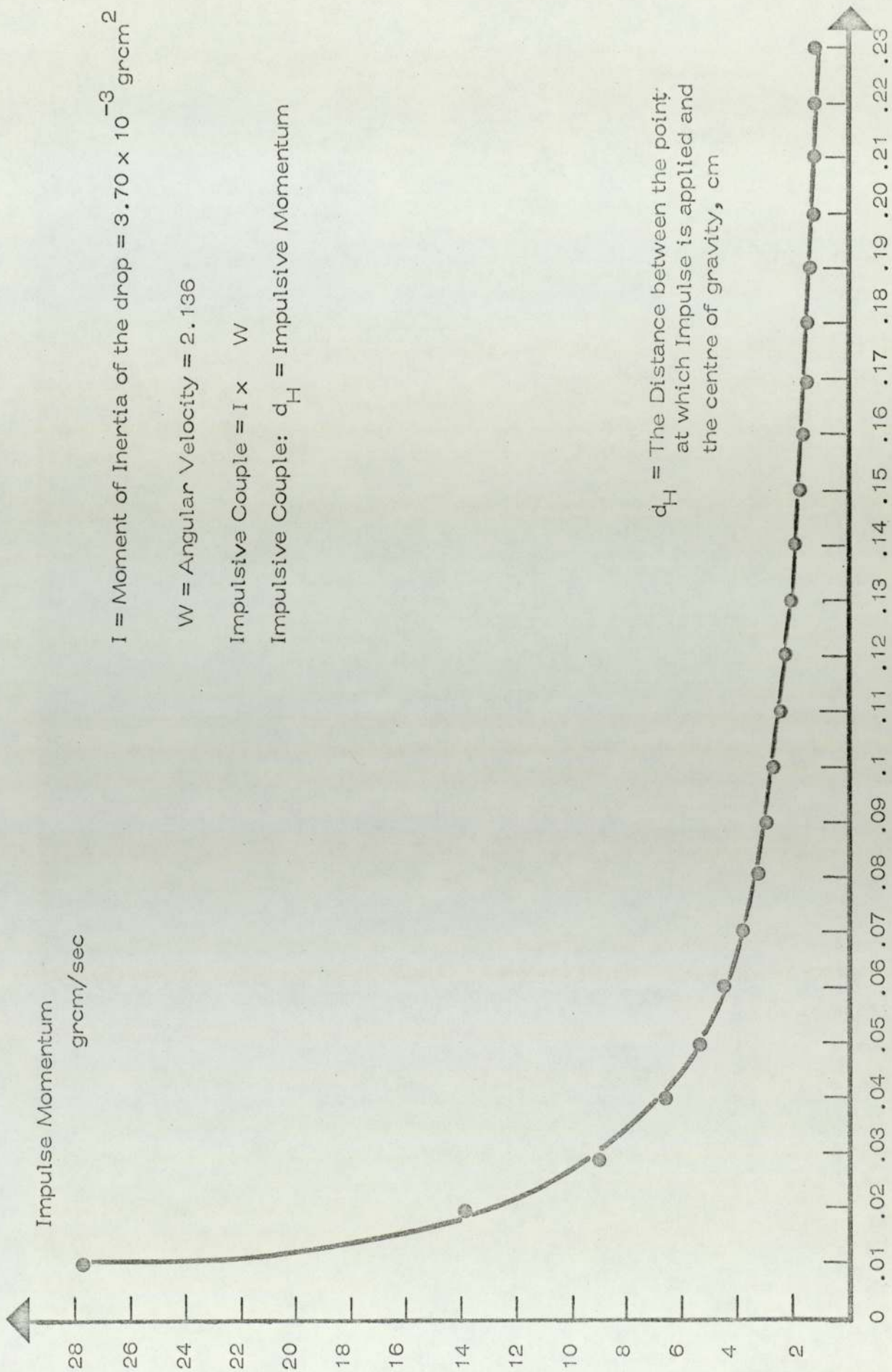d_H = The Distance between the point at which Impulse is applied and the centre of gravity, cm

Table 6

Diameter of the drops (cm)	Length of the drop (cm)	Length of the cone (cm)	Radius of the hemisphere (cm)	Metal
0.385	0.872	0.6795	0.1925	Tin
0.350	0.650	0.4750	0.1750	Tin
0.385	0.872	0.6795	0.1925	Lead
0.350	0.650	0.4750	0.1750	Lead

Centre of the gravity $X = \dfrac{3l^2+3a^2+81a}{4(2a+l)}$	Moment of inertia of the hemisphere about an axis through the centre of gravity	Moment of inertia of the cone about an axis through the centre of gravity	Moment of inertia of the whole drop gr cm ^{2}
0.597	3.63×10^{-3}	7.10×10^{-2}	7.55×10^{-2}
0.434	1.57×10^{-3}	2.10×10^{-3}	3.70×10^{-3}
0.597	5.60×10^{-3}	1.12×10^{-1}	1.177×10^{-1}
0.434	2.40×10^{-3}	3.30×10^{-3}	5.77×10^{-3}

Table 7

Metal	ℓ cm	Δw	I grcmsec^{-1}	d H cm
Tin	0.872	5.555	2.09	0.200cm
Tin	0.650	5.555	2.10	0.010cm
Tin	0.650	5.555	12.00	0.002cm
Tin	0.872	5.555	12.00	0.035cm

ℓ = length of the drop

Δw = angular velocity of the drop

I = impulsive momentum

dH = the distance between the point at which impulse momentum applied and the

centre of gravity

obtained for the tin drops, as there is no available data for deviating

lead drops. For the tin drops of 0.650cm in length, the distance

between the centre of gravity and the point at which momentum is

applied is 0.01cm for an impulse of $2.1grcmsec^{-1}$ and 0.002cm for

an impulse of $12grcmsec^{-1}$. Similarly, these distances are 0.2cm

for an impulse of $2.1grcmsec^{-1}$ and 0.035cm for an impulse of

$12grcmsec^{-1}$ for tin drops of 0.870cm in length.

Apart from this hypothetical approach the existence of small

holes (figures 36 and 37) on tin and lead drops and their position

with respect to the centre of gravity was found to be suitable to

calculate impulsive momentum imparted to these drops. However,

no holes were observed on the bismuth drops. The distance from

the top of the tail to the hole was measured. The holes occur in two

different regions. The first region was near to the tail, where as

the second region was very close to the centre of gravity. The

distances between the holes of the second region and the centre of

gravity were also measured and it was found to be very similar to

those obtained by the hypothetical approach. As it was described

earlier, the cause for the deviation could be linked to the formation

of the vapour rings and their eventual collapse[58]. These holes are

present in the region where the pulsating vapour rings occur. There

is considerable evidence of simultaneous boiling regimes occurring

on molten tin drops. Upon quenching the tin drops, the hemispherical
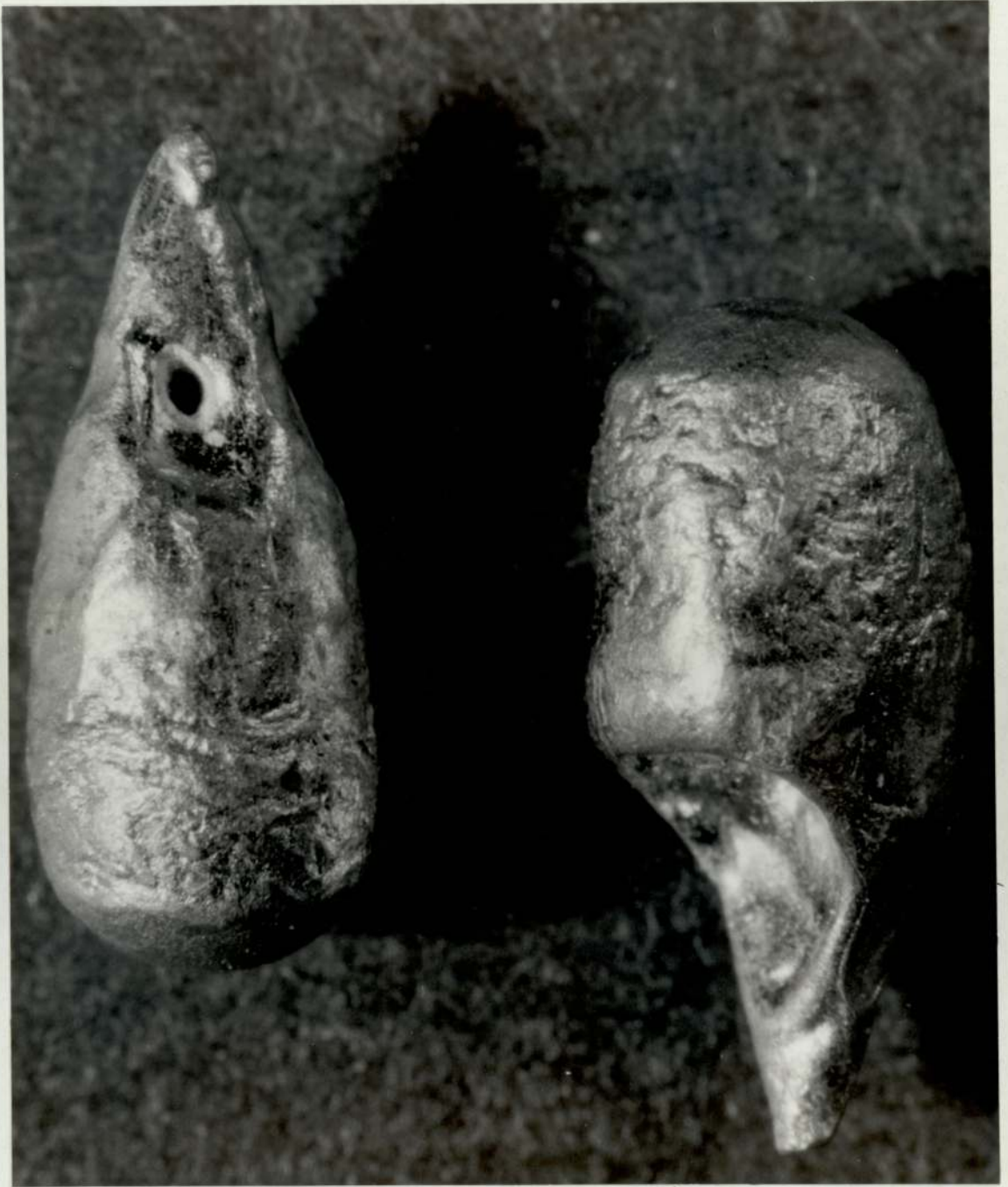
FIGURE 36.   Lead Drops Showing Hole Formation
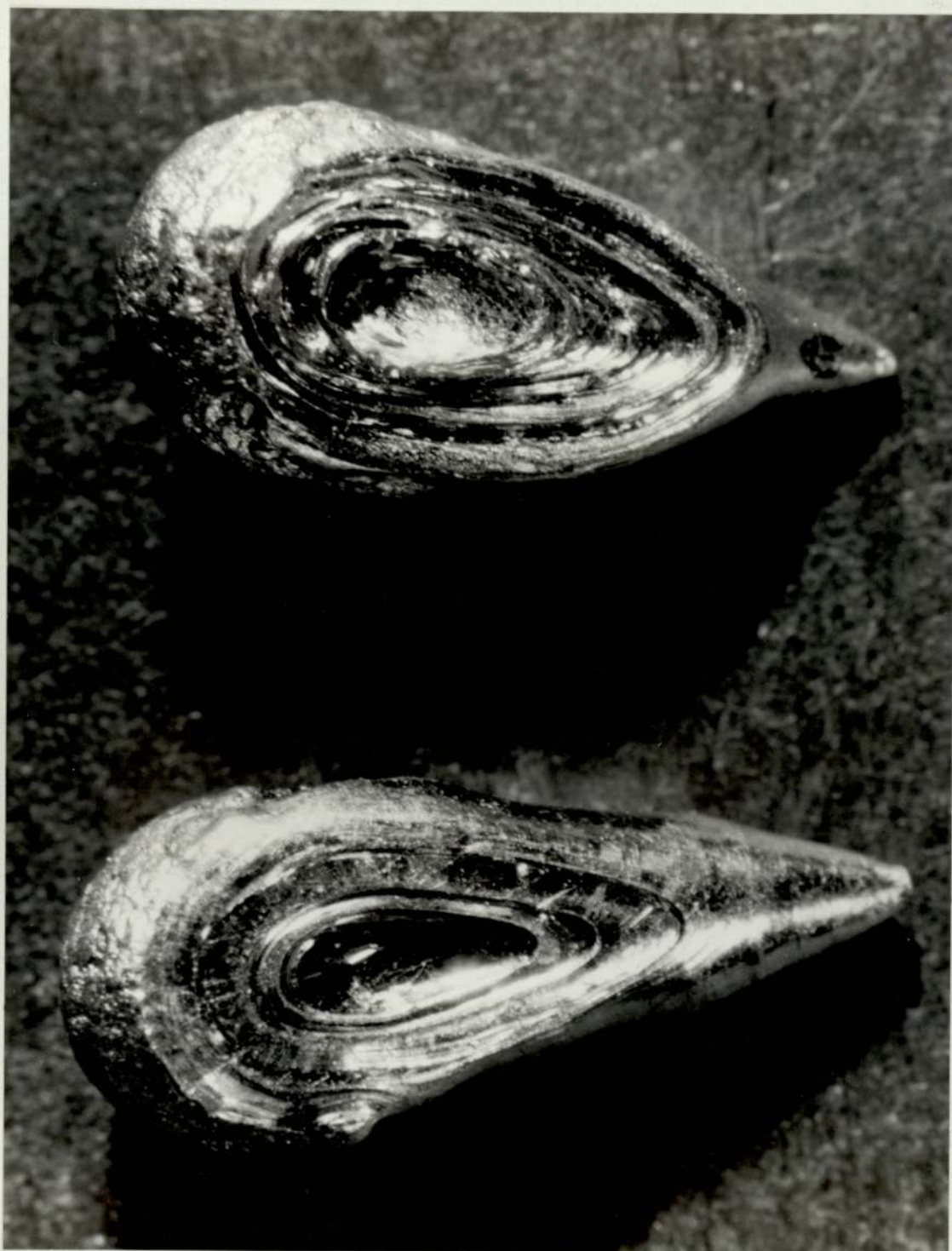
0.2 cm

FIGURE 37. Ripple Formation on the Reproducible Tin Drops

0.2 cm

front zones were found to be very rough, unlike the tail zone which

was very smooth (figures 5 and 37). In addition, it was found that

ripple formation had taken place around those holes mentioned above

and they were very similar to those which occurred when molten tin

at relatively higher temperatures (600°C) was poured into a flat

metal container placed on the floor of the water tank. The temperature

of the water was well above the corresponding threshold temperature

and was about 95°C. It was observed that as soon as the molten tin

come into contact with the metal surface, a stable vapour blanket

was established on the tin drop. This blanket remained stable for

at least 2 - 5 seconds. After this time has elapsed, the vapour

blanket as a whole oscillates and begins to collapse starting from

the edges of the stationary tin drop and propagating along the surface

towards the centre. Towards the end of the progagation what remains

is a single spherical vapour bubble. Wherever this bubble collapsed

a hole was found at that point. Around these holes there are very

regular ripple formations as shown in figure 38. The ripples over

almost the entire tin surface. There are grounds for believing that

these ripples were formed because of a collapsing vapour blanket

and its propagation velocity. The formation of ripples on a fluid

surface is a familiar occurrence in fluid mechanics. The develop-

ment of ripples in this case results from a relative tangential

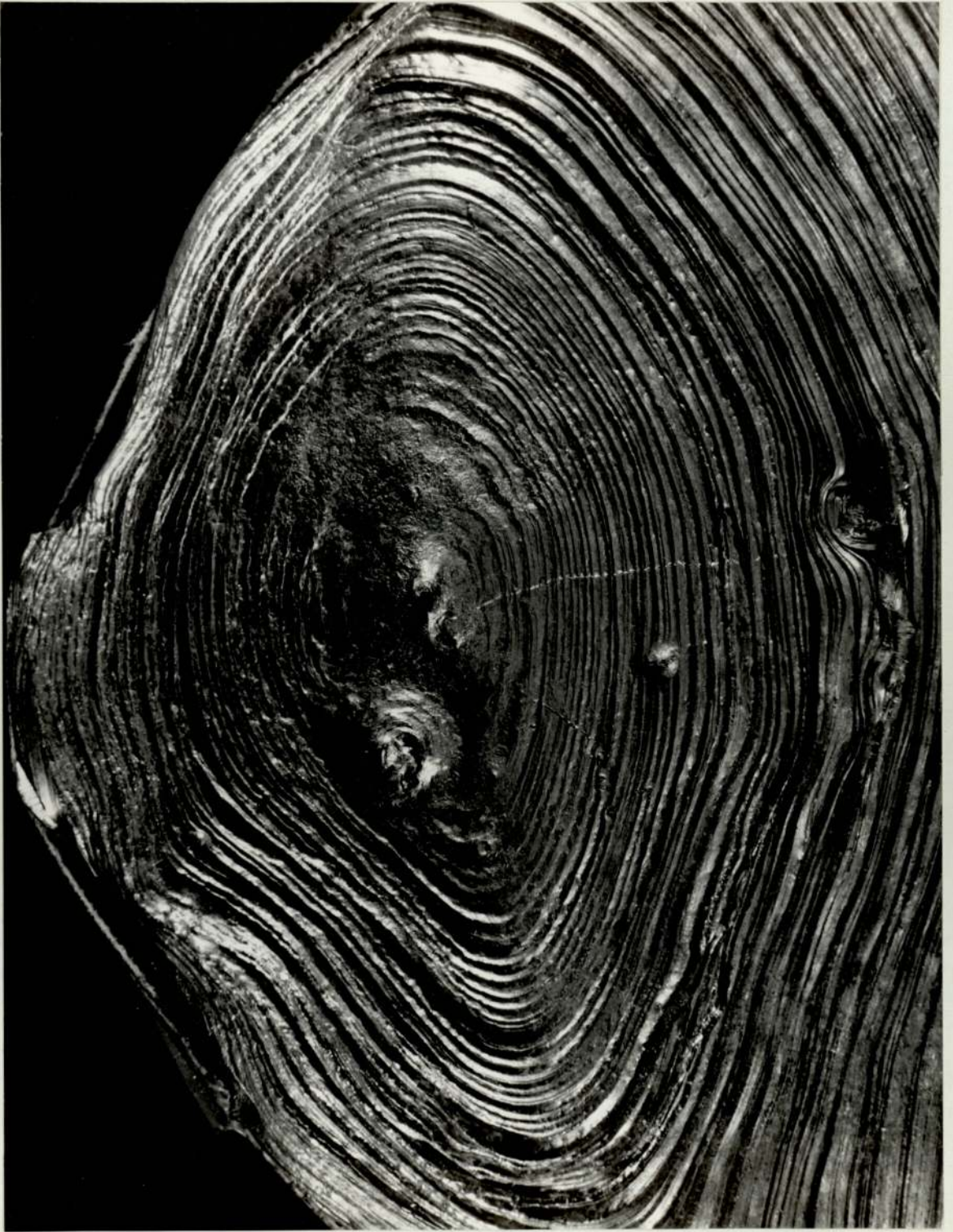velocity arising from the propagating vapour collapse. The collapse

FIGURE 38.   Ripple Formation on the Stationary Tin Drops

of the vapour blanket and its propagation over the surface of the

falling tin drops could also cause the similar ripples observed on

these drops.

The contraction of most metals (including tin and lead) causes

shrinkage cavity formation during the solidification process.

However, some metals do expand during the solidification and

bismuth is one of them. As a result, it is expected that the shrink-

age cavities will appear on lead and tin drops, but will not on bismuth.

As can be seen from figures 39 and 40 slight fragmentation of the tin

and lead drops occurs at those points where the holes are present.

Assuming that these holes result from the collapse of a vapour

blanket (or bubbles) adjacent to the metal drops, impulsive momentum

can be evaluated. (1) The positions of the holes with respect to the

centre of gravity were measured by using a travelling microscope

and these distances were used to evaluate impulsive momentum.

Results were obtained for lead and tin drops of same sizes and

they were 0.650 and 0.872cm in length respectively. The impulsive

momentum and the corresponding values of R_m (the maximum radius

of a single vapour bubble causing rotation of the lead drops) are

shown in figures 41, 42, 43 and 44. The results for tin drops are

shown in table 8 . These results indicate that when a single vapour

bubble collapses near to the tail zone of tin and lead drops of 0.650cm

in length the impulsive momentum lay between 0.123 and 0.141grcmsec^{-1}

FIGURE 39.   Partially Disintegrated Tin Drops

0.2 cm

FIGURE 40.   Partially Disintegrated Lead Drops

0.2 cm

Figure 41

d_H = Average distance between the holes and centre of gravity of the lead drops is 0.2798cm
Diameter of the drop=0.385 cm
Length of the drop=0.872cm

Figure 42

Frequency

D_H = Average distance between the holes and the centre of gravity of the lead drops is 0.286cm

Diameter of the lead drops = 0.350cm

Lenght of the lead drops = 0.650cm

Impulsive Momentum grcmsec^{-1}

.04 .05 .06 .07 .08 .09 .1 .11 .12 .13 .14

14
13
12
11
10
9
8
7
6
5
4
3
2
1

Frequency

R_m, the maximum radius of the vapour bubble cm

.05 .055 .06 .065 .07 .075 .08

Figure 43

Frequency

D_H = the distance between the holes and the centre of gravity is 0.0726cm

Diameter of the drops = 0.385cm

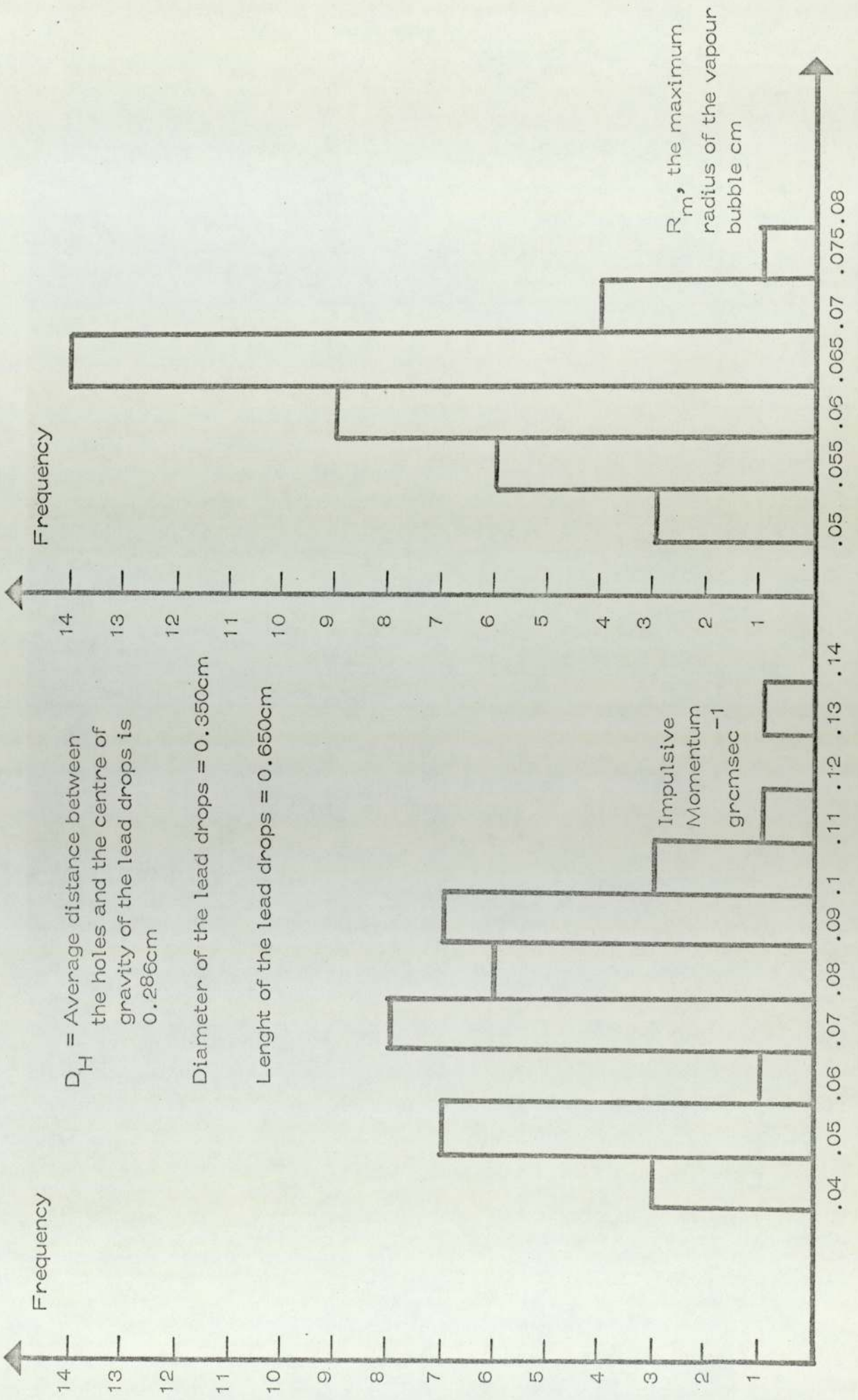Lenght of the drops = 0.872cm

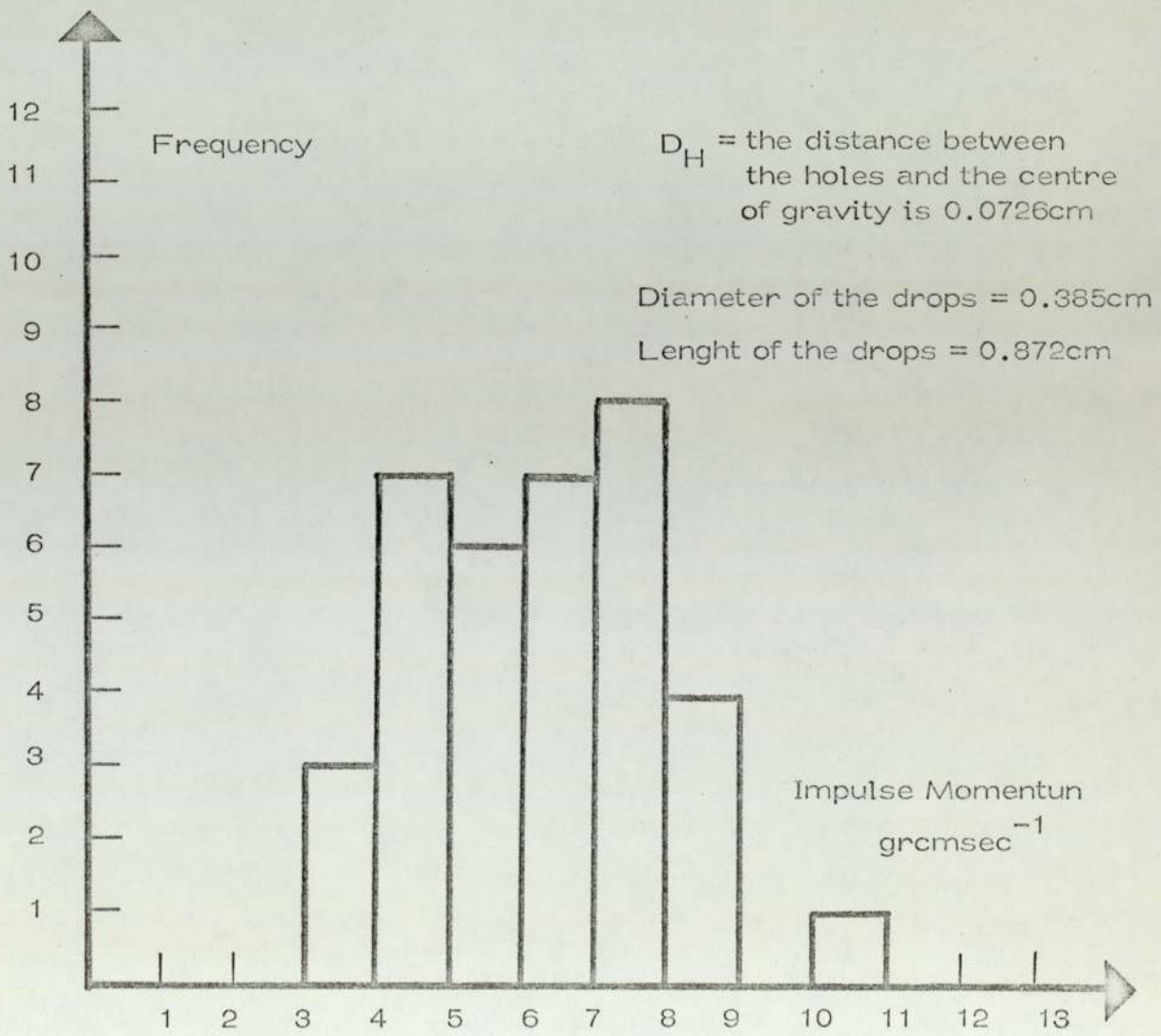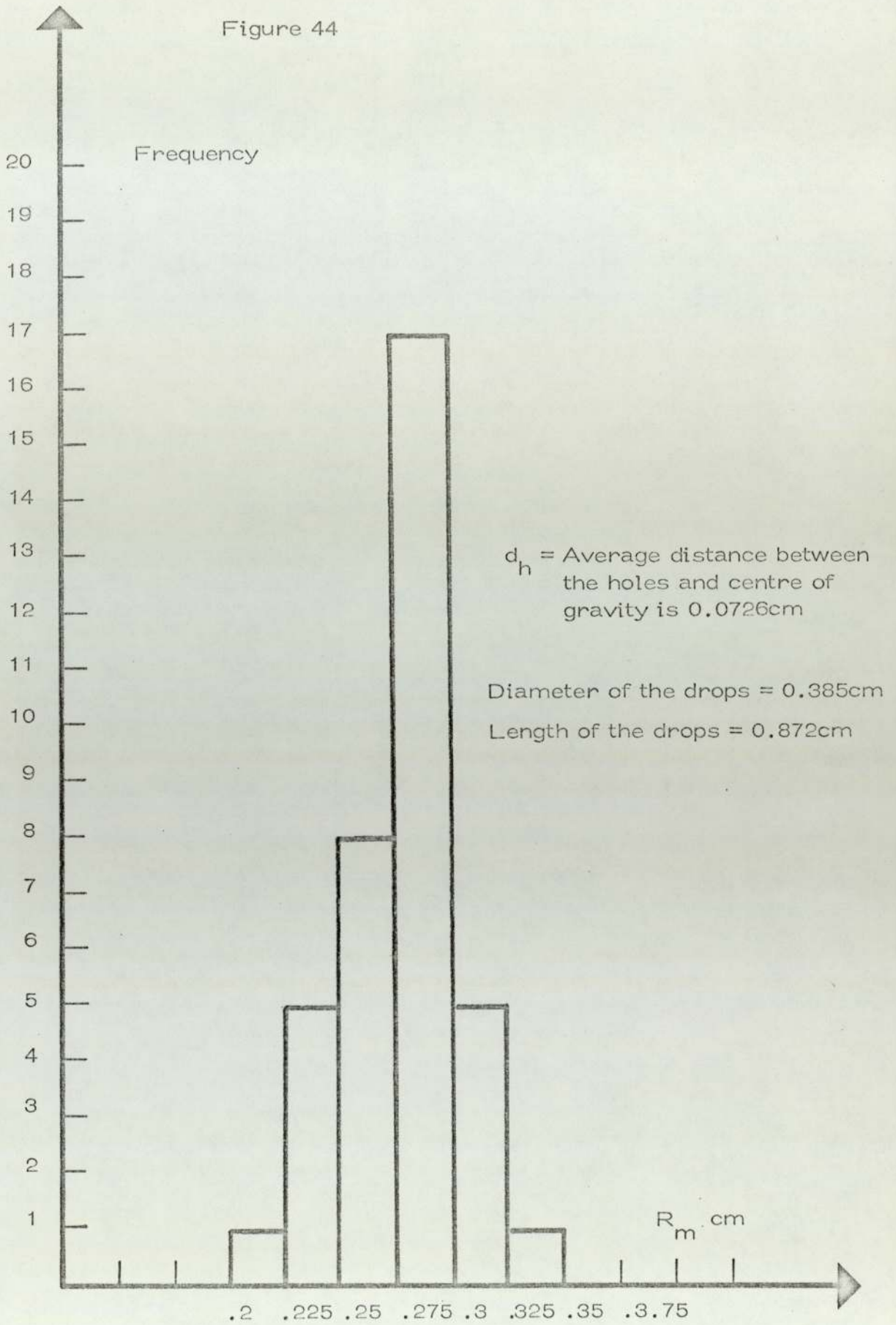Impulse Momentun grcmsec^{-1}

Figure 44

Table 8

Momentum grcmsec^{-1}	R_m cm	Size of the drop length	Average distance between the holes and the centre of gravity of the tin drop
0.786	0.140	0.650cm	0.0172cm
0.123	0.075	0.650cm	0.1100cm.
2.210	0.195	0.872cm	0.1260cm
17.660	0.395	0.872cm	0.0158cm
	Tin drops		

for tin and 0.04 and 0.14grcmsec^{-1} for lead drops. The corresponding values of R_m are between 0.075 and 0.079cm for tin and 0.05 and 0.08cm for lead drops. These seem to be reasonable sizes for a single vapour bubble for the metal drops of radius 0.175cm. However, the findings demonstrate that if the bubble collapse occurs in the region which is near to the centre of gravity of the drops, the corresponding values of R_m still seem to be quite large.

When the molten tin drops at higher temperatures (600°C) fall into water at about 90°C or into liquids which have low-boiling points such as acetone and carbon tetrachloride, it was observed that they definitely establish a vapour blanket around them.

The collapse of this blanket occurs about 3 - 6 seconds after entering the water. This result shows that the vapour blanket stays stable during the fall of molten tin drops and the collapse always occurs at the bottom of the container.

If the molten tin drops are allowed to fall into these volatile liquids one after the other, their fall is vertical. Since the time interval between the fall indivual drops is less than the time taken for the vapour blanket to collapse, the drops land on to each other, resulting in a vertical 'tower' formation. This is shown in figures 45a and 45b. The vapour blanket around the indiviual drop eventually collapses but the drops were by then welded together. Thus, the usual consequences of this collapse are not witnessed and so the tin 'tower' remains in

FIGURE 45a.　　Tower formation of the Tin drops.
If the molten tin drops are allowed to fall
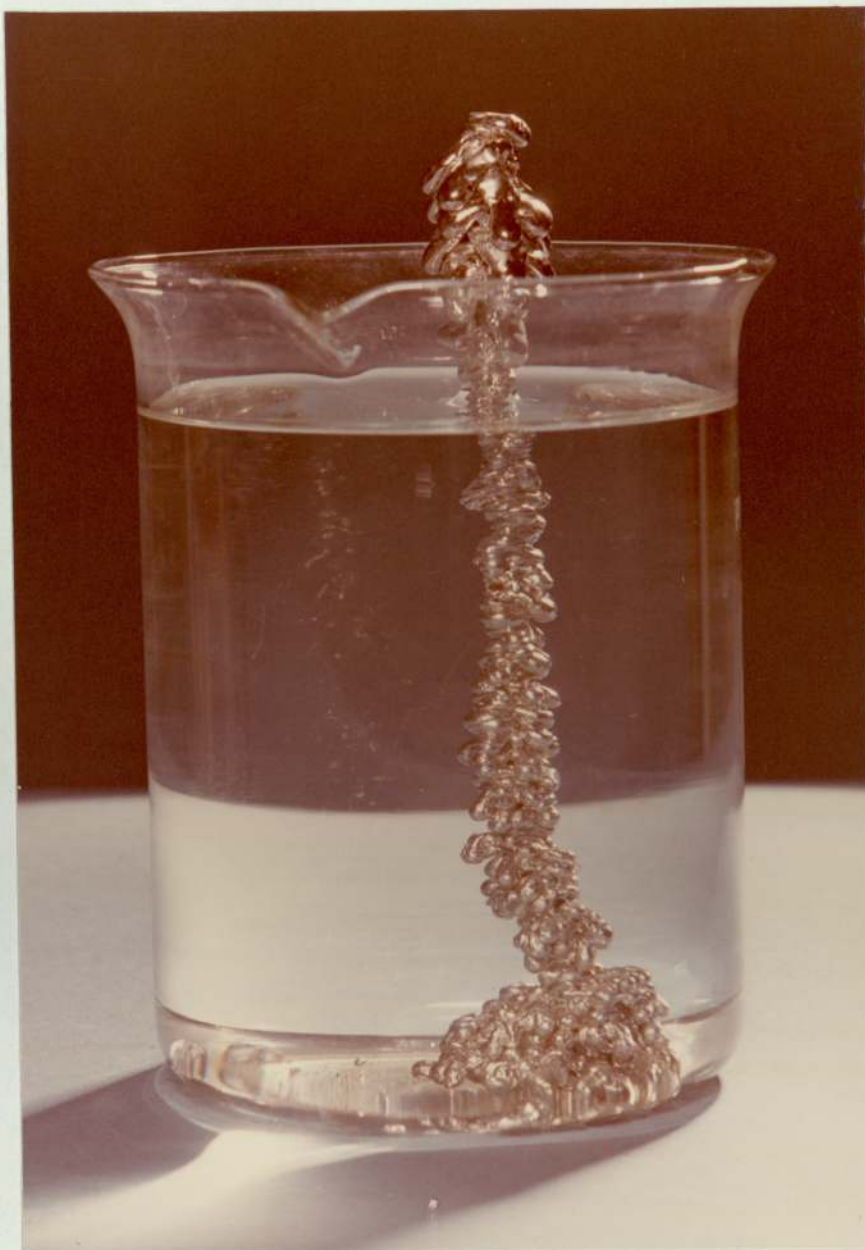into volatile liquids one after the other,
their fall is vertical.

FIGURE 45b.   Tower formation of the tin drops.

tact. It should be noted however that the very lower part of the tower is quite fragile and it can be easily broken. In fact, one of these towers was broken into two pieces from those fragile points. Towards the top of the tower, the tin drops are more strongly welded to each other. The explanation for this behaviour is that the drops which enter the liquid first travel relatively longer distances and hence cool down more. As the tower height increases, the incoming travelling drops travel smaller and smaller distances in the volatile liquids. As a result, they do not cool down as much as the previous ones and hence upon their contact with the drop at the top of the tower, they stick on more strongly. In addition, the drops which form the upper part of the tower are flattended whereas the drops at the lower end of the tower are not. A typical example of the necessary metal and water temperatures to establish such a stable vapour blanket were $500^{\circ}C$ and $90^{\circ}C$ respectively. These two values are in accordance with those values obtained by Witte et al[58] for hot solid spheres. When an unstable pulsating vapour blanket is present, the molten tin drops deviate from their vertical path upon the collapse of this blanket which occurs 20 to 30 milli seconds after the drops have entered the water.

Conclusions

This study has attempted to provide information on the explosions

between molten metals and water. In order to study this phenomenon

an apparatus which can provide small reproducible molten metal

drops was constructed. This reproducibility enabled the present work

to produce regular and quantitative results.

The explosions between molten metals which were studied during

this investigation and the water are not chemical. They are physical

explosions and closely related to the boiling of the water (coolant)

around the molten metals.

The initial metal and the coolant temperatures are the most

important factors which govern the explosions. The explosive

interaction can be prevented by the alteration of one of these variables.

The results show that there exists a temperature for the coolant

(water) above which no explosions can occur. This temperature is

called threshold or cut-off temperatures and is a function of initial

metal temperatures, with water at or above threshold temperatures

explosions can be prevented.

One of the basic difficulties in obtaining useful experimental

results on molten metal-water interactions is that there is no good

standard method of calibrating an explosion. These difficulties have

been overcome to some extent as molten metal drops of known

configuration were obtained.

Using a metal temperature of 300°C and water at room temper-
ature, metal drops were produced which entered the water in a
straight vertical line but were then observed to deviate suddenly and
sharply from their course without losing their pear-like shape. This
metal temperature was just below that necessary to produce explosive
interactions for the given water temperature. The deviation of metal
drops from straight vertical lines in the water produced quantitative
results. These results were used to check the proposed theories
for the explosions. Assuming that the forces causing the deviation
of the metal drops result from the collapse of a single vapour bubble
adjacent to the metal drop, the maximum radius of the vapour bubble
were found to be 0.19 and 0.35cm. These seem too large for single
bubble collapse to be a complete answer for an initiation of the
fragmentation process at least for tin drops of radius 0.15 and 0.19cm.
In some cases where the temperature of the molten metal is very
close to that necessary to produce explosive interactions, a combination
of deviation and fragmentation occurs. Initially, the drops of molten
metal (tin lead and bismuth) fall in vertical straight lines, but a few
centimetres below the water surface, they disintegrate producing a
hollow crust (figures 46 and 47) which keep its pear-like shape and
some very finely divided particles. In fact the internal part of the
drop seems to be ejected outwards. Photographs of this phenomenon
were taken using stroboscopic illumination. These photographs
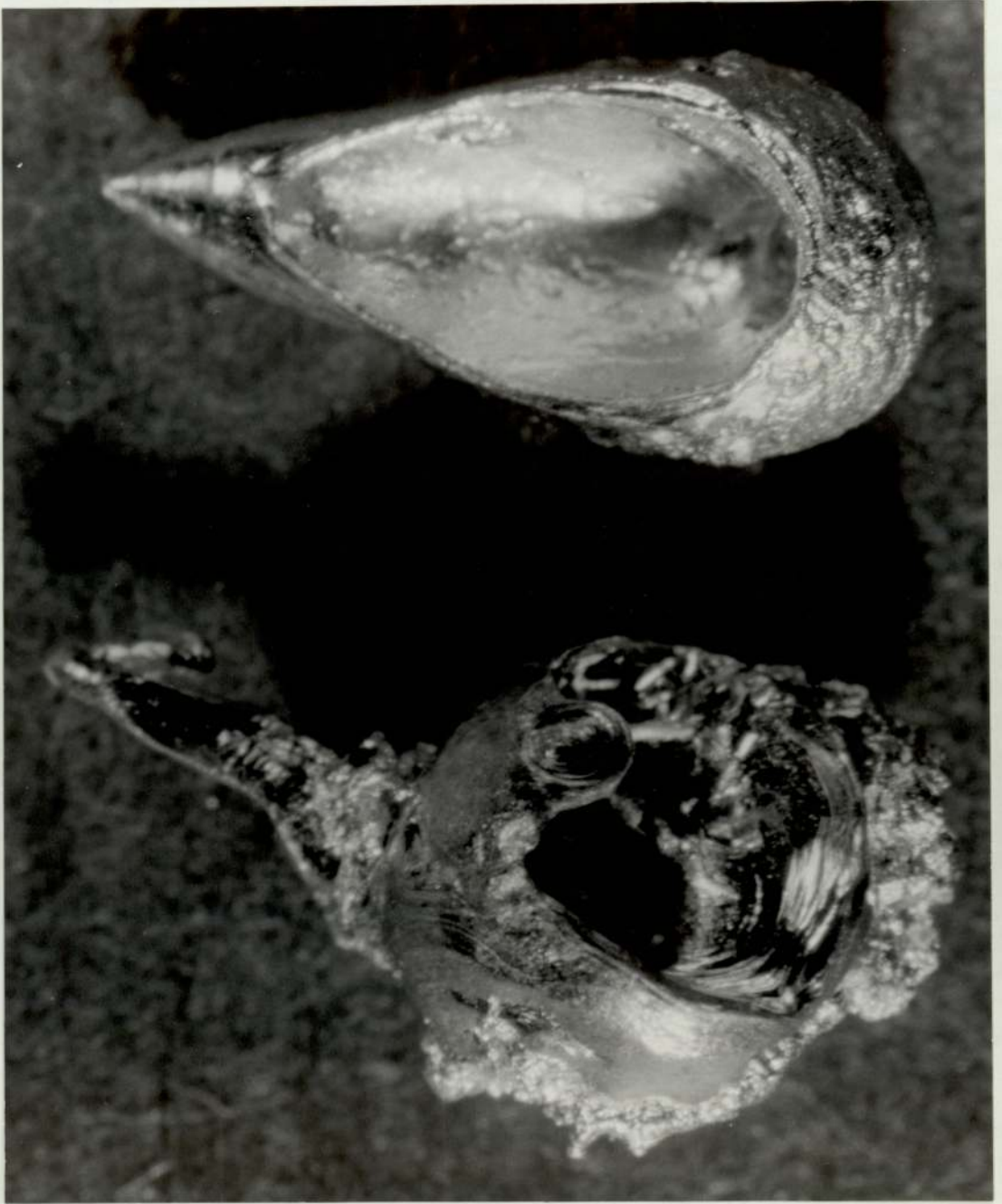
FIGURE 46. The hollow crust of Tin drops caused by
            Deviation-Fragmentation phenomenon.

0.2 cm

FIGURE 47.   Lead drops showing hole formation near to their
centre of gravity and also the hollow crust.

←————————→

0.2 cm

indicate that the crust accelerates as soon as the initial break-up occurs. The deviation of this hollow crust from the straight line is considerable and the values of the angles of deviation were found to be within 0.47 and 0.50 radions. If the temperature of the falling molten metal drops is slightly increased above that necessary to cause deviation fragmentation the whole drop disintegrates into very finely divided particles. It seems very likely that these three series of events (deviation, deviation-fragmentation and fragmentation) are inter-related and the same mechanism is the cause of these phenomena.

On the basis of present experiments it can be concluded that vapour collapse and the corresponding instantaneous heat flux are the main causes of fragmentation in molten metal-water explosions.

The experimental results obtained from aluminium-water inter-actions prove the existence of internal pressure within the aluminium drops. This pressure is due to instantaneous vapourisation of the entrapped water. However, the mechanism which causes the entrap-ment of water is not fully understood. It should be noted that the vapour collapse or the onset of transition boiling does not fully account for the fragmentation. The results demonstrate that the transition boiling occurs around molten metals even above the threshold temperatures for the coolant. A possible mechanism for the frag-mentation is that the high speed liquid jet formed during the later

stages of the vapour collapse penetrates the molten metal and produces a very fine dispersion of the coolant inside it. The instantaneous vapourisation of the coolant inside the molten metal causes the fragmentation.

The deviation of metal drops occurs when the liquid jet due to the collapse of the thin unstable vapour blanket strikes the drop. However, the temperature of the drop is such that the jet can only push the metal drop away from its vertical path. If the temperature of the metal drop is sufficiently high enough the jet is able to penetrate it. However, the crust of the drop solidifies.

As a result, vapourisation of the liquid jet pushes the hollow crust away while fragmenting the interior. Complete fragmentation occurs if the temperature of the metal drop is further increased. Since the solidification of the crust is not complete, the pressure due to the instantaneous vapourisation of the liquid jet breaks up the whole drop causing extensive fragmentation.

Bibliography

1   Johnson and Page, Final year Chemistry course project, University of Aston, 1972

2   G W P Rengstorff, A W Lemmon and A O Hoffman, Review of Knowledge on Explosions between Aluminium and Water, presented to the Aluminium Assoc, April 1969

3   G Long, Explosions between Aluminium and Water Cause and Prevention, Metal Progress, Vol 71, p107, May 1957

4   F E Brauer, Metal-Water Explosions, Nuclear Science and Engineering, Vol 31, p551, 1967

5   K Flory, R Paoli, and R Mesler, Molten Metal-Water Explosions, Chemical Engineering Progress, Vol 65, p50, 1967

6   S G Lipsett, Explosions from Molten Materials and Water, Fire Technology, p118, May 1966

7   L C Witte, J E Cox and J E Bouvier, The Vapour Explosion, Journal of Metals, p39, February 1970

8   L C Witte, T J Vyas and A A Gelabert, Heat Transfer and Fragmentation during Molten Metal-Water Interactions, Journal of Heat Transfer, p521, November 1973

9   J O Elgert, and A W Brown, In-pile Molten Metal-Water Reactions, US Atomic Energy Commission Publications, 100 16257, 1956

10   H M Higgins, The reaction of Molten Uranium and Zirconium

Alloys with Water, Aerojet General Report, No Agc – AE – 7, p18, April 30, 1965

11 L F Epstein, Analytical Formulations for the Reaction Rate of Metal–Water Reactions, Vol 6, US AEC (GEAP 3272), p37, September 30, 1958

12 P D Hess and K J Brondyke, Molten Aluminium–Water Explosions and their Prevention, Metal·Progress, Vol 95, part 4, p33, April 1969

13 R H Bradley and L C Witte, Explosive Interaction of Molten Metals Injected into Water, Nuclear Science and Engineering, Vol 48, p387, 1972

14 R M Paoli and R B Mesler, Explosion of Molten Lead in Water, Proc of the 8th Intern Conf on High Speed Photography, John Wiley and Sons, New York, 1968

15 J M Genco and A W Lemmon Jr, Physical Explosions in Handling Molten Metals and Slags, Foundry Men's Society Transactions, Vol 78, p317, 1970

16 H M Higgins and R D Schultz, USA EC Report, IDO-28000, Aeroject General Corporation, 1957

17 K D Maischak and W Feige, Ursach en und Verhutung von Al – H_2O Explosion, New Hutte, Vol 15, p662, 1970

18 K H Hsiao, J E Cox, Pressurisation of a Solidifying Sphere, Journal of Applied Mechanics, Vol 39, p71, 1972

19   R W Miller et al, Trans American Nuclear Soc, Vol 6, p138,
      1963

20   R W Wright et al, USA EC R and D Report, STL 372-50,
      Annual Summary Report, Contract No AT(04-3)-372, 1966

21   T Enger and E Hartman, Explosive Boiling of Liquified
      Gases on Water, Shell Pipe Line Corp, R and D Lab, Houston,
      Texas, 1972

22   G T Boyle, Vapour Production from LNG Spills on Water,
      Shell Research Limited, UK, 1973

23   S J Board, C L Farmer and D H Poole, Fragmentation in
      Thermal Explosions, Int J of Heat Mass Transfer, Vol 17,
      p331, 1974

24   D L Katz and CM Sliepcevich, LNG-Water Explosions Cause
      and Effect, Hydrocarbon Processing, Vol 50, No 11, p240,
      1971

25   D Laber and A W Lemmon Jr, Explosion of Molten Aluminium
      and Water, Annual Summary Report to the Aluminium Assoc,
      December 1970

26   Wikto Zyskowski, Thermal Interaction of Molten Copper with
      Water, Int J of Heat Mass Transfer, Vol 118, p271, 1975

27   J O Hinze, Critical Speeds and Sizes of Liquid Globules,
      Applied Scientific Research, Vol A1, p273, 1948

28   J O Hinze, Forced Deformation of Viscous Globules, Applied

Scientific Research, Vol A1, p263, 1948

29   W M Rohsenow, Editor, Development in Heat Transfer,

Edward Arnold (Publishers) Ltd, London, p169, 1972

30   S S Kutaleladze, A Hydrodynamic Theory of Changes in the

Boiling Process under Free Convection Conditions, 1ZV Akad,

Nauk, SSSR, Otd Tekh, Nauk NO4, p529, 1951

31   J W Westwater and J G Santangelo, Photographic Study of

Boiling, Industrial and Engineering Chemistry, Vol 47, p1605,

1955

32   N Zuber, On the Stability of Boiling Heat Transfer, Transactions

of the ASME, Paper No 57 HT-4, April 1958

33   H Forster and N Zuber, Growth of a Vapour Bubble in a

Super-heated Liquid, Journal of Applied Physics, Vol 25,

p474, 1954

34   J G Leidenfrost, De Aquac Communis Nonnullis Qualitatibus

Tractatus, (A tract about some qualities of common water),

Disburg on Rhine, 1756. An original copy of this treatise is

in the Yale University Library.

35   V Paschkis and G Stolz Jr, Quenching as a Heat Transfer

Problem, Journal of Metals, Vol 8, p1074-5, 1956

36   V Paschkis and G Stolz Jr, How Measurement Lead to

Effective Quenching, The Iron Age, p95, November 1956

37   V Paschkis, The Co-efficient of Heat Transfer during

Quenching, (in German), Hart Techn Mitt, Vol 15, n4, p189, 1960

38 V Paschkis and G Stolz Jr, Research and Development with Respect to Heat Transfer in Quenching, Armed Forces Technical Information Agency Report, No AD 281854, Arlington 12, Va, USA

39 D J Buchanan, UKAEA Report Culham Laboratory, A Model for Fuel-Coolant Interactions, 1973

40 D J Buchanan and T A Dullforce, Nature, Vol 245, p32, 1973

41 Lord Rayleigh, On the Pressure Developed in a Liquid during the Collapse of a Spherical Cavity, Phil, Mag, 34, p94, August 1917

42 W H Besant, Hydrostatics and Hydrodynamics, Art 158, Cambridge University Press, London 1859

43 M S Plesset and R B Chapman, Collapse of an Initially Spherical Vapour Cavity in the Neighbourhood of a Solid Boundary, Journal of Fluid Mechanics, 47, p283, 1971

44 N L Hancox and J H Brunton, Phil Trans, Roy Soc, London, A260, p121, 1966

45 T B Benjamin and A T Ellis, Phil Trans, Roy Soc, London, A260, p221, 1966

46 J P Christiansen and J A Reynolds, Application of Vortex to Study the Mixing of two Liquids, Computational Physics Group Experimental Division B, Culham Laboratory, 1971

47 G I Taylor, Scientific Papers, Vol 3, paper 32, 1963

48 R S Peckover, Unpublished work, performed at Culham
Laboratory (reference from Buchanan et al, 1973, article
page 11, UKAEA Res Group Preprint Culham), 1971

49 G K Batchelor, Proc Roy Soc, A213, p349, 1952

50 D J Buchanan, Analysis of the Formation of a Vapour Layer
at a Liquid – Hot Wall Interface, UKAEA Res Group Preprint,
Culham Lab, Abingdon, Berkshire, 1972

51 S J Board and R W Hall, Propagation of Thermal Explosions,
1-Tin/Water Experiments, CEGB Report RD/B/N2850, 1974

52 H E Edgerton and J K Germeshausen, Stroboscopic Light
High Speed Motion Pictures, Jr Soc, Motion Picture Engineers,
23, p284, 1934

53 H E Edgerton and J K Germeshausen and G E Grier, High Speed
Photographic Methods of Measurement, Jr Appl Phys, 8, no 1,
2-9, 1937

54 A T Ellis, Observations on Bubble Collapse, Calif Inst of Tech,
Hydrodynamics Lab Report, 21-12, December 1952

55 A T Ellis, Techniques for Pressure Pulse Measurements and
High Speed Photography in Ultrasonic Cavitation, Proc 1955,
NPL Symposium on Cavitation in Hydrodynamics, paper 8,
HM Stationary Office, London 1956

56 W S Bradfield, Liquid-Solid Contact in Stable Film Boiling,

I and EC Fundamentals, Vol 5, No 2, p200, May 1966

57 W S Bradfield, RO Barkdoll and J T Byrne, Film Boiling

on Hydrodynamic Bodies, Convair Scientific Research Lab,

Note 37, p8, December 1960

58 J W Stevens and L C Witte, Destabilisation of Vapour Film

Boiling Around Spheres, Int J Heat Mass Transfer, Vol 16,

p669, 1973

59 F J Walford, Transient Heat Transfer from a Hot Nickel

Sphere moving through Water, Int J Heat Mass Transfer, 12,

1621-1625, 1969

60 S J Board, A J Clare, R B Duffey, R S Hall and D H Poole,

An Experimental Study of Energy Transfer Processes Relevant

to Thermal Explosions, Int J Heat Mass Transfer, Vol 14,

p1631, 1971

61 Sir H Lamb, Hydrodynamics (6th Edition), Cambridge University

Press, 1957